Lawrence Berkeley National Laboratory
Recent Work

Title

Separation of Salt from Water-Soluble Polymers Using High-Pressure Carbon Dioxide

Permalink

https://escholarship.org/uc/item/24q5988q

Authors

Magin, P.
Bonnin, M.
Prausnitz, John M.

Publication Date

1991-07-03

Lawrence Berkeley Laboratory

UNIVERSITY OF CALIFORNIA

Materials & Chemical Sciences Division

To be published

Separation of Salt from Water-Soluble Polymers Using High-Pressure Carbon Dioxide

P. Magin, M. Bonnin, and J.M. Prausnitz

May 1991

DISCLAIMER

SEPARATION OF SALT FROM WATER-SOLUBLE POLYMERS USING HIGH-PRESSURE CARBON DIOXIDE

Peter Magin, Marianne Bonnin and John M. Prausnitz

Department of Chemical Engineering and Chemical Sciences Division
Lawrence Berkeley Laboratory
University of California, Berkeley, CA 94720

Contents

SEPARATION OF SALT FROM WATER-SOLUBLE POLYMERS USING HIGH-PRESSURE CARBON DIOXIDE

Peter Magin, Marianne Bonnin and John M. Prausnitz

Department of Chemical Engineering and Chemical Sciences Division
Lawrence Berkeley Laboratory
University of California, Berkeley, CA 94720

I. ABSTRACT

The results presented in this work show that, at a pressure range between 6.5 and 80 atm and at a temperature of 40°C, high-pressure carbon dioxide induces a liquid-liquid phase separation in aqueous solutions containing about 3-10wt-% of hydroxyethylcellulose (low-viscosity fraction), 25-35wt-% of an alcohol and 0.15-0.3wt-% of an alkali salt. Most of the polymer was found in the heavier liquid phase, whereas the salt distributes more or less evenly between the two liquid phases. The partitioning of the salt could be utilized in a new purification method for hydroxyethylcellulose (HEC).

Following previous work on the system HEC/sodium acetate/isopropanol/water/carbon dioxide, we investigated the dependence of the compositions of the two coexisting liquid phases on pressure and on initial alcohol concentrations. Upon raising the pressure, alcohol and carbon dioxide accumulated increasingly in the lighter phase; polymer, salt and water accumulated in the heavier phase. A lower initial alcohol content did not change the salt distribution, but increased the phase separation pressure. By replacing isopropanol (the co-solvent used in previous work) with tertiary butanol, the lowest operating pressure of the devised purification process could be reduced from 61 to 6.5 atm.

Based on this new purification method, a new production process for hydroxyethylcellulose is proposed in this work. It is premature to claim that the suggested process is superior to the current industrial process. To allow a substantial assessment of the qualities of the new process, additional work would have to be carried out, including the investigation of the influence of higher salt contents than those in our experiments and the addition of other by-products, such as ethylene glycol, to the feed of the phase-separation experiments.

Furthermore, it is not known whether the reaction of cellulose to HEC could be conducted efficiently in the proposed way. Since, in the new process, the recycling of the organic solvent is carried out through the extraction of teriary butanol from aqueous solutions with carbon dioxide, it would be worth while to investigate of the thermodynamic behavior of the ternary system tertiary butanol/water/CO_2.

Experiments were carried out with a low-viscosity and a high-viscosity fraction of HEC. No liquid-liquid phase separation could be observed in aqueous-organic solutions of the high-viscosity fraction. Therefore, it would be useful to examine the thermodynamic behavior of solutions of crude HEC, as it is before fractionation.

It would be useful to insert a mechanical stirring device into a chamber for phase equilibrium experiments. Highly viscous polymer solutions required several days to attain equilibrium in our equipment, where the cell content was mixed hydrodynamically. For the high-viscosity HEC, a liquid-liquid phase split was not achieved, perhaps because of insufficient mixing. The pressure may have been raised too fast to allow the solution to equilibrate in the liquid-liquid region of the phase diagram.

Phase-equilibrium experiments were also carried out with solutions of the microbial polysaccharide xanthan gum and the appropriate by-product salt. The distribution of the polymer and the salt among the two liquid phases was different, but the analytical results for xanthan gum were of low accuracy. Therefore, it is not possible to claim the practicability of a purification of this polymer through a CO_2-induced phase separation.

Phase equilibrium experiments with concentrated polymer solutions require much time. Therefore, assistance of a molecular thermodynamic model for multi-component polymer solutions is desirable. Attempts have been made to apply a recently developed equation of state for aqueous solutions of salts and common gases to the polymer solutions used in our experiments. However, it is difficult to obtain experimental data for parameters reflecting the interactions between the polymer and the other solutes. These interaction parameters are required for the adaptation of the present equation of state to polymer solutions. The results of this thermodynamic calculation effort were not yet sufficient to compare them with the experimental data of this work.

II. INTRODUCTION

The experimental results presented in this work provide new data for the phase equilibria of a system containing a water-soluble (cellulose derivative) polymer, an alkali salt, an organic co-solvent, water and CO_2. The collected data, together with the results of previous work on this system, may provide a basis for a new purification process for water-soluble polymers. The examined polymers were hydroxyethylcellulose (HEC) and xanthan gum. In the production of these polymers, several by-products, e.g. sodium acetate or dipotassium phosphate, have to be removed. In current industrial practice, this removal is achieved by washing the crude product with aqueous-organic solvents, e.g. aqueous alcohols. The alcohol prevents the polymer from dissolution, but it also reduces the capacity of the washing solution to dissolve the by-product salts. In the experiments presented in this work, high-pressure carbon dioxide was used to induce a liquid-liquid phase separation in an aqueous-organic polymer solution at 40°C.

For HEC, the polymer and an appropriate salt partitioned between these two phases. Most of the polymer stayed in one phase, whereas the salt distributed more or less evenly between the two liquid phases. The different behavior of these two components could form the basis of a new purification process. The new process may have the advantage that the application of high-pressure CO_2 reduces the amount of alcohol needed for the purification.

Based on the novel purification process for water-soluble polymers, a new overall production process for HEC is proposed in this work.

Hydroxyethylcellulose

Hydroxyethylcellulose (HEC) is a nonionic, water-soluble cellulose ether, used e.g. as thickener, binder, suspender or film former. In 1985, annual world consumption totaled about 10^5 tons, at a price of ca. $4.60/kg (1). HEC is prepared by the basic catalyzed reaction of ethylene oxide with alkali cellulose. Alkali cellulose is obtained by soaking cellulose in an aqueous solution of sodium hydroxide to

disrupt the crystalline regions of the cellulose to make the hydroxyl groups accessible for the alkylating agent ethylene oxide.

The reaction

$$ROH \cdot NaOH + n\, CH_2CH_2O \rightarrow R(OCH_2CH_2)_nOH + NaOH$$

is carried out in a slurry, where isopropanol or other alcohols are used as diluents. $ROH \cdot NaOH$ represents the alkali cellulose. Figure 1 shows an idealized structure of hydroxyethylcellulose. Ethylene glycol and polyethylene glycol appear as by-products due to the basic catalyzed hydrolysis of ethylene oxide. Moreover, the necessary neutralization of the sodium hydroxide yields a large amount of sodium salt. For most applications, a purified product is desired or necessary. According to information from the supplier of the HEC used, the salt (sodium acetate, if the base is neutralized with acetic acid) has to be removed from a mixture which contains 0.3-0.5 kg salt per kg polymer. This is currently done by washing the crude polymer with aqueous solutions of alcohols (typically isopropanol) or acetone, which have to be recycled. No quantitative information was available for this purification method. The removal of all low-molecular-weight impurities is very cost-intensive (1).

Xanthan Gum

Xanthan gum is an anionic, water-soluble microbial polysaccharide, produced in a batch fermentation process utilizing the aerobic extra-cellular synthesis by the bacterium Xanthomonas campestris. Figure 2 shows the structure of xanthan gum. Commercial production of xanthan gum commenced in 1964. Five years later xanthan gum was approved by the Federal Drug Administration as a food additive without specific quantity limitations (2). Xanthan gum is currently used as a thickening, sus-pending and stabilizing agent in the food, cosmetic and pharma-ceutical industries. Its molecular weight ranges between 2 and 50 million g/mol (3). In 1987, the US market for the food-grade product amounted to ca. 2200 tons, with the price range between \$13.20 and \$15.40/kg (\$7.70-\$11.00/kg for industrial-grade products) and an annual growth rate of 5% (4).

In the production process, acid groups are formed as part of the polysaccharide molecules. To maintain the pH between 6.0 and

7.5, a range suitable for the fermentation, 0.5 wt-% of dipotassium phosphate is used as a buffer. After the nutrient carbohydrate (typically glucose) is entirely consumed by the bacteria, the final aqueous fermentation broth contains about 1.5 wt-% of xanthan gum (5).
Thus, it contains about 0.33 kg phosphate per kg polymer. For food-grade products, this phosphate and other impurities have to be removed. Since the less pure, industrial grade polymer is about $5/kg cheaper, one third of the food-grade product price is due to this final purification step. Currently, xanthan gum is recovered by precipi-tation out of the fermentation broth with isopropanol, ethanol or methanol in the presence of potassium chloride, filtered and then purified by washing with the same organic solvents. With methanol or ethanol, the required weight ratio of alcohol to fermentation broth is about 3 (6,7). For commercial production, it is essential to recycle this vast amount of alcohol.

In the experiments we added alcohol to an aqueous solution of xanthan gum and dipotassium phosphate, which resembled, in salt and polymer concentration, the final fermentation medium. After inducing a phase split with high-pressure carbon dioxide, the polymer and the salt accumulated in the heavier, water-rich phase. Upon raising the pressure, xanthan gum, unlike the salt, seemed to distribute more evenly among the two liquid phases.

The separation of these two components did not occur to an extent that would make an application of this phase split feasible in the purification of xanthan gum.

In a typical supercritical extraction process, a supercritical fluid (SCF) is used to selectively dissolve a specific, non-volatile component from a multi-component mixture. In the systems discussed in this work, however, compressed carbon dioxide is a poor solvent for either the polymer and the salt; in our experiments, we used carbon dioxide as a phase splitter.

Polymer solutions can exibit a liquid-liquid phase separation at the lower critical solution temperature (LCST) - that is, the temperature at which the polymer-solvent mixture separates into a polymer-rich and a solvent-rich phase. LCST phenomena can be related to the chemical nature of the components of the mixture, the molecular weight of the components, especially the polymer, and the critical temperature and critical pressure of the solvent. As the single-phase polymer solution is heated isobarically to conditions near the critical point of the solvent, the polymer and solvent thermally expand at different rates, which means that their free volumes change at different rates. The thermal expansion of the

solvent is much greater than that of the polymer. Near its critical point, the solvent is expanded so much that it no longer is able to solubilize the polymer. Hence, the polymer falls out of solution.

If the molecular weight of the polymer is close to one million, the LCST phase separation can occur at a temperature as low as 120°C below the critical temperature of the solvent. Still, the critical temperatures of common solvents may be high enough to cause thermal degradation of the polymer (9).

The LCST can be shifted to lower temperatures by introducing a supercritical fluid (SCF) to the polymer solution. The overall effect of the SCF is to lower the LCST curve, as illustrated in Figure 4 (10).

To our best knowledge, LCST phenomena of the polymer solutions studied in this work have not been examined before. In the experiments presented in this work, we shifted the LCST of an aqueous-organic polymer solution to 40°C by adding carbon dioxide at elevated pressures. We chose 40°C as operating temperature because it is approximately the lowest temperature easily maintained in a thermostat against room temperature without the support of a refrigerator.

The objective was the removal of salts from aqueous-organic polymer solutions through a liquid-liquid extraction by phase separation. The water-soluble polymer and the appropriate (by-product) salt were dissolved in a mixture of water and alcohol. The maximum content of alcohol was determined by the limited solubility of the polymer in aqueous-organic solutions. The maximum content of water was limited by the fact that, below a certain alcohol concentration, no phase separation could be observed at 40°C and pressures below about 80 atm. Water has a much higher critical temperature (374.2°C) than those of the common alcohols (ca. 240°C). Since the LCST depends on the solvent's critical temperature, with pure water as the solvent, the pressure of carbon dioxide at 40°C would have to be much higher to achieve a phase separation.

III. EXPERIMENTAL PROCEDURE

The apparatus used for our experiments and the measuring principle of the density of the liquid phases was identical as the ones described in previous work (11).

1.   Concentration Measurements

To determine the concentrations of the contents of the cell, discrete volumes of different phases were sampled by means of two VICI six-port switching valves with zero dead volume. These two-position valves are made from Hastelloy-C and were tested for 200°C and 350 bar. Their operating principle is illustrated in Figure 9. The content of the cell was pumped through a sampling loop of known volume; when equilibrium was attained, the fluid that was present in the loop at that moment was separated from the recirculation flow by turning the valve to the "sampling" position. The sample was rinsed out of the loop, diluted with pure water and then analyzed.

It was important to know the exact volumes of both sampling loops to calculate the concentrations inside the cell. The necessary volumetric calibration was achieved by sampling two different sodium acetate solutions of known concentration. The content of the sampling loop was rinsed out and diluted with a known amount of pure water, and the concentration was measured by atomic absorption spectroscopy, as discussed later. The volume of the loop V_{loop} was then easily obtained by

$$V_{loop} = V_{diluted} \left(c_{diluted} / c_{loop} \right)$$

c is the concentration of sodium acetate. To minimize errors arising in the preparation of the samples, several calibration experiments were carried out and the resulting values for both loops were averaged.

a) Concentration of Carbon Dioxide

The concentration of carbon dioxide in the samples was determined by a volumetric method. After turning the sampling valve, the sampling loop was connected to a burette with CO_2-saturated water. The water inside the burette and the connected reservoirs of the sampling apparatus for carbon dioxide (see Figure 10) was saturated by routing CO_2 through the lines for 20 minutes.

Then the content of the sampling loop was slowly expanded to room pressure and the volume of gas going out of solution was monitored through the rising level of the CO_2-saturated water in the burette. The level in the burette was determined with an accuracy of 0.2 ml. The temperature of the CO_2 was measured with an accuracy of 0.1°C with a thermo-couple and an OMEGA ENGINEERING Digital Temperature Indicator. The thermocouple was calibrated with icewater. Room pressure was measured with an accuracy of 0.01 bar with a precision mercury barometer. The amount of CO_2 in the sampling loop was then calculated using the ideal-gas law, which is justified for CO_2 at room temperature and pressure.

$$m_{CO2} = V_{CO2}\, P_{room}\, M_{CO2}\, /\, T_{CO2}\, R$$

M_{CO_2} is the molecular mass of CO_2. With this method, the error margin of the carbon dioxide concentration measurements was about 3% at maximum. The carbon dioxide used came from a commercially available gas bottle and was filtered with a NUPRO 5 μm filter-element.

b) Concentration of Salt

The salt concentration was measured with a PERKIN-ELMER Atomic Absorption Spectrometer model 2280. Its primary light source is a hollow cathode lamp filled with a noble gas.

The dilute aqueous sample solution is converted into atomic vapor in an air-acetylene flame and penetrated by the light beam of the cathode lamp. Under appropriate flame conditions, most of the atoms are excited by absorption of light energy of element-specific wavelengths. Therefore, the lamp cathode has to be made of the same element as the one that is to be detected.

The amount of light absorbed increases with the number of atoms in the light path. The detector measures the amount of the light of a certain, variable wavelength after passing the flame. A quantitative determination of the amount of atoms in the light path can be made through instrument electronics.

Sodium was analyzed at a wavelength of 589.0 nm. The corresponding value for potassium was 766.5 nm. Plastic bottles were used for storing the calibration standards to prevent absorption of alkali metal ions at, or release from, glass walls. For each sample, two or three measurements were carried out.

Consistently, the deviation from the mean value amounted to less than 2%. Compared to this deviation, dilution errors were neglegible. Both salts used were supplied by FISHER SCIENTIFIC, with purity specifications of 99.98 wt-% for K_2HPO_4 and 99.5 wt-% for NaAc.

c) Concentrations of Polymer and Alcohol

The concentrations of the alcohols and polymers in the samples were determined by a form of liquid chromatography called size-exclusion chromatography. Other than in most forms of liquid chromatography, which depend on adsorption phenomena, separation occurs on the basis of the "effective molecular diameter" (see Figure 11). Adsorption is not desired and falsifies results. "Small" solute molecules diffuse into the pores of the packed particles while entry of "large" molecules is hindered; the components of the solute mixture leave the column in the order of decreasing molecular size. Thus, separation characteristics depend to a large extent on the pore-size distribution of the given column packing. This principle is illustrated in Figure 12.

The application of high pressure to the chromatography system provides increased speed, resolution, sensitivity and reproducibility. A high-pressure liquid chromatography assembly consists of the solvent (mobile phase) container, the solvent delivery pump, a packed, thermostatized column, a detector, an integrator and recorder and a waste container. The solvent delivery pump used was a RAININ Rabbit HPX piston pump. For our measurements, 26 bar at a flow rate of 0.8 ml/min were sufficient.

The column used was a BIORAD Bio-Gel SEC-30XL column with an internal diameter of 7.8 mm, packed with hydroxylated polyether based material. These columns operate consistently in the pH-range from 2 to 12 and are typically used for protein analysis. The hydrophilic packing with an average pore size of 250 Å and a particle size of 60000 Å separates molecules with weights from about 10^3 to 10^6. The column was maintained at 36°C with a RAININ column heater block.

A KNAUER Differential Refractometer Type 198.00 was used as a detector. It was thermostatized at the same temperature as that of the column. The detector converts the difference between the refractive index of pure water and that of the mobile phase of the chromatograph column continuously into an electronic signal.

To calculate the peak areas of individual components, the signal of the differential refractometer is processed by an IBM AT personal computer with the NELSON ANALYTICAL Chromatography Data System 4000 software, via a model 760 intelligent interface.

The chromatograph was calibrated by injecting different solutions of selected components and by relating resulting peak areas to the known concentrations. Unfortunately, the peak areas for the calibration standards were not constant. After about 15-20 runs, the peak area for the same calibration standards had deteriorated significantly; the sensitivity of the detector had declined for every component; the calibration had to be repeated. This problem arose especially during the analysis of xanthan gum solutions.

Several times, the optical flow cell of the detector was removed and cleaned with hot nitric acid. Each time, this procedure improved the sensitivity by factor 10, but even the use of a 0.5 μm filter for the sample solutions could not prevent the sensitivity from declining with time. Perhaps, small clusters of undissolved polymer molecules adhered to the glass walls of the optical flow cell. One of the numerous calibrations which had to be carried out is reported in Figure 13.

Due to errors from sample injection and possible fluctuations in component retention, three measurements were carried out for each sample and averaged. The aqueous sample solutions analyzed with the chromatograph contained the polymer, the appropriate salt and an alcohol. Two liquid chromatography plots are shown in Figure 14. The alcohols always separated well from the other components, but the salts had retention times very close to those of the polymers. Therefore, the peak areas of these two components overlapped, formed a combined peak, and could not be integrated separately.

Since the concentration of the salt was determined previously by atomic-absorption spectrometry, the "polymer part" could be evaluated by substracting the "salt part" from the combined salt-polymer peak area. Hence the calibration of the liquid chromatograph had to be conducted for the respective salt, too. However, this simple method is only valid, if the polymer and the salt do not interfere, i.e. if a linear additve relation exists between the peak areas of salt and polymer.

Our calibration experiments indicated, that for all concentrations which did not exceed 0.06 g/l Xanthan + 0.02 g/l K_2HPO_4 and 0.7 g/l HEC + 0.08 g/l NaAc respectively, interference of the salt and the polymer was very small and the peak areas of these two components almost exactly linear additive.

The actually measured combined salt/polymer peak areas were, at maximum, 3% larger than the sum of the expected individual peak areas for each component, calculated from the calibration for the individual components.

In Table 2, peak areas are reported for a typical sample containing HEC, sodium acetate and tertiary butanol, respectively xanthan gum, dipotassium phosphate and the same alcohol. The relatively broad distribution of the peak area values of xanthan gum were typical. For this polymer, the maximum deviation from the mean value was about 11%, whereas for all other components it was below 1%.

The maximum deviation from the mean value in the calibration was about 6% for xanthan gum and below 1% for all other components. Therefore, the overall error for the xanthan gum analysis was ca.18%, for the other components analyzed with the chromatograph ca. 3%. Dilution errors were comparatively small. The wide error margin for xanthan gum solutions may be due to the relatively small xanthan peaks and, therefore, a small relative distance to the baseline noise of the detector. Higher concentrations of this polymer yielded larger peaks, but involved an unbearably rapid decline of the sensitivity of the detector.

The supplier of our HEC specified 3 wt-% of sodium carbonate as an impurity in their product; our measurements indicated a content of 3.75 wt-%. The analytical results were corrected, using our value. The original potassium content of the xanthan gum used was determined to 2.5 wt-%. Since xanthan gum is an anionic polymer, this potassium content was not an impurity; the potassium cations are part of the polymer. Accordingly, only the salt analysis results were corrected in the experiments with xanthan gum. The concentration of water was indirectly determined by substracting the sum of the concentrations of the other compounds from the overall density of the concerned phase.

The alcohols used were isopropanol, secondary butanol and tertiary butanol in the experiments with HEC and isopropanol and tertiary butanol with xanthan gum. Our isopropanol was supplied by FISHER SCIENTIFIC, the specified purity was 99.96 wt-%. The secondary butanol came from the MATHESON, COLEMAN + BELL Company, the tertiary butanol from the J.T.BAKER Inc., both with no purity specifications. The water was purified with a BARNSTEAD Ultra Pure Water System.

The HEC used was supplied by UNION CARBIDE. This company offers the polymer in various grades. We used the low-viscosity fraction QP 09L (with a specified viscosity of a 5 wt-% aqueous solution of 0.075-0.112 Pa·sec at 25°C; the molecular weight is ca. 70000 g/mol) and the high-viscosity fraction QP 4400H (the corresponding values are 4.8-6.0 Pa·sec at 2 wt-%; the molecular weight was not determined).

Our xanthan gum was supplied by the ALDRICH Chemical Company; specifications of their product were requested but not given.

2. Experimental Procedure

All experiments were carried out in the same way: Before each experiment, the equilibrium cell was rinsed with pure water, which was filled into the equipment, pumped through the recirculation lines for one hour and then removed. This was repeated until the salt content of the washwater was well below 0.1% of the desired salt content of the next experimental polymer solution. The last rinsing step was carried out with acetone. Then the lines were dried under vacuum for several hours.

The solutions were prepared by mixing the polymer and the salt with water, using a mechanical stirrer at low rotational speed, until a homogeneous solution was obtained. The desired amount of alcohol was added dropwise in the case of tertiary butanol to prevent the polymer from reprecipitation.

A slight vacuum was applied to the cell through the top outlet of the equilibrium apparatus and the solution was sucked in slowly through the bottom drain (see to Figure 5). The cell was filled well above the suction inlet of the upper recirculation line to provide enough liquid for the content of the recirculation lines, which were still empty. The temperature inside the oven was raised to 40°C and the content of the cell was degassed for one hour. Then the bottom recirculation pump was switched on. When the density meter showed a constant reading, indicating that the cell content was homogeneous, the "initial sample" was separated from the bottom recirculation line by turning the sampling valve (see Figure 9). Analysis of this sample determined the feed composition of the following phase equilibrium experiment. The content of the sampling loop was always rinsed out with 100 ml pure water, an amount proven to be sufficient, and diluted to 200 ml. Depending on the composition, further dilution was sometimes required for the analytical measurements.

The sampling valve was switched back to the equilibrating position. Pressure was gradually applied in steps of 3 to 6 atm, if the pressure, at which the phase separation would occur, could previously be estimated by experience. Otherwise, the pressure was raised in steps of 1 to 2 atm. Equlibrium pressures were only approached by adding, not by releasing cell pressure, which would have resulted in an uncalculable loss of alcohol as the only significant component in the gaseous phase, besides carbon dioxide.

The CO_2 feed pump was used to reach pressures above the gas bottle pressure (about 70 bar). The carbon dioxide from the bottle was liquified at about 10°C before entering the pump. Thus, the desired pressure in the cell was obtained quickly because liquid carbon dioxide is almost incompressible. The cell was separated from the gas feed and the system was allowed to equilibrate.

The hydrodynamic mixing in the cell was not very efficient. Equilibration could take up to three or four days, due to the high viscosity of the polymer solutions.

In experiments in which the desired phase separation was achieved, the equilibrated system inside the cell contained three phases: two liquid phases, referred to as the (lighter) "top phase" and the (heavier) "bottom phase", and one gaseous (CO_2-rich) phase. At equilibrium, the maximum relative volume expansion of the liquid cell content, compared to the initial solution at room pressure, amounted to ca. 10%, at a CO_2 concentration of 31wt-% in the top phase and 4-wt% in the bottom phase.

Sometimes, the volume of the top phase was very small and this phase did not cover the inlet of the top recirculation line; the top phase could not be sampled and analyzed. However, after analyzing the bottom phase, the mass balances would yield the concentrations of all components in the top phase, except carbon dioxide (the amount of the alcohol in the gaseous phase had to be estimated for this purpose, using to the mass balance of other experiments). The volume of the liquid phases could only be measured optically with an accuracy of 2 ml. With a top phase volume of 2 to 10 ml, the results obtained through the mass balance were too inaccurate and therefore useless.

Unlike the two liquid phases, the gaseous phase could not be analyzed at all. But the mass balance of the experiments showed that, besides carbon dioxide, the gaseous phase contained only the alcohol to a significant amount.

When the density and the pressure were stable over several hours at 40°C, equilibrium was obtained.

Since there were two liquid phases in the cell, both contained entrainment from the other phase. To remove suspended parts of the other phase from the phase to be sampled, the recirculation pump of this other phase was stopped for two hours before sampling. The sampling loop was separated from the recirculation line, and the CO_2 concentration was measured according to the corresponding section on page 16.

Rinsing out of the other contents of the sampling loop was carried out in the same way as that for the initial sample.

When both liquid phases were sampled, the pressure was either further increased for another equilibrium, or released through the upper purge line. The cell was emptied through the bottom drain. While the apparatus was cleaned through several rinsing cycles, the samples were analyzed as described in the analytical section.

IV. EXPERIMENTAL RESULTS

The analytical results at equilibrium are reported in distribution coefficients and separation factors. In this work, we defined the distribution coefficient as the ratio of the concentration (g/l) of a given component in the top phase to the concentration of this component in the bottom phase. Where not otherwise stated, the separation factor was defined as the ratio of the distribution coefficient of the salt to the distribution coefficient of the polymer. To compare the experimental results with regard to the applicability of the liquid-liquid phase separation for a purification of the polymer, we evaluated the salt content of the polymer before and after the phase separation, i.e. in the feed and in the bottom phase, respectively. The amount of polymer dissolved in the top phase was considered a "loss".

We tried to keep the alcohol content and the phase separation pressure low, but these two objectives appeared to be contradictory.

The concentrations in g/l are reported in the appendix.

1. Short Review of Previous Results

The system carboxymethylcellulose(CMC)/K_2SO_4/isopropanol/water/ CO_2 was examined in previous work (11). As HEC, CMC is a water-soluble cellulose derivative with a similar range of applications. In the same mixture of isopropanol and water, its solubility is smaller than that of HEC.

In one experiment, phase separation was achieved at 52.3 atm and 40°C with an initial solution containing 14wt-% isopropanol, 3.4wt-% CMC and 1.4wt-% potassium sulfate. The separation factor was 3.5; the salt content of the polymer was reduced from 30% (feed) to 24% (bottom phase). 15% of the overall amount of polymer was dissolved in the top phase.

In another experiment, with 21wt-% isopropanol, 3.0wt-% CMC and 1.3wt-% potassium sulfate at the same temperature, the phase separation occurred at 37.4 atm and 40°C, and the separation factor was 24; the salt content of the polymer was reduced from 29% to 22%, hereby losing 2% of the polymer in the top phase.

Therefore, the CO_2-induced phase separation may be used as a purification process for CMC. Since these results were promising, we tried to apply an analogic phase split to solutions of HEC and the appropriate salt. The low-viscosity fraction of HEC has less than half the molecular weight of CMC and is, unlike CMC, uncharged.

2.   Experiments with Hydroxyethylcellulose (HEC)

2.1   The HEC (low-viscosity fraction) / Isopropanol - System

The preparation of the homogeneous initial polymer solutions was accomplished in 1-2 h. After adding the alcohol to the previously prepared aqueous solution, some polymer precipitated, but dissolved again quickly. The solutions filled into the cell were always clear at room temperature and pressure.

Initial Concentrations

Figure 15 shows the initial compositions of the solutions filled into the cell. Sodium acetate is referred to as "salt". The experiments #1 and #2 were conducted by our predecessor (11).

Since, under economical aspects, a low alcohol content is desirable, the isopropanol/polymer ratio in the initial solutions was lowered in exp. #3,#4, and #5, compared to that in exp. #1 and #2.

Volumes and Pressures at Equilibrium

The volumes of the two liquid phases and the lowest pressures at which the phase separation was observed are reported in Figure 16. The lighter top phase was always clear and much less viscous than the very turbid bottom phase. The reducing of the isopropanol/water ratio in exp. #3 and #4, compared to that in the first two experiments, resulted in very small top phases which could not be sampled; no distribution coefficients or separation factors could be evaluated for exp. #3 and #4. A minimum initial isopropanol concentration of ca. 300 g/l was necessary to achieve a top phase of sufficiently large volume to be sampled. Therefore, in exp. #5, the initial alcohol concentration was increased to 340 g/l, well over the concentrations in exp. #3 and #4 (278 and 270 g/l, respectively).

CO_2-Solubility in Both Liquid Phases

Figure 17 shows that the CO_2-solubility of both liquid phases was much higher than that in pure water. Unlike water, isopropanol is entirely miscible with CO_2 at 40°C and 100 atm (14). Therefore, the isopropanol might have enhanced the CO2-solubility in both phases, especially in the alcohol-rich top phase.

The CO_2-solubility of both phases in exp. #5 was smaller than those in the first two experiments, requiring a higher pressure to achieve a phase separation. Since HEC is not soluble in CO_2, the relatively high polymer concentration in the bottom phase of exp. #5 might have reduced the CO_2-solubility, compared to exp. #1 and #2.

Distribution Coefficients

The distribution coefficients for each component are reported in Fi-ure 18 (The water distribution coefficient of exp. #1 could not be evaluated, because at that time no density meter was available for the top liquid phase). The lighter top phase was always rich in CO_2 and alcohol, whereas the water, salt and the polymer accumulated in the bottom phase. Comparing exp. #1 and #2 with exp. #5, an increased distance of the distribution coefficients from value 1 is notable, reflecting the increased dissimilarity of the two coexisting phases upon raising of pressure.

The distribution coefficient of the salt was higher than that of the polymer, which was crucial for our separation objective.

Separation of Salt and Polymer

The separation factor of the salt and the polymer was smaller for exp. #5 than that in the first two expperiments. It amounted to 4.9 for exp. #1, 9.1 for exp. #2 and 4.7 for exp. #5. The relatively high initial polymer concentration in exp. #5 did not seem to serve our separation purpose; by hampering the dissolution of the carbon dioxide, it delayed the phase separation to higher pressures.

As Table 3 shows, HEC could be purified in the experiments with isopropanol. The best separation results were obtained in exp. #2, at a phase-separation pressure of 65.2 atm.

2.2   The HEC (low-viscosity fraction) / Tertiary Butanol - System

Like isopropanol, tertiary butanol is, as the only C_4-alcohol, entirely miscible with water at room temperature and pressure. It has the same critical temperature as isopropanol (235°C). The phase separation temperature of polymer solutions can be related to the solvents critical temperature (see introduction).

The preparation of the polymer solutions with tertiary butanol as the co-solvent required at maximum 3-4 h, more than with isopropanol. Upon addition of tertiary butanol to the previously prepared aqueous polymer solution, some polymer reprecipitated and dissolved very slowly. Therefore, tertiary butanol was added dropwise from a burette into the continuously stirred solution, which resulted in a small loss of alcohol by evaporation. The solutions filled into the cell were clear.

Initial Concentrations

Figure 19 shows the initial concentrations. Sodium acetate is referred to as "salt". In exp. #7a,7b and #8a,8b,8c,8d respectively, the initial solutions were identical; samples were taken at different pressures.

Equilibrium Pressures and Volumes of the Two Liquid Phases

The volumes of the two liquid phases at equilibrium are reported in Figure 20. As in the experiments with isopropanol, the top phase was clear and much less viscous than the turbid bottom phase.

Not expecting phase separation pressures in the range of 6-12 atm, in the first experiment with tertiary butanol, #7a, the pressure was raised in steps too large to determine the lowest phase separation pressure for this initial composition. Therefore, experiment #6 was prepared with approximately the same initial composition as that of exp. #7, and the pressure was raised in smaller steps of less than 1 atm. (The difference between the initial alcohol concentration of exp. #6 and #7 was not desired and reflects the loss of alcohol during the preparation of the polymer solution, which could only be estimated roughly.)

In the experiments with tertiary butanol, the lowest equilibrium pressure, at which phase separation could be observed, was much lower than those with isopropanol.

With initial concentrations of 336 g/l tertiary butanol and 39.4 g/l HEC (exp. #6), the lowest observed pressure, at which a phase separation occurred, was 6.5 atm. In exp. #1, at initial concentrations of 308 g/l isopropanol and 38 g/l HEC, the corresponding pressure was almost ten times higher. Upon replacing isopropanol with tertiary butanol, we could make a major step forward in the applicability of the here proposed new purification process by reducing the necessary operation pressure by factor 10.

Although a lower initial concentration of tertiary butanol than that in exp. #6 and #7 would lead to higher phase separation pressures, it still seemed desirable, considering the advantage of a low alcohol content for industrial application. Therefore, the initial alcohol concentration of exp. #8 was relatively low.

Density of Equilibrated Phases

In Figure 21, the equilibrium density of the single-phase solution (before the phase split) and that of the two separated liquid phases is plotted versus pressure for exp. #8. Obviously, the phase split occured at an equilibrium pressure of ca. 20 atm. The density of the two phases parted increasingly with pressure, indicating that the composition of the phases become more dissimilar.

CO_2-Solubility in Both Liquid Phases

In Figure 22, the solubility of CO_2 in both liquid phases is compared with the solubility of CO_2 in water, at 40°C. In the bottom phase, the solubility was apparently the same as that in water. In the alcohol- and CO_2-rich top phase it was significantly larger.

For tertiary butanol, the necessary CO_2-concentration to achieve a phase separation was much lower than for isopropanol: 13 g/l CO_2 in both coexisting phases in exp. #6, whereas with isopropanol, the minimum CO_2-concentration for a phase split amounted to 73 g/l in the bottom phase and 97 g/l in the top phase (see Figure 17).

This difference in CO_2-solubility may indicate, that in the presence of CO_2 tertiary butanol is less compatible with water than isopropanol, although both alcohols are completely miscible with water.

Distribution Coefficients

The difference in composition of the two liquid phases is also reflected in Figure 23, where the distribution coefficients of all components are shown for exp. #6-8; the top phase was rich in alcohol and carbon dioxide, whereas the water, salt and polymer accumulated in the bottom phase. Both effects were enhanced by raising of pressure and CO_2-content. We presumed that, since CO_2 and the alcohol, as bad solvents for both HEC and sodium acetate, were accumulated in the top phase, they drove the polymer and the salt out of the top phase. The increasing dissimilarity of the two liquid phases upon raising of pressure was also observed in the experiments with isopropanol (see Figure 20), but that dissimilarity was much more significant in exp. #8 with tertiary butanol, considering the different ordinate scales of the diagrams in Figures 18 and 23.

The distribution coefficients in exp. #6 and #7, also reported in Figure 23, were relatively close to the value of 1 and did not exhibit the same distinct pressure dependence as in exp. #8c,d. This was not surprising, since the pressure was much lower than those in exp. #8c and d. The accumulation of water, salt and polymer in the bottom phase and that of carbon dioxide and alcohol in the top phase of exp. #6 and 7 were consistent with those observed in the other HEC experiments.

Separation of Salt and Polymer

The separation factor is shown in Figure 24. Because the initial alcohol concentrations in exp. #6 and #7 were significantly different from that in exp. #8, the separation factors of these two different series of experiments are shown in different symbols.

The value of the separation factor of 3.4 to 4, reproduced four times (exp. #6,7a,7b,8a), supported our purification objective. The maximum value of 6.8 at 40 atm (exp. #8c) was probably not significant; at 40 atm, both the salt and the polymer distribution coefficient were very low and small absolute errors in the concentration measurements caused a large effect on the ratios which defined the distribution coefficients and the separation factor.

As notable in Figure 23, the values of the salt and the polymer distribution coefficient became increasingly alike with increasing pressure, thus resulting in the lowest separation factor at the highest pressure of 63 atm in exp. #8d. Therefore, we considered pressures of around 60 atm unfavorable for our purification objective.

In exp. #7b and #8a, at approximately the same equilibrium pressures, the separation factors were about the same, although the initial alcohol concentrations were different (see Figure 19, pg. 36). This indicated that the separation of the salt and the polymer was not very sensitive to changes of initial alcohol content.

The results for the salt removal, as shown in Table 4, supported our purification objective. More polymer was "lost" in the top phase than in the experiments with isopropanol (see Table 3, page 34); but the phase separation pressure was much lower.

Considering the cost-factors pressure, polymer-loss and salt removal efficiency, exp. #7a seemed to give the most favorable results for our devised purification process.

The salt removal effectivity in exp. #8b and #8c was worse than that in exp. #8a and therefore, in Table 4, no quantitative results are shown for these two experiments.

Secondary Butanol

In the presence of CO_2, tertiary butanol is much less compatible with water than isopropanol. Thus, the phase separation pressure of an aqueous-organic polymer solution is very sensitive to little changes in the chemical nature of the organic co-solvent (the chemical structure of tertiary butanol is similar to that of isopropanol, see Figure 25).

We presumed that the "increased organic nature" (meaning the increased dissimilarity to water) of tertiary butanol, which, as a C_4-alcohol, has one methyl group more than isopropanol, turned the scale to lower phase separation pressures.

Therefore, secondary butanol, another C_4-alcohol with a structure similar to isopropanol, was selected as the organic co-solvent for the next experiment. Secondary butanol is "more organic" than tertiary butanol in that, unlike tertiary butanol, it is not completely miscible in water. Water dissolves a maximum of 15wt-% secondary butanol at room temperature and pressure. In a solution with 130 g/l secondary butanol in water, 25 g/l HEC was the highest polymer concentration which could be achieved. In the preceding experiments

with isopropanol and tertiary butanol, the initial alcohol and polymer concentrations were much higher.

A phase separation was observed at 50 atm. Though the top phase volume amounted to only 5 ml, fortunately, the inlet of the top recirculation line was covered completely, and both phases were sampled and analyzed. The distribution coefficients of the salt and the polymer were very close; and therefore the separation factor, with a value of 1.3, much lower than in any previous experiment. For that reason, no other experiments were conducted with secondary butanol. As for all other experiments, the analytical results for this experiment (#9) are reported in detail in the appendix.

Both the lower maximum alcohol concentration in an aqueous solution and the slightly higher critical temperature of secondary butanol (265°C), compared to that of tertiary butanol (235°C), probably caused the relatively higher phase separation pressure in the experiment with secondary butanol.

2.3 The Systems HEC (high-viscosity fraction) / Isopropanol and HEC (high-viscosity fraction) / Tertiary Butanol

The HEC of the high-viscosity fraction was more difficult to handle than the low-viscosity fraction: The solubility of the high-viscosity fraction in the water-alcohol mixtures was much lower and the polymer dissolved more slowly. The initial polymer solutions, containing between 7 and 17 g/l polymer of the high-viscosity fraction, were extremely viscous. If stirred too long, the solutions formed a stiff paste.

No liquid-liquid phase separation could be observed. Instead, upon application of CO_2-pressure, the polymer precipitated. Since the equilibrium cell did not feature mechanical stirring devices, the solid polymer sedimented to the bottom and formed a stiff, rugged aggregate firmly attached to the walls of the cell, occupying one quarter to one third of the cell volume. The large polymer molecules were probably entangled in a network and lost their ability to float in the liquid, enclosing large quantities of the liquid cell contents. Bubbles of liquid phase were conspicuously caught in the precipitated polymer network.

The liquid phase could still be recirculated through both recirculation lines and was sampled. After the pressure was released and the liquid phase removed from the cell, the polymer aggregate remaining in the chamber almost completely resisted to dissolve in

pure water. Numerous rinsing cycles, in one case stretched over 3 days, were required to remove all solid polymer.

Since part of the liquid was enclosed in the polymer network of the precipitated aggregate, the hydrodynamic mixing of the cell contents was severly hampered; even after 2 or 3 days of recirculating the liquid phase, the density was not as stable over a long period of time as in the experiments with the low-viscosity fraction of HEC. Therefore, equilibrium was most probably not obtained when the liquid phase was sampled, and the analytical results, reported in detail in the appendix, have to be considered with caution. The salt content of the precipitated polymer was not determined.

In two experiments with isopropanol, HEC precipitated at 77 and 78 atm, respectively. The corresponding initial concentrations were 16.8 g/l HEC, 358 g/l isopropanol (exp. #10) and 13.6 g/l HEC, 268 g/l isopropanol (exp. #10*), respectively. With an initial concentration of 7.7 g/l HEC and 354 g/l tertiary butanol (exp. #11), the polymer precipitated at 6.6 atm.

Precipitation of the polymer upon application of CO_2-pressure does not serve our objective of a new liquid-liquid extraction process. The advantage of working with a solution would be lost.

Also, the precipitated polymer seemed to dissolve more slowly in water than the original polymer used for the initial solution and formed stiff networks under CO_2-pressure, presumably indicating an undesirable property change of the HEC.

3. Experiments with Xanthan Gum

Aqueous Solutions of xanthan gum were much more viscous than solutions of HEC at the same polymer concentrations; xanthan gum dissolved more slowly than HEC and had a lower solubility in water. The preparation of a 1.4wt-% aqueous xanthan gum solution required about 4 h of mixing with our electrically propelled stirrer. 1.4wt-% is the concentration of xanthan gum in the aqueous medium after completion of the fermentation. The fermentation broth also contains 0.5wt-% dipotassium phosphate as a buffer (see introduction). In exp. #13,#15 and #16, the initial aqueous polymer solution (before adding the alcohol) resembled, in polymer and salt concentration, the final fermentation medium after filtration of the bacteria debris. (The fermentation process requires the presence of other salts, but in very small concentrations: 0.06 wt-% ammonium nitrate, which is most

probably consumed by the bacteria, and 0.01 wt-% magnesium sulfate.)

Initial Compositions of Polymer Solutions

Figure 26 gives the initial concentrations of all experiments with xanthan gum solutions. Dipotassium phosphate is referred to as "salt". All solutions were slightly cloudy, due to remnants of bacteria debris. In exp. #12 neither liquid-liquid phase separation nor polymer pre-cipitaion was observed at equilibrium at 77.3 atm.

In exp. #13, with isopropanol as the co-solvent, xanthan gum precipitated at 76.4 atm and formed flakes of aggregated polymer molecules, which slowly sedimented to the bottom. After reducing the pressure to about 3 atm, the sediment did not adhere to the cell walls and was easily removed from the chamber. Although, before sampling, the density was stable over a long period of time, the precipitated polymer surely hampered the mixing and equilibrating of the cell content.

Therefore, the analytical results for this experi-ment, in detail reported in the appendix, should be viewed with caution. According to the analysis of the liquid phase, three quarters of the overall amount of polymer in the initial solution precipitated out of solution and merely all of the salt remained in solution. After releasing the cell pressure and removing of the cell content, separation of the precipitated polymer from the liquid phase by filtering with a fritted funnel and a laboratory vacuum pump was not possible; the filter frit was plugged by the swollen polymer. The precipitated xanthan gum had absorbed much of the liquid phase during the release of pressure. The precipitation of the polymer in exp. #13 does not serve the purpose of separating the polymer from the salt.

Volumes of the Two Liquid Phases

As seen in Figure 26, the initial alcohol concentration was decreased for the experiments following exp. #13 to prevent precipitation of the polymer.

In the experiments with tertiary butanol, #14,#15 and #16, a liquid-liquid phase separation was achieved. Figure 27 gives the equilibrium volumes, pressures and temperatures for these experi-ments. In exp. #14, at a pressure of 36.6 atm, about 80% of the polymer precipitated and sedimented to the bottom of the cell, while

the rest of the polymer remained in solution in the bottom phase. No polymer could be detected in the top phase. In the exp. #15, the mass balance of xanthan gum indicated that a small amount of polymer may have precipitated. The bottom phase was very turbid; no solid polymer could be observed. In this experiment, samples were taken at three different pressures. The lowest phase separation pressure observed was 44.1 atm.

In exp. #16a, the top phase was very small and did not cover the inlet of the top recirculation line. The top phase could not be sampled and analyzed. As substantiated in the section "Experimental Procedure", an indirect calculation of the top phase composition through a mass balance was too inaccurate to be useful. A minimal initial concentration of tertiary butanol of about 250 g/l proved to be necessary to obtain a sufficient top phase volume to be sampled.

In exp. #16b and c, the temperature inside the cell was raised to 50 and 60°C, respectively, to study, very qualitatively, the influence of the temperature on the volume of the phases (all other experiments in this work were conducted at 40°C).
No additional carbon dioxide was added to the already present amount from exp. #16a. Compared to that in exp. #16a, the top phase volume in exp. #16b and c was slightly smaller. The pressure was higher due to the increased temperatures. Sampling of the top phase was not possible. The analysis of the bottom phases indicated no significant changes in the composition of the liquid phases in exp. #16a,b and c.

CO_2-Solubility in the Two Liquid Phases

In Figure 28, the solubility of CO_2 in both liquid phases of exp. #14 and #15 is compared to that of pure water at 40°C. As in the experiments with HEC and tertiary butanol, the CO_2-solubility in the bottom phase was relatively small and close to that of water, whereas, in the top phase, the CO_2-concentration rose sharply with the increasing pressure.

In exp. #8 (HEC, low-viscosity fraction), with an initial tertiary butanol concentration of 280 g/l, the minimum concentration of CO_2 to induce a phase separation was 26 g/l in the bottom and 31 g/l in the top phase, at 20.7 atm. In exp. #14 (xanthan gum), with a higher initial concentration of tertiary butanol (322 g/l), the corresponding CO_2-concentration to achieve a phase separation was much higher and amounted to 40 g/l in the bottom phase and 68 g/l in the top phase, at 36.6 atm. These two experiments are compared here

because both initial polymer solutions had a similar apparent viscosity (but different initial polymer concentrations).

Distribution Coefficients

The distribution coefficients for exp. #14 and 15 are reported in Figure 29. As observed in the HEC experiments, the distribution coefficients of the CO_2 and the alcohol increased with higher pressure; both components accumulate in the top phase. The bottom phase was rich in salt and water. Unlike in the HEC experiments, accumulation of water and salt in the bottom phase *with increasing pressure* was hardly recognizable, especially for the salt.

Since the analytical results for xanthan gum concentrations were affected with a very large error margin, the reported distribution coefficients for this polymer have to be valued with caution. Unlike in the HEC experiments, the polymer distribution coefficient in exp. #15a and c was larger than the corresponding salt distribution coefficient.

The difference between these two distribution coefficients was large enough to support this statement, despite the inaccuracy of the analytical results for xanthan gum concentrations.

It seemed that xanthan gum distributed more evenly among the two liquid phases when the pressure was raised.

Separation of Salt and Polymer

Since the distribution coefficient of the polymer seemed to be larger than that of the salt, in the application of a CO_2-induced phase separation for a xanthan gum purification process, the salt would have to be extracted through removal of the *bottom* liquid phase from the equilibrated system. (In the previous HEC experiments, the salt distribution coefficient was larger than that of the polymer, and therefore the salt would have to be extracted through removal of the *top* phase from the system.)

The separation factor, here defined as the inverse of that for the HEC systems, amounted to 3.5 for exp. #15a and 5.7 for exp. #15c. If there was some precipitated polymer in the bottom phase, the separation factors would be lower.

The results of the quantitaive evaluation for the salt removal were unfavorable for a possible purification process. Most of the polymer would be lost if the salt would be removed from the system through the bottom phase.

V.OUTLINE FOR A MOLECULAR-THERMODYNAMIC MODEL FOR AQUEOUS POLYMER/SALT/CO_2/SOLVENT EQUILIBRIA

1 Introduction

To guide future experiments and to aid process design, it is useful to carry out isothermal-isobaric flash calculations on the five-component, three-phase systems experimentally studied here. We chose for particular attention the water-isopropanol-CO_2-HEC-potassium sulfate system at 40 °C. This model, developed in parallel with the experimental study, may help to explore the multi-variable phase diagram of our system. Using flash calculations simultaneously with experimental runs, we can then attempt to optimize the separation under given constraints. Furthermore, the development of a model helps to reach a better understanding of the fundamental phenomena governing the distribution of the components between the two phases.

Supercritical CO_2 has been extensively studied as a solvent for extraction of natural aromas. But the liquid-liquid phase equilibria induced by supercritical CO_2 in a mixture of water and an organic compound offer also a wide range of applications. Elgin and Weinstock (18) were the first to investigate ternary systems of water, supercritical ethylene and a water-soluble organic liquid, and to propose possible applications for the separation of organic from water.

The use of supercritical solvents for the energy-efficient recovery of alcohols from aqueous solutions has recently been proposed by several investigators. Paulaitis et al. (21) and Mc Hugh et al. (16) examined the recovery of ethanol with carbon dioxide, ethylene and ethane. Kuk and Montagna (14) presented results for the recovery of ethanol and isopropanol using supercritical carbon dioxide.

According to Elgin and Weinstock, ternary systems containing a supercritical gas and two relatively non-volatile liquids can exhibit three types of behaviors (figure 25). Type-1 behavior is typical of systems with a solute which has a strong affinity for water, such as ethanol. As pressure increases, the miscibility gap between the supercritical fluid and the solute narrows until they form a single

phase. Type-2 behavior is followed by systems that have a lesser tendency to form hydrogen bonds, but still have active hydrogen atoms and donor atoms in their structure. For a range of pressures, the supercritical fluid induces an immiscibility between water and the solute. This "salting-out" phenomena can be used as a basis for the extraction of the solute from water. Systems where a solute-water immiscibility exists even when no supercritical solvent is present, exhibit type-3 behavior. As pressure rises, the miscibility gaps for both the water-solute and the solute-fluid binaries close up. Depending on the temperature, a given system can shift from one type of behavior to another. It can also show a more complex behavior like the appearance of four-phase equilibrium regions.

The water-isopropanol-CO_2 system has been studied by Paulaitis et al. (19) and Radosz (22). This system shows type-3 behavior at 40°C and at pressures ranging from 95 to 140 atm (figure 26) , but can also exhibit four-phase equilibria .

To calculate the thermodynamic functions necessary to compute the equilibrium phase compositions of our system, we require a molecular-thermodynamic model. Cubic equations of state or Helmholtz (or Gibbs) excess energy models can possibly be used for flash calculations. However, conventional excess-Gibbs-energy models, since they use different reference states and parameters for the two phases, are not useful for systems at pressures near the critical pressure of one of the major components of the mixture. A cubic equation of state was succesfully used by Panagiotopoulos to represent a variety of systems containing water, supercritical CO_2 and an organic compound (23). However this approach is not immediately useful for systems containing electrolytes. The model proposed by A. Harvey and J.M Prausnitz (24), originally developed for aqueous systems with dissolved hydrocarbons and electrolytes, is suitable for our purposes. We use it here to represent interactions between water, alcohol, CO_2 and salt.

To account for the effect of the polymer on the chemical potentials of the components, we use a perturbation model which combines an osmotic expansion and Pitzer's equations.

We discuss the methods used to estimate the parameters of the model. Some significant parameters could, however, not be determined experimentally as planned. These parameters had to be adjusted through flash calculations to an experimental phase-

equilibrium point before the program could give realistic results. It is possible then to explore the region surrounding this point, by extrapolating it with respect to the variables of the separation (pressure, alcohol-to-water ratio, salt content, polymer content).

2 Computational Framework

Figure 27 shows the structure of the equilibrium system whose compositions we wish to calculate. The gas phase (v) contains mainly near-critical CO_2 with unknown concentrations of isopropanol and water. The composition of this phase has not been measured. The alcohol-rich liquid phase (α) consist of 50 to 60%w water, 30%w isopropanol, 9%w CO_2, less than 1%w HEC and about 0.3%w salt. The polymer-rich phase (β) contains about 60 %w water, 25 %w isopropanol, 5 to 10%w HEC , 5 to 10%w CO_2 and less than 5%w salt. Both phases are rich in water. The pressure is in the range 30 to 75 atm and the temperature is fixed at 40°C.

To solve the five-component, three-phase equilibrium, the following equations have to be solved :

At given T and P :

$$\Phi_i^v \, y_i = \Phi_i^\alpha \, x_i^\alpha = \Phi_i^\beta \, x_i^\beta \tag{1}$$

where Φ_i is the fugacity coefficient of component (i) and x_i^α, x_i^β, y_i, z_i are the mole fractions of component (i) in the top-liquid phase (α), the bottom-liquid phase (β), the vapor phase (v) and the feed, respectively.

Conservation of mass gives :

$$a x_i^{\alpha} + b x_i^{\beta} + (1-a-b) y_i = z_i \qquad \text{for } i=1 \text{ to } 5 \qquad (2)$$

where a and b are the volume ratios of the top(α) and bottom(β) liquid phases to the total volume. Note that z_{CO_2} is an unknown since only the CO_2 pressure is fixed in the cell. The constraints on the mole fractions give:

$$\sum_{i=1}^{5} x_i^{\alpha} = \sum_{i=1}^{5} x_i^{\beta} = \sum_{i=1}^{5} y_i^{v} = 1 \qquad (3)$$

The system has 18 unknows (5*3 mole fractions, the two volume ratios a and b, and the CO_2 feed mole fraction) and 18 independent equations (10 phase-equilibrium equations, five mass-balance equations, and three constraints on the molde fractions); it is therefore fully defermined. The molecular-thermodynamic model has to provide the fugacities as functions of density, temperature and mole fractions. However, our system is far too complex to be described by the common models available. Therefore, we have to make simplifying assumptions. The choice of these assumptions has much influence on the performance of the final model. Our assumptions are determined by the experimental results and by the empirical understanding of the phenomena involved.

1- Using the experimental fact that the polymer almost entirely remains in the bottom liquid phase, we assume that no polymer is present in the top phase.
2- We assume that the interactions between water, isopropanol, CO_2 and salt due to the presence of the polymer in the bottom phase (β) can be accounted for through a linear perturbation model.
3- Finally, we assume the gas phase to be pure CO_2.

The system of equations which are to be solved is now :

$$\Phi_i^{\alpha} x_i^{\alpha} = \Phi_i^{\beta} x_i^{\beta} \qquad \text{for water, isopropanol and salt} \qquad (4)$$

$$\Phi_{CO_2}^{v} y_{CO_2} = \Phi_{CO_2}^{\alpha} x_{CO_2}^{\alpha} = \Phi_{CO_2}^{\beta} x_{CO_2}^{\beta} \qquad (5)$$

where the left-hand term is known as an input,

the mass balance equations:

$$(1-a)x_i^\alpha + a x_i^\beta = z_i \qquad (6)$$

where a is the volumetric ratio of the bottom-liquid phase to the total liquid volume, and :

$$\sum_{i=1}^{5} x_i^\alpha = \sum_{i=1}^{5} x_i^\beta = 1 \qquad (7)$$

The problem has been reduced to a liquid-liquid equilibrium calculation where the fugacity of one component is fixed (CO_2) in phase v, α, and β, but its feed mole fraction is not known. This system can be solved using a first-order algorithm described by King (25). By making these assumptions, we redefine the requirements as follows :

- We need a liquid-solution model or an equation of state able to represent the liquid-liquid water-isopropanol-CO_2-salt equilibrium at high pressures. For a predictive model, the parameters need to be determined à priori. We aim to calculate the partitioning of the salt between the two liquid phases; therefore we require good estimations of the dielectric properties of the two liquid phases. A. Harvey's model has been chosen.

- We need to develop a perturbation model which describes the effect of the polymer on the activities of the other components in our liquid solution. The parameters used in the perturbation must be experimentally accessible.

3 Calculation of the Fugacities

The fugacities of the components are calculated in a framework consistent with the assumptions above to solve equations (4) and (5). Since the polymer concentration is neglectible in the alcohol-rich phase (α), Harvey's model can be used to express the fugacities of the components in this phase. For the polymer-rich phase (β), Harvey's model is extended to our mixture through a perturbation term.

1. Alcohol-Rich Phase (α)

The fugacity coefficients of the components are calculated from:

$$RT \ln(\phi_i^{\alpha}) = \left(\frac{\delta A^r}{\delta n_i^{\alpha}} \right)_{T,V,n_i^{\alpha}} + RT \ln \left(\frac{P}{rRT} \right) \tag{8}$$

where the residual Helmholtz energy A^r is relative to the Helmholtz energy of the uncharged ideal gas at the same temperature, density and composition. A^r is given by the sum of three contributions :

$$A^r = A^I + A^{II} + A^{III} \tag{9}$$

Following Harvey, A^I is the contribution arising from all short-range intermolecular forces other than those due to the permanent electric charges of the ions; it is calculated with the Lennard-Jones potential.

$$u_{ii}(r) = 4 \, \varepsilon_{ii} \left[\left(\frac{\sigma_{ii}}{r} \right)^{12} - \left(\frac{\sigma_{ii}}{r} \right)^{6} \right] \tag{10}$$

For uncharged species, $\varepsilon_{ii}(T)$ and σ_{ii} are obtained from experimental pure-component data. Adjustable binary parameters k_{ij} and k_{ji} are introduced in the combining rule for the attractive-energy parameter ε_{ij} for interactions between unlike molecules:

$$\varepsilon_{ij} = \left(\varepsilon_i \varepsilon_{jj}\right)^{1/2} \left[1 - k_{ij} + \left(k_{ij} - k_{ji}\right)\frac{x_i}{x_i + x_j}\right]$$

(11)

Values for k_{ij} are fitted to binary vapor-liquid equilibrium data.

A^{II} is the contribution from charging the ions and A^{III} accounts for charge-charge interactions. Both terms require the dielectric constant of the fluid mixture as a function of temperature, density and composition. For this calculation, a systematic procedure is used (26), where the only information required is a size parameter for each species.

The ion-charging contribution is calculated considering the ions as charged hard spheres interacting in a continuum of given dielectric constant (primitive model). The reversible work required to charge an ion in solution can thus be established (25).

The charge-charge interactions are also modeled with the primitive model for the ions. A reasonable solution for the thermodynamic properties of this model is obtained using the Mean Spherical Approximation (26). The iterative procedure necessary has however, been reduced to a simple calculation by assuming that every ion has the same single diameter σ_{mix} :

$$\sigma_{mix} = \frac{\displaystyle\sum_{ions} x_i \sigma_{ii}}{\displaystyle\sum_{ions} \sigma_{ii}}$$

(12)

2. Polymer-Rich Phase (α) Fugacities

We consider a system containing water, isopropanol, CO_2 and potassium sulfate with the same molalities as in the phase to be represented. The chemical potential of a component (i) of this mixture (*) can be calculated using Harvey's model :

$$\mu_i^* (T,P,x_i^*) - \mu_i^o (T,P^o,x_i=1) = RT \left[\ln (\phi_i^*) + \ln \left(\frac{x_i^* P}{f_i^o} \right) \right]$$

(13)

where f_i^o is the fugacity of the pure component at the pressure of reference P^o. The chemical potential of any component (i) in the real mixture can then be divided into two contributions and related to the fugacity of this component :

$$\mu_i^\beta (T,P,x_i^\beta) - \mu_i^* (T,P,x_i^*) + \mu_i^* (T,P,x_i^*) - \mu_i^o (T,P^o,x_i=1) = RT \left[\ln (\phi_i^\beta) + \ln \left(\frac{x_i^\beta P}{f^o} \right) \right]$$

(14)

Combining equations (10) and (11) we obtain an expression for the fugacity coefficient of component (i) in phase (β) :

$$RT \ln (\phi_i^\beta) = \mu_i^\beta (T,P,x_i^\beta) - \mu_i^* (T,P,x_i^*) + \left[\ln (\phi_i^*) + \ln \left(\frac{x_i^*}{x_i^\beta P} \right) \right]$$

(15)

We then assume that the difference of the chemical potential of component (i) in the hypothetical mixture (*) and that in the real mixture has the form :

For the non-ionic solutes :

$$\mu_i^\beta(T,P,x_i^\beta) - \mu_i^*(T,P,x_i^*) = RT \, m_4^\beta \, a_{i4}$$

(16)

where the indices are chosen as follows :

(1)　　water
(2)　　isopropanol
(3)　　CO_2
(4)　　HEC
(5)　　potassium sulfate

m^β_4 designates the molality of the polymer in phase (β) and a_{i4} is a parameter linearly related to the osmotic second virial coefficient characterizing the interaction of the polymer with component i in water. This osmotic expansion formulation has been inspired by studies on mixtures of proteins (27,28).

For the ionic solutes we apply Pitzer's equations (29) to our system :

$$\mu_i^\beta(T,P,x_i^\beta) - \mu_i^*(T,P,x_i^*) = RT\left(2\Delta_{45}m_4^\beta + 3\,m_4^{\beta^2}\Gamma_{445} + 6(\nu_+\nu_-)m_4^\beta\, m_5^\beta\,\Gamma_{455}\right)$$

$$(17)$$

where Δ_{45}, Γ_{445} and Γ_{455} are Pitzer's polymer-salt interaction parameters in water.

The chemical potential change for water is derived from equations (14) and (15) using the Gibbs-Duhem equation . We obtain :

$$\mu_i^\beta(T,P,x_1^\beta) - \mu_i^*(T,P,x_1^*) = -M_1RT\left(m_4^\beta + a_{24}m_2^\beta m_4^\beta + a_{34}m_3^\beta m_4^\beta + \Delta_{445}m_4^{\beta^2} + \right.$$

$$\left. 6\,m_5^\beta\, m_4^{\beta^2}\,\Gamma_{445} + 3(\nu_+\nu_-)m_5^{\beta^2}\, m_4^\beta\,\Gamma_{455}\right)$$

$$(18)$$

4 Dielectric Constant

Since we want to describe a system where ions are distributed between the two liquid-phases, it is essential to estimate the dielectric properties of these two phases. The dielectric constant of phase (α) (no polymer) is calculated with the procedure proposed by Harvey (24). In the polymer rich-phase, the presence of the polymer is likely to decrease the dielectric constant of the bottom-phase, thus making it more similar to the one of the top phase. This effect is taken into account through a volumetric mixing rule of the mean polarization of the solution (P_{mix}), considering the mixing between a solution of the same molality than the phase (β) but wherefrom the polymer is absent and the pure polymer.

$$P_{mix} = \left(1 - \frac{V_{pol}}{V_{tot}}\right) P_{sol} + \left(\frac{V_{pol}}{V_{tot}}\right) P_{pol} \tag{19}$$

where Vtot and Vhec are the total volume and the volume occupied by the polymer respectively. The dielectric constant of the reference solution is calculated using Harvey's procedure.
The dielectric constant D and the mean polarizations are related through :

$$P = \frac{(D-1)(2D+1)}{9D} \tag{20}$$

The dielectric constant of the polymer is set equal to 2 .

5 Determination of the Parameters

Table 1 gives the interaction parameters which need to be estimated before running the flash calculations. They are restricted to 2-body interactions parameters, except the higher order terms in Pitzer's equations.

Table 1 : Estimation of the parameters between species i and j

i\j	water	alcohol	CO2	HEC	salt
water	sat.	VLE	VLE	LS	osm.
alcohol	VLE	sat.	VLE	LS *	-
CO2	VLE	VLE	sat	-	setch.
HEC	/	LS *	-	LS	LS *
salt	osm.	-	setch.	LS *	/

sat. :   Pure component saturated liquid and vapor densities
VLE :   Vapor-liquid equilibrium data
osm. :   Binary osmotic data
setch. :   Setchenov constant
LS :   Light-scattering measurements

* indicates that the parameter could have theoretically been determined with this method, but was not estimated with sufficient accuracy.

The parameters determined via light scattering as well as the parameter derived from the Setchenov constant and the osmotic data stand for solute-solute interactions in water.

5.1 Pure Component Parameters

The water Lennard-Jones parameters were fitted to data taken by Raatschen (32) . The CO_2 data used were from the IUPAC tables (30). The results show an average agreement between the calculated and experimental densities of 0.2 % for water and for CO_2. For isopropanol however, the deviations are higher; they reach 2% for the liquid phase, 10% for the vapor phase. Even when other sets of data are used, the calculated data still show a systematic underprediction of the density of the vapor phase.

5.2 Binary Parameters.

Despite the poor representation of the pure isopropanol densities by the EOS, the properties of the water-isopropanol (36) and CO_2-isopropanol (32) binaries can be very well fitted with the two binary parameters $k_{ij}(T)$ and $k_{ji}(T)$. These are assumed to be linearly dependent on temperature. The liquid-vapor equilibrium data of the water-CO_2 binary (33,34) were adjusted with less than 0.5 % discrepancies, as well as the osmotic data of aqueous potassium sulfate (35).

Salt-isopropanol parameters could have been adjusted from saturation pressure data for the isopropanol-potassium sulfate system. No data were found however for this system. Similar systems have been investigated by Sada and Morisue (36), and their data provide a possible rough estimation of these parameters which prove to play an key role in the partitioning of the salt between the two liquid phases.

5.3   Interaction Parameters Involving the   Polymer.

5.3.1   Theory

Two methods were available to estimate the polymer-polymer, polymer-salt, polymer-alcohol interactions: osmometric measurements and light scattering. Both have been attempted, with limited success, however. Osmometric measurements were carried out on a Knauer Membrane Osmometer with cellulose-acetate membranes. The measurements failed because of the tendency of the cellulose derivative polymer to adsorb on the membrane, thus creating a very high pressure drop accross the membrane. It seems to be possible however to conduct these measurements in the presence of salt, as further measurements have shown later.

The light-scattering measurements theoretically provide a way to evaluate the second and third osmotic virial coefficients for a macromolecule in water. For a solution of the polymer in water, the difference between the intensity of the light scattered by the solution and the one scattered by the solvent, or Rayleigh factor (R_θ) can be related, assuming a dilute solution, to the dependence of the chemical potential of the polymer on the concentration. The following expression is derived (37) :

$$\frac{K c}{R_\theta} = \frac{1}{M} + 2 A_2 c + 3 A_3 c^2 + \dots$$

(21)

where K is the optical constant determined experimentally through refractive-index measurements of solutions of different concentrations, c is the concentration, M the molecular weight of the macromolecule and A_2 and A_3 are the second and third osmotic virial coefficients, respectively.

5.3.2 Experimental Results

The equipment used is a multiangle spectrometer from Brookhaven Instruments Corporation, using a BI-200SM goniometer and BI-correlator.

The samples have to be prepared so that no dust is enclosed in the aqueous solutions. The sample tubes are washed with water in a sonicator, washed with hot isopropanol dried and closes with plastic caps. A Barnsted ultrapure-water system provides nanopure water. The polymer is first dissolved in water and the solutions are introduced into the sample tubes trough a Millipore GV 0.2 nm filter unit with a 2.5-cc syringe without removing the tube cap. This procedure provides a way to minimize the introduction of dust particles into the samples.

The HEC supplied by Union Carbide contains about 5%w sodium acetate. The complete removal of the salt by rinsing the solid polymer with solutions of acetone of water proved not to be efficient enough to separate all the salt from the polymer. We could, however, obtain three samples of 2 %w, 5 %w and 10%w sodium acetate. The scattering of these three solutions could give us, by extrapolation at 0%w salt, a reasonnable estimate of the polymer molecular weight and of the polymer-polymer interaction coefficient in water, a_{44} (Figure 28).

The data taken at different angles and increasing concentrations between 0.25 g/l and 5g/l were analysed by a Zimm Plot Analysis software provided by Brookhaven Intruments Corporation. The data were treated by the least square analysis method and extrapolated to zero angle and zero concentration to give the desired properties. We obtained for the HEC studied :

$$Mw = 70000 \ g/mol$$

$$a_{44} = 12731 \ kg/mol$$

For the mixed-solvent systems, the presence of the sodium acetate salt in the polymer required that the data be corrected by substracting the sodium acetate-polymer interaction contribution to the excess scattered light. The non-corrected results obtained are

presented in figures 28, 29 and 30. To obtain the polymer-solute interaction coefficients in water, we need to substract as well the scattered intensity due to the polymer-polymer interactions in water from the scattered intensity of the mixed solvent system. As shown on Figures 31 and 32, the deviations between points from a system are bigger than the differences between two systems. Therefore, we could not use these data.

From the data, we can however, conclude that the potassium sulfate tends to increase the chemical potential of the polymer in solution, while the isopropanol has the opposite influence. These effects have been observed for a range of concentrations lower than that in our real system, while the weight ratios between the solutes have been kept as close as possible to those in the real system.

5.4 Conclusion

Some required parameters were evaluated with satisfactory precision. Some significant parameters, however, remain unknown : the isopropanol-salt k_{ij} parameters, the polymer-salt, and polymer-isopropanol. In addition, the molar volume of the polymer used in the mixing rule for the calculation of the dielectric constant in the polymer-rich phase is also unknown. The composition of the vapor phase which has to be specified for each calculation can also be considered as a parameter in the calculation.

6 Computation of the Phase Compositions

The computer code used as a basis for the flash calculation is the one proposed by Harvey (24). The method used was developed by Topliss (39). A few modifications have been made to adapt the calculation to our problem. Since the perturbation model introduced here is treating the salt as one species, we now solve the flash equations considering the potassium sulfate as one component, instead of two ions as in the former formulation. The CO_2 feed composition in our system is an unknown. It is reevaluated during the iteration procedure through a mass balance taking into account the known fugacity of CO_2 in the gas phase.

For the real system, about 100 iterations are needed to reach a convergence of the phase-equilibrium and mass-balance equations with a threshold of 10^{-5}. This takes less than one minute real time on an IBM 3090.

7 Results

7.1 Computation of the Water-Isopropanol-CO_2 Vapor-Liquid Equilibrium Phase Diagram

The tie-lines for the water-isopropanol-CO_2 system were calculated in the L-V region at 102 bars and 60 °C (Figures 33 and 34). Since the binary parameters have been adjusted from LV data, it is no surprise to obtain agreement with the experimental data only in the low-isopropanol concentration range. In the two phases of our real system, the water mole fraction is always greater than 0.8, therefore these calculations can be considered satisfactory enough for our purposes.

7.2 Prediction of the Appearance of the Second Liquid Phase in the Water-Isopropanol-CO_2 system

It is possible to predict the appearance of the second liquid phase in the water-isopropanol-CO_2 system by raising the pressure at a given feed composition. The iterative procedure used to solve the set of equations calls a subroutine to calculate the density. When liquid and vapor densities are simultaneously roots of the density equation, the liquid density is the one which is chosen. As a result, when the pressure increases so that the system enters the L-L region of the phase diagram, the flash calculations show a discontinuity in the density of the second phase (Figure 35).

This procedure was repeated for two different isopropanol-to-water ratios (Figure 36). As this ratio rises the pressure at which the second phase appears is lowered. The boundary between the liquid region and the liquid-liquid region could also be detected close the the L-L-V curve.

7.3 Water-Isopropanol-CO_2-HEC Liquid-Liquid Equilibrium at 40 °C.

When 5 to 10%w HEC is added to a feed mixture containing water, isopropanol and CO_2 in proportions similar to the ones of our real system, the pressure necessary to observe a phase split is very much lowered. Hydrogen bonds form between the HEC molecule and

the water; less water is therefore available for the alcohol which becomes less soluble. The amount of water linked to the polymer is about 10% of the total number of water molecules of a 10%w HEC-water solution. The sharp increase in the viscosity of the solution when the HEC is added suggest that the interactions between the chains are strong. The thermodynamic environment created by the presence of the HEC chains is significantly different from that of the former isopropanol-water-CO_2 solution. Although in our experimental conditions, the solubility of CO_2 in water is not affected by the presence of the polymer, no CO_2 solubility measurements have been made in the water-isopropanol-HEC system.

Some computations of the liquid-phases compositions for the salt-free system confirm a number of intuitive qualitative effects of the experimental variables. An increase in the pressure enhance slightly the solubility of the CO_2 in the polymer-phase; more isopropanol is driven out this phase creating, therefore, a larger alcohol-rich phase. No quantitative predictions could however be obtained since two very significant parameters remain unknown: the polymer-alcohol and the polymer-CO_2 interaction parameters.

An increase of the isopropanol-to-water ratio has a similar effect on the solubility of the CO_2 and on the volume of the two phases.

The polymer-alcohol and polymer-CO_2 parameters have a strong influence on the structure of the two phases. However, for very different sets of the previous parameters, only two types of phase diagram were obtained for a fixed proportion of the two phase volumes chosen so that $\alpha = 0.7$:

- If the water content of the alcohol-rich phase is high (about 50%w) , then the isopropanol content of both phases is relatively low (about 23 and 35 %w) and the solubilities of the CO_2 in the two liquid phases is low (3.5 %w in the water-polymer phase and 12 % in the alcohol rich phase),

- if the water content of the alcohol-rich phase is low (43%w), the isopropanol content of both phases is higher (about 30 and 40%w) as are the carbon dioxide solubilities in both phases (4%w and 15%w).

7.4 Water-Isopropanol-CO_2-HEC-Potassium Sulfate System.

We try to reproduce an experimental point with the following characteristics:

Table 2 : Composition of the system in weight percent

80.2 atm 40°C	water	alcohol	CO_2	HEC	salt
feed	52	35.8	7.5*	11	0.3
top	41.2	47.2	10.7	0.7	0.27
bottom	56	29.3	6.0	8.2	0.31

* The CO2 feed composition has been estimated through a mass balance.

Volume ratio of the two liquid phases:

$$\alpha = \frac{V\ bottom}{V\ bottom + V\ top} = 0.7\ (\pm 0.05)$$

The experimental errors on the compositions are high (10%), except for the isopropranol and the salt content. Other experiments carried out under similar conditions confirm however that the structure of the system at equilibrium is fairly described by these set of compositions.

The presence of the salt affects slightly the composition of the two phases, provided that the salt content in the feed does not exceed 0.2%w. We have tried to adjust the polymer-alcohol (a_{24}), polymer-CO_2 (a_{34}) and isopropanol-salt binary parameters to reproduce the experimental tie-lines and the proportions of the two-phases. The two types of structures described for the salt-free system are again obtained. Depending on which values are assigned to the parameters, one or the other structure is obtained, providing that the volumes of the two liquid phases are kept equal to the experimental values.

The calculated salt distribution coefficient is very sensitive to the Pitzer's polymer-salt first-order interaction coefficient. When this parameter is increased, the polymer is driving the salt out of the polymer-rich phase, thus increasing its distribution coefficient (Ks). But this coefficient never reaches values of the order of one, as experimentally observed. It remains about one order of magnitude lower (0.1). If the salt-polymer coefficient increases further, then the salt almost entirely abandons the polymer-rich phase and goes into the alcohol-rich phase. The lowest Ks obtained for this configuration is about 10. It seems therefore that the present model does not allow similar concentrations of the salt on both liquid phases. This model probably leaves out one essential physical phenomenon allowing this partitioning to happen. So far, the influence of the polymer on the dielectric constant of the polymer-rich phase has not been taken into account. However, a number of flash calculations, assuming different quantitative influences of the HEC on this dielectric constant did not lead to any improvement of the model.

This failure to represent the partitioning of the salt can be attributed to a number of characteristics of the model.

We notice first that the water-isopropanol-CO_2 tie-lines are not very well represented. However, it is not possible to know whether this is a cause or a consequence of the failure to obtain good agreement for the partitioning of the salt. If the water tie-lines are well represented, the isopropanol partitioning is slightly underestimated while the CO_2 partitioning is systematically much overestimated (Figure 37).

The absolute values of the salt fugacities coefficients computed by the model are large in both phases; and they are sensitive to the feed composition as well as to the parameters. Therefore, when the salt distribution coefficient becomes close to one, the slightest change or error in the computation of these coefficients has a very strong effect on the convergence of the compositions.

The CO2-salt interactions are described by a simple linear model which assumes the carbon dioxide to be in its molecular form in solution. We may therefore make significant errors in predicting the solubility of CO2 in the two liquid phases, which plays a key role for the partitioning.

Finally, for simplicity, the model assumes that no polymer is present in the top phase. The presence of HEC in the alcohol-rich phase may, however, be a significant factor the salt partitioning.

8 CONCLUSION

The theoretical model in its current form is able to represent quantitatively the water-isopropanol-CO2 system far from the critical region. When polymer is present, the computed compositions agree qualitatively with our empirical understanding of the system. No experimental point can be used for comparison since the HEC used has an initial salt content that we cannot reduce to zero. Further, measurement of the third virial polymer-solute coefficients through light-scattering is a delicate task which did not give very precise results. We, however, were able to test different reasonable sets of parameters, which showed that they do not affect strongly the fact that no salt distribution coefficient close to unity could be predicted.

Some further work and changes in the method may improve the performances of the model :

- Additional light-scattering measurements may give an estimate of the two missing parameters (isopropanol- and salt-polymer interactions), the isopropanol-salt binary parameter could be derived from vapor pressure measurements.

- Measurements of CO2 solubilities in the water-polymer-isopropanol system would help to determine the polymer-CO2 binary interaction coefficient.

- The flash calculations can easily be modified to allow a polymer distribution coefficient different from zero. If this coefficient were fixed to its experimental value for example, the same thermodynamic model would still be valid.

- An important task would be to improve the model for the salt-carbon dioxide interactions.

VI. A NEW PRODUCTION PROCESS FOR HYDROXYETHYLCELLULOSE

Current Process

Figure 30 shows schematically the current, heterogeneous, production process of the water-soluble cellulose derivative hydroxyethylcellulose (HEC). Batch processes remained dominant in 1985. Continuous processes are considered more economical, although transporting the slurry in the heterogeneous, continuous production process is difficult.

Cellulose is soaked in aqueous solutions of sodium hydroxide. The base disrupts the intermolecular hydrogen bonding of the cellulose and makes the hydroxyl groups of the anhydroglucose units easily accessible for the alkylating reagent, ethylene oxide. An organic diluent such as isopropanol, tertiary butanol, acetone or toluene is added to suspend and disperse the activated cellulose and promote an even reagent distribution, which is most important for the uniformity of the reaction. In the reaction, water competes with cellulose for the alkylating reagent, and due to the hydrolysis of ethylene oxide, ethylene glycol is formed as a by-product. Throughout the entire process, the water concentration is kept low to prevent the reaction product HEC from dissolution.

In the next step, the base is neutralized. The product is filtered and sodium salt and other by-products are removed by washing the crude product with aqueous organic solvents, which have to be recycled. After filtration, the product is dried in a nitrogen atmosphere.

Suggested Process

The new, continuous production process set forth in this work is shown in Figure 38. Since we wanted to utilize the examined CO_2-induced phase separation of *homogeneous* polymer solutions as a purification method for HEC, we considered it advantageous to devise an *entirely homogeneous* production process, based on the novel purification method. The reaction of the cellulose to HEC and the dissolution of the produced polymer are conducted in one stage.

To achieve alkali-soluble HEC, the number of cellulosic hydroxyl groups per anhydroglucose unit that needs to be substituted is

smaller than then number to achieve water-soluble HEC. Therefore, a smaller amount of the alkylating reagent ethylene oxide is required to obtain alkali-solubility of the product than that to obtain water-solubility. In the new process, the alkali cellulose is dispersed in the inert organic co-solvent, tertiary butanol, and a relatively small amount of ethylene oxide is first used to yield an alkali-soluble product. Simultaneously, some water is added to dissolve the reacted cellulose in the aqueous-organic alkaline solution, thereby making the process homogeneous.

Upon adding more ethylene oxide, the remainder of the reaction to the water-soluble state is entirely carried out in a solution (which gives the product superior quality relative to that of the product of the current, heterogeneous industrial process) and, subsequently, a liquid-liquid phase split is induced by high-pressure carbon dioxide. HEC accumulates in the water-rich phase, the organic solvent in the CO_2-rich phase. The salt formed in the simultaneously conducted neutralization step distributes more or less evenly between the two phases. Figure 39 shows a schematic chart of the envisioned continuous purification step. Several stages of phase-separation operations have to be conducted to separate the by-products and the HEC entirely from one another and from the solvents carbon dioxide and tertiary butanol, which are recycled.

The suggested new process may have three potential advantages:

a) Uniform reaction is an inherent problem in heterogeneous processes. *Uniformity* of substitution, rather than merely high rate of molar substitution of the cellulosic hydroxylgroups, is the criterion of optimum water-solubility of the final product; high water-solubility is desirable in most applications of HEC. Homogeneous processes (like that suggested here) produce a more even distribution of substituents on the cellulose units due to a better reaction uniformity than that of heterogeneous processes, thus yielding a product with improved properties such as a higher solubility in water.

b) From a technical point of view, processing a solution is preferable to processing a slurry because, in a homogeneous process, there is no danger of accumulation of sediments in pipelines and pumps.

c) In both processes, the organic solvent/diluent is recycled. In the suggested process, the turnover of organic solvent in the recycling circuit may be comparatively lower by inducing a liquid-liquid phase separation through high-pressure carbon dioxide.

Unfortunately, no quantitative information about the current process was available. Though it was not in the scope of this work to prove the economic superiority of the suggested process, an attempt was

made to compare quantitatively the efficiency of the purification steps of both processes.

In one experiment, we tried to reduce the salt content of the original HEC, as obtained from the supplier, by washing the polymer with a mixture of isopropanol and water at ambient conditions. This is the method used in industry to purify the crude product. With a total of 810 ml isopropanol and 90 ml water, the salt content of the solid HEC was reduced from 3.8 to 2.0wt-% in three stages. 14wt-% of the polymer dissolved and was lost.

Starting with the same amount of polymer as above, a quantitative evaluation was made of experiment #7a (see pages 35ff) as a one-stage, discontinuous liquid-liquid extraction process: with 330 ml of tertiary butanol and 380 ml of water, the salt content of the HEC in the water-rich phase was reduced from 6.4 to 4.2wt-%, whereas 22% of the original amount of polymer was dissolved in the alcohol-rich top phase and would be lost in an one-stage extraction. Equilibrium pressure (mostly CO_2) was 12 atm at 40°C.

Data from experiment #2 (see pages 30ff) were evaluated likewise: with 430 ml isopropanol and 550 ml water, the salt content of the HEC in the water-rich phase was reduced from 5.9 to 3.0wt-%, losing 12% of the polymer. At 40°C, the equilibrium pressure was 65 atm.

These preliminary results indicate that in the suggested process, the amount of organic solvent needed may be lower than that in the current industrial process to obtain the same purified HEC. With tertiary butanol as the organic co-solvent, the loss of polymer in a one-stage process would be higher in the suggested process, but could probably be compensated in a multi-stage process.

As the results of our experiments show, both isopropanol and tertiary butanol are highly soluble in carbon dioxide at high pressures.

Thus, the recycling of the organic solvent seems to be feasible by extraction of the alcohol from the water and liquid by-products with carbon dioxide (see Figure 40), rather than by energy-intensive separation techniques such as rectification.

Mixtures of water, isopropanol and CO_2 separate into two liquid phases at elevated pressures; carbon dioxide as a compressed gas or supercritical fluid can selectively extract isopropanol from aqueous solutions to give alcohol concentrations greater than that corresponding to the isopropanol/water azeotrope, but the minimum operating pressure would be approximately 88 atm at 40°C. Sub-ambient temperatures would be required to reduce significantly the

minimum operating pressure below 88 atm (16). Although no corresponding data were available for tertiary butanol, we presume that the minimum operating pressure for an extraction of tertiary butanol from aqueous solutions would be significantly lower than that with isopropanol; by replacing isopropanol with tertiary butanol, we reduced the phase separation pressure of our polymer solutions from above 60 atm to about 10-20 atm; in the presence of CO_2 tertiary butanol is less compatible with water than isopropanol.

In the process set forth in this work, a sufficient amount of water has to be added to dissolve the produced HEC molecules immediately after they are formed. For this reason, a higher water content may be necessary in the proposed process, compared to that in the current (heterogeneous) industrial process (the water concentration in the reaction step of the industrial process was not available). Since water competes with the cellulose for the reagent ethylene oxide, the effectiveness of the ethylene oxide as an alkylating agent for cellulose may be comparatively lower in the proposed process.

Acknowledgements

References

(1)   Encyclopedia of Polymer Science and Technology (1982), 2nd Ed. J.Wiley & Sons, Vol.3, pg. 226-246

(2)   Encyclopedia of Chemical Technology (1980), J.Wiley & Sons, Vol.12, pg. 64

(3)   Encyclopedia of Polymer Science and Technology, 2nd Ed. (1987), J.Wiley & Sons, Vol.17, pg. 902

(4)   Encyclopedia of Polymer Science and Technology, 2nd Ed. (1987) J.Wiley & Sons, Vol.17, pg. 916

(5)   Ullmanns Enzyklopädie der technischen Chemie, 4.Auflage (1981), Verlag Chemie, Weinheim, pg. 275

(6)   Journal of Biochemical and Microbiological Technology and Engineering (1961), Vol.III, No.1, pg. 51-63

(7)   Polysaccharide (Xanthan) of Xanthomonas Campestris, ARS-NC-51 (Nov.1976), U.S. Department of Agriculture

(8)   Encyclopedia of Polymer Science and Technology, 2nd Ed. (1987) J.Wiley & Sons, Vol.17, pg. 908

(9)   M.A.McHugh, V.J.Krukonis, Supercritical Fluid Extraction (1986), Butterworths, pg. 102

(10) J.M.L.Penninger, M.Radosz, M.A.McHugh, V.J.Krukonis (editors), Supercritical Fluid Technology (1985), Elsevier, pg. 165

(11) K.A.Bartscherer, Phasengleichgewichtsthermodynamik wässriger Polymere, Diplomarbeit (1990), Department of Chemical Engineering, University of California, Berkeley

(12) R.H.Perry, C.H.Chilton, Chemical Engineer's Handbook, 5th Ed. (1970), McGraw Hill, New York, pg. 3-71

(13) R.E.Gibson, O.H.Loeffler, J. amer. chem. soc. 63(1941), pg. 898

(14) J.M.L.Penninger, M.Radosz, M.A.McHugh, V.J.Krukonis (editors), Supercritical Fluid Technology (1985), Elsevier, pg. 154

(15) R.Wiebe, V.L.Gaddy, J. amer. chem. soc. 63(1941), pg. 475

(16) J.M.L.Penninger, M.Radosz, M.A.McHugh, V.J.Krukonis (editors), Supercritical Fluid Technology (1985), Elsevier, pg. 157

(17)   C.J King   Separation Processes 2nd edition Mc Graw   Hill. New York 1980   chapter 2

(18) Elgin and Weinstock J. Chem. Eng. Data 4,3 (1959)

(19) M.E Paulaitis, R.G Kander, J.R DiAndreth Ber, Bunsenges Phys. Chem. (1984)

(21) M.E Paulaitis, J.M.L Penninger, R.D Gray, P. Davidson Chemical Engineering at Supercritical Fluid Conditions (1983) , Butterworth

(22) M. Radosz personnal communication (1983)

(23) A.Z. Panagiotopoulos, Doctorate Dissertation, Massachussets Institute of Technology (1986)

(24) A.H Harvey, PhD Dissertation , University of California at Berkeley (1988)

(25) M. Born, Z. für Physik 1 45 (1920)

(26) T.W Coperman, F.P Stein, FLuid Phase Equilibria 35, 165 (1987)

(27) E. Edmont, A.G Ogston Biochem. Journal 109, 569 (1987)

(28) C. A Haynes, J.M Prausnitz, work in progress

(29) K.S Pitzer J. Phys. Chem. 77, 268 (1973)

(30) Carbon Dioxide International Tables of the Fluid State. IUPAC

(31) E. Sada and T. Morisue. J. Chem. Eng Japan vol 8, 3 (1981)

(32) M. Radosz. J. Chem. Eng. Data 31 (1984)

(33) R.Wiebe and V.L Gaddy J. Am. Chem. Soc. 63 (1941)

(34) K. Tödheide and E.U Franck Z. Physik. Chem. NF 37 (1963)

(35) M.K Goldberg J. Phys. Chem. Ref. Data vol 10, 3 (1981)

(36) E. Sada and T. Morisue. J. Chem.Eng Japan vol 8, 3 (1981)

(37) Modern Theory of Polymer Solutions H. Yamakawa, (1971), Harper and Row

(38) R.J Topliss , Doctorate Dissertation, University of California (1985)

Table 1: Typical Chromatography Results for Polymer Solutions (Peak Areas in μVsec. as evaluated by the integrator of the chromatography system; the reported concentrations for tertiary butanol were calculated with different calibrations for this alcohol)

Analysis Number	Xanthan + K_2HPO_4 (0.06 + 0.018g/l)	tertiary Butanol (1.27g/l)
1 2 3	108950 115533 93838	1657172 1645284 1650026
average for three runs	106107 $\approx$ 106100	1650827 $\approx$ 1650800
	HEC + NaAc (0.31 + 0.019g/l)	tertiary Butanol (2.47g/l)
1 2 3	1347270 1367250 1351864	8424422 8444414 8457813
average for three runs	1355461 $\approx$ 1355500	8442216 $\approx$ 8442200

Table 2: Salt Removal in Exp. #1,2 and 5

exp. #	salt content of HEC (feed) in wt.-%	salt content of HEC (bottom phase) in wt.-%	HEC lost in top phase, in % of HEC in feed
1	5.6	3.7	14
2	5.9	3.0	12
5	4.0	3.7	2

Table 3: Salt Removal in Exp. #6-8a

exp. #	salt content of HEC (feed) in wt.-%	salt content of HEC (bottom phase) in wt.-%	HEC "lost" in top phase, in % of HEC in feed
6	5.3	4.1	12
7a	6.4	4.2	22
7b	7.0	3.7	33
8a	6.5	5.8	6
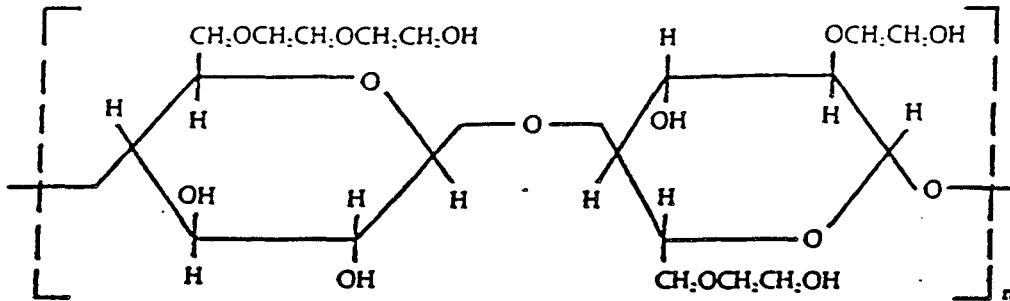
Figure 1: Structure of Hydroxyethylcellulose

M⁺= Na. K. ½Ca
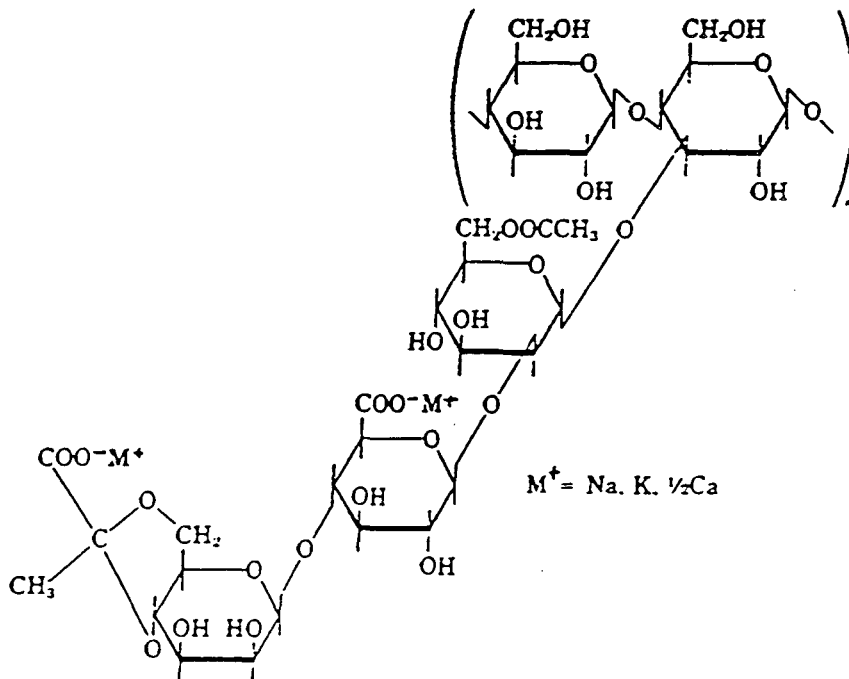
Figure 2: Structure of Xanthan Gum
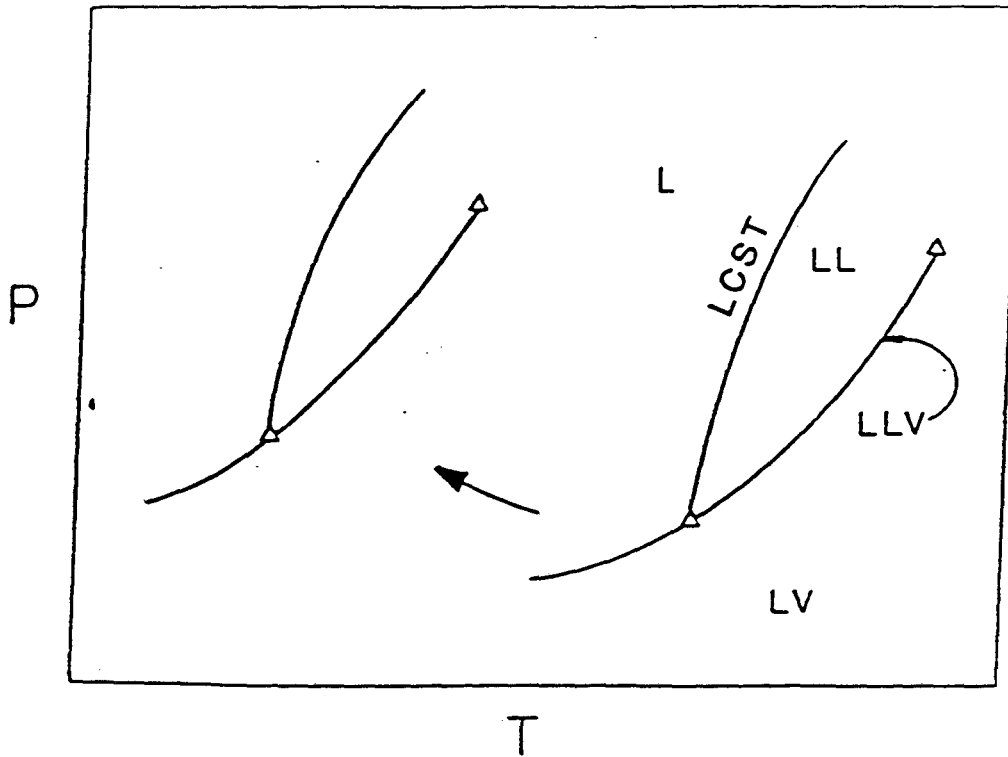
Figure 3: Influence of a Supercritical Fluid on the Phase Diagram of a Polymer Solution
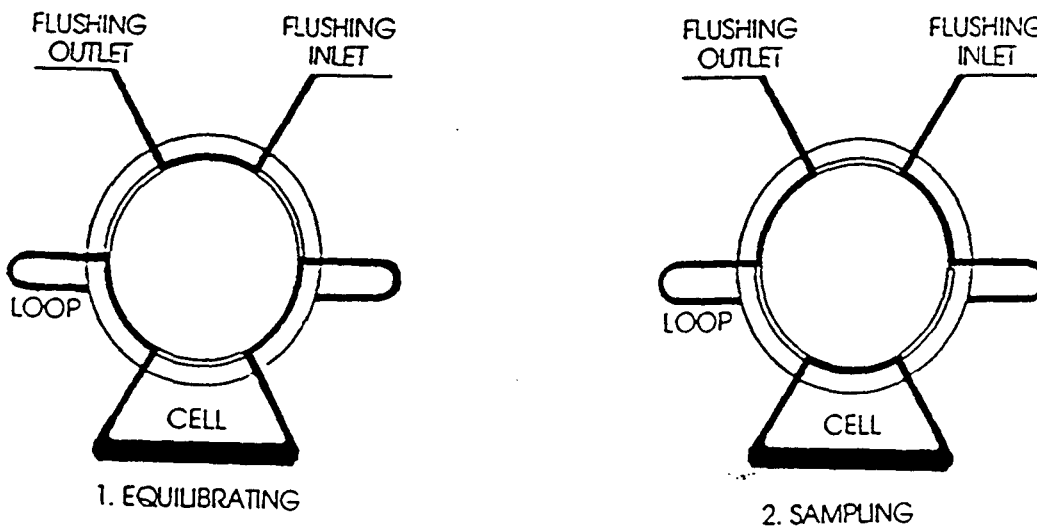
Figure 4: Operating Principle of Sampling Valves
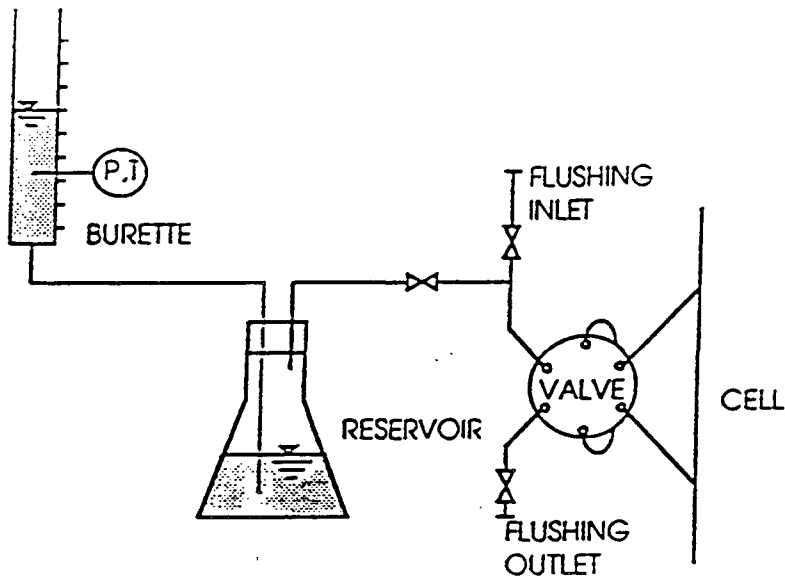
Figure 5: Equipment for CO_2-Measurements

EFFECTIVE DIAMETER
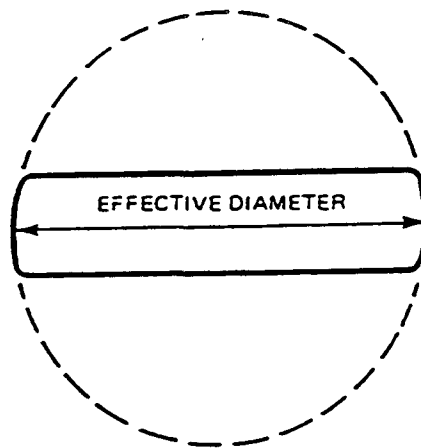
Figure 6: Effective Molecular Diameter
(The effective molecular diameter of a long, narrow molecule is defined by the diameter of a sphere with a diameter equal to the length of the molecule

DIRECTION OF SOLVENT FLOW
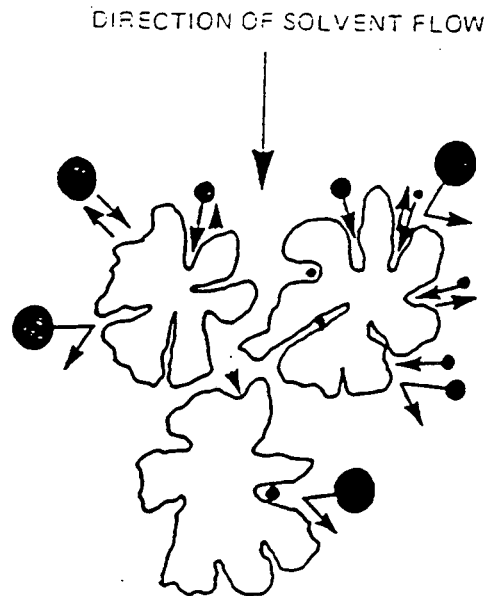
Figure 7: Principle of Size-Exclusion Chromatography

□ NaAc
○ isopropanol
■ HEC

concentration in g/l
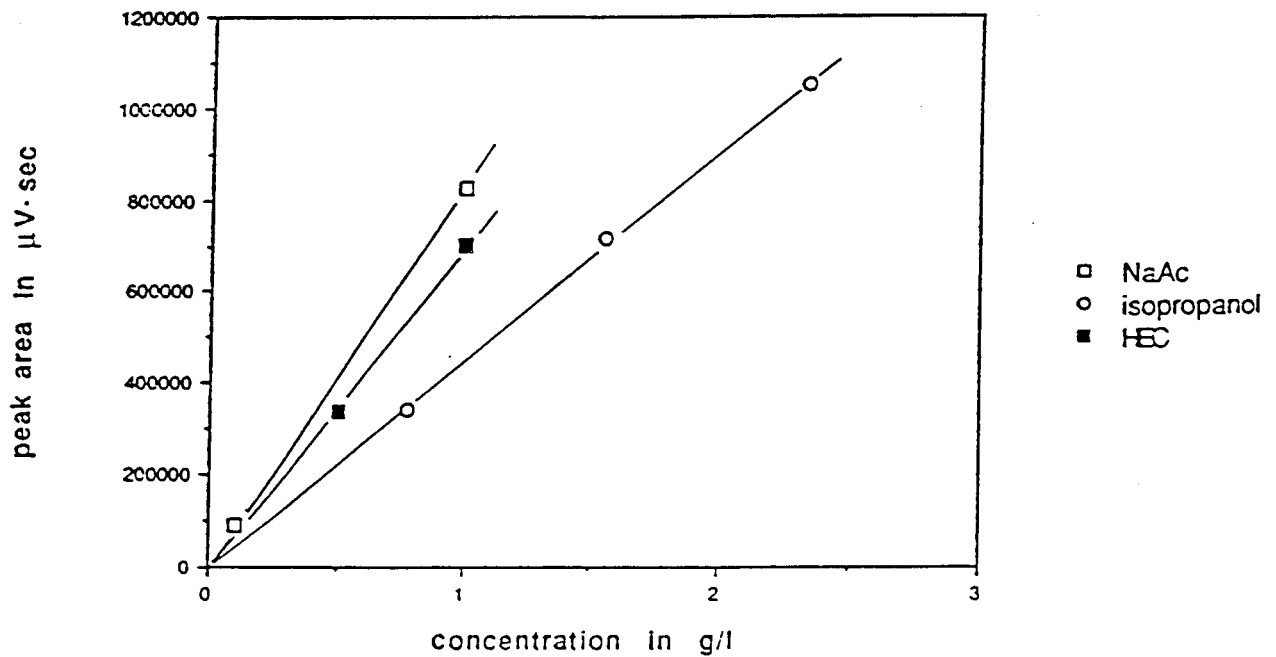
Figure 8: A Typical Calibration of the Chromatograph for Sodium Acetate, Isopropanol and Hydroxyethylcellulose
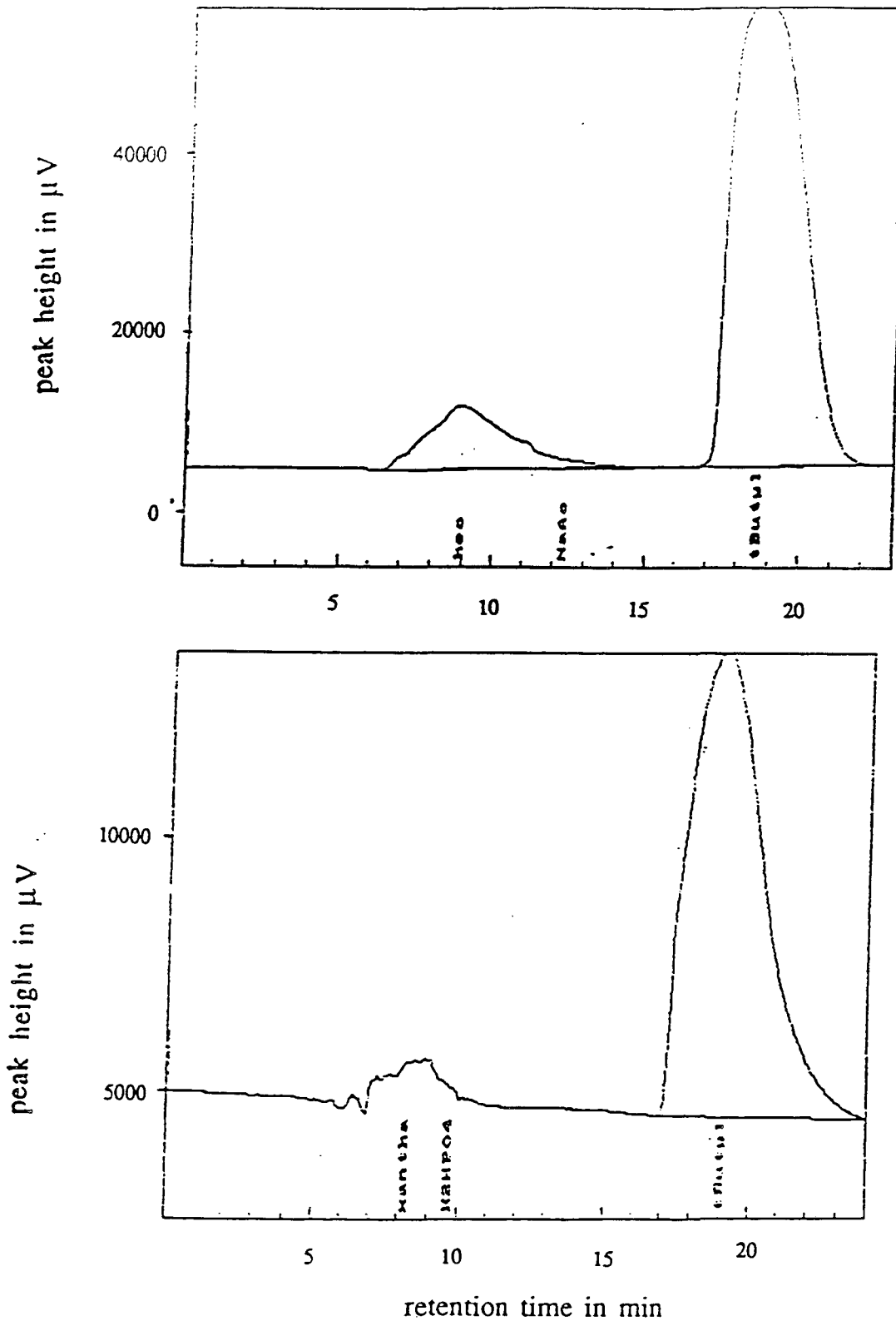
Figure 9: Two Chromatography Plots
(above: 0.31 g/l HEC, 0.02 g/l NaAc, 2.65 g/l tertButanol
below: 0.06 g/l Xanthan, 0.018 g/l K_2HPO_4, 1.27 g/l
tertButanol)
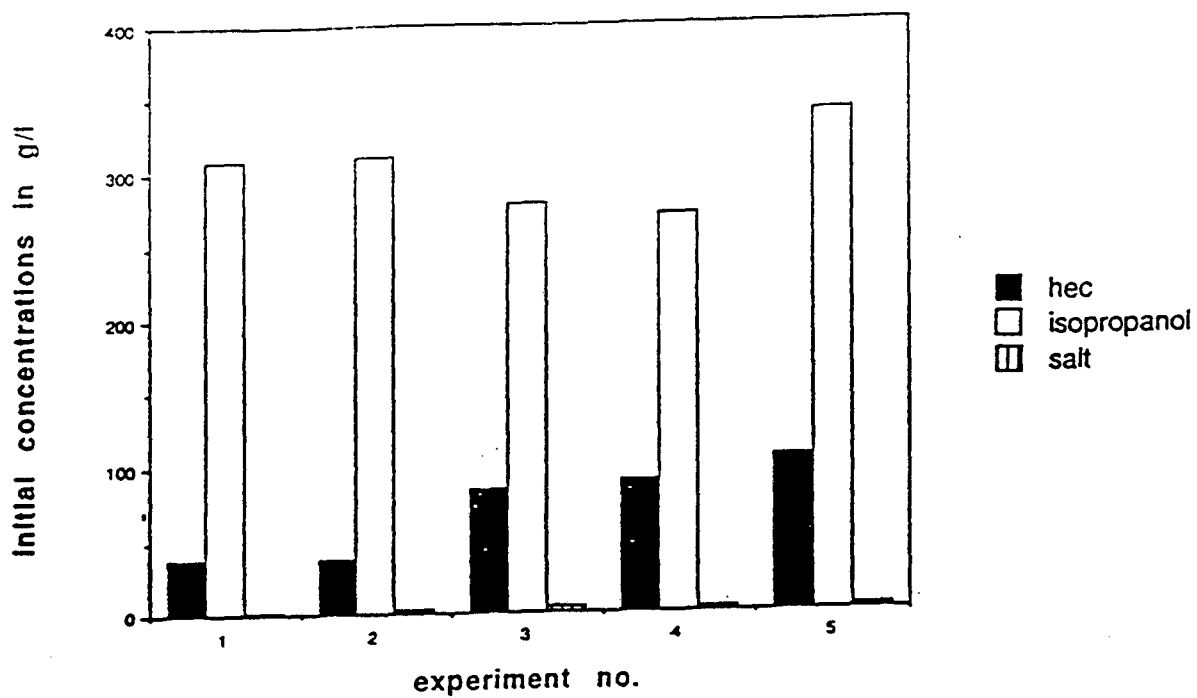
Figure 10: Initial Compositions of Polymer Solutions #1-5
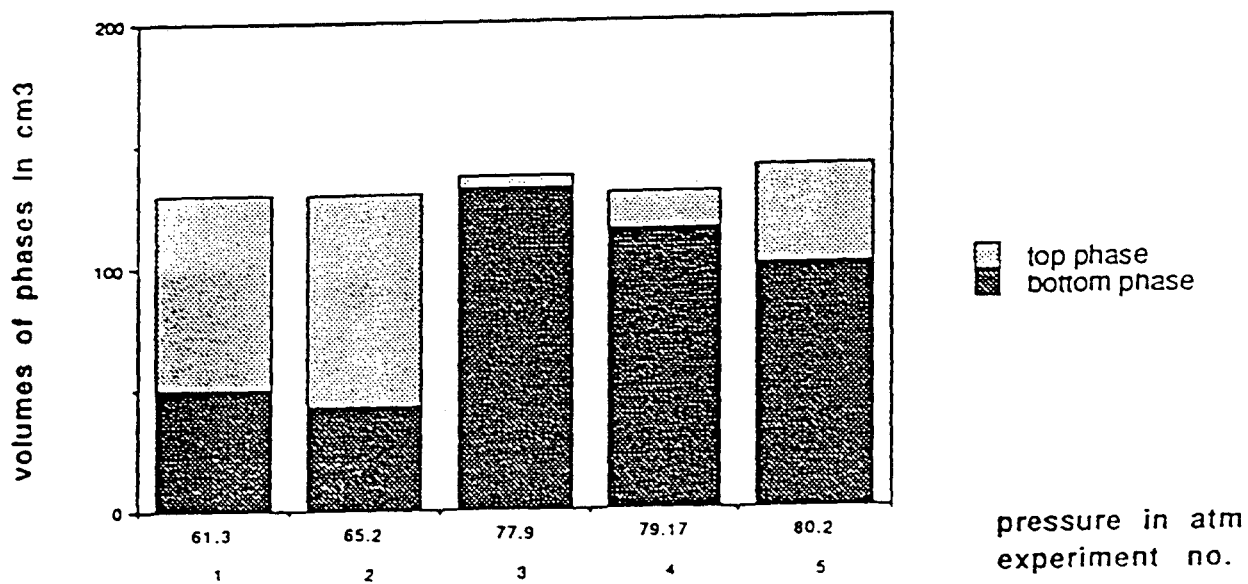
Figure 11: Volumes of the Two Liquid Phases at 40°C in Exp. #1-5
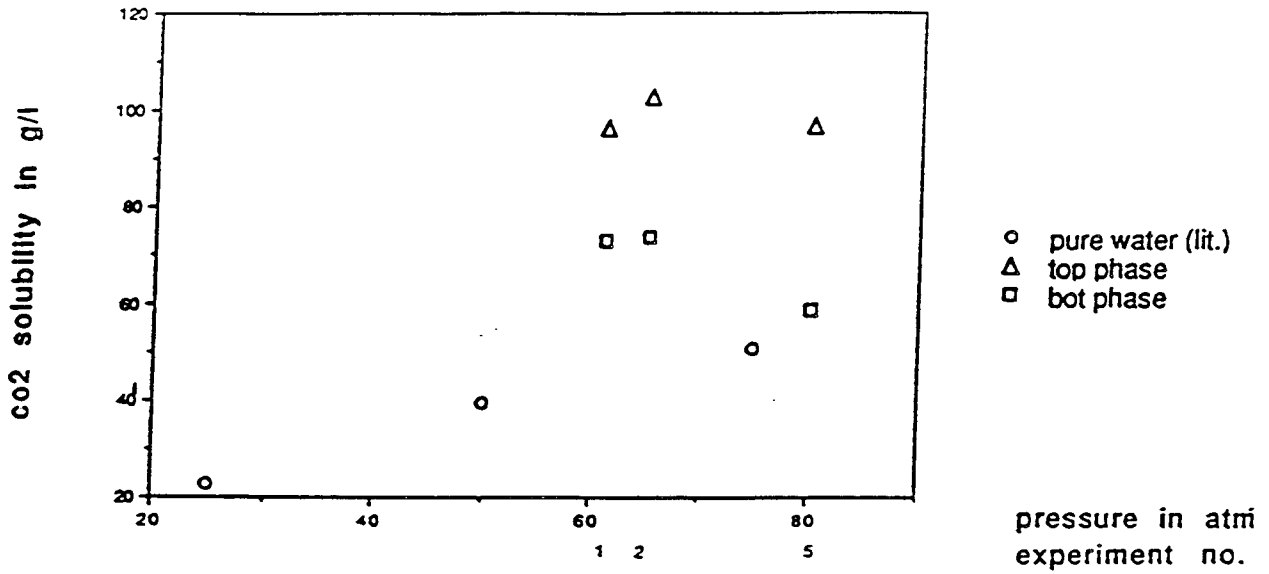
Figure 12: CO₂-Solubility in Both Liquid Phases in Exp. #1,2 and 5
And in Pure Water at 40°C (data for water from (15))
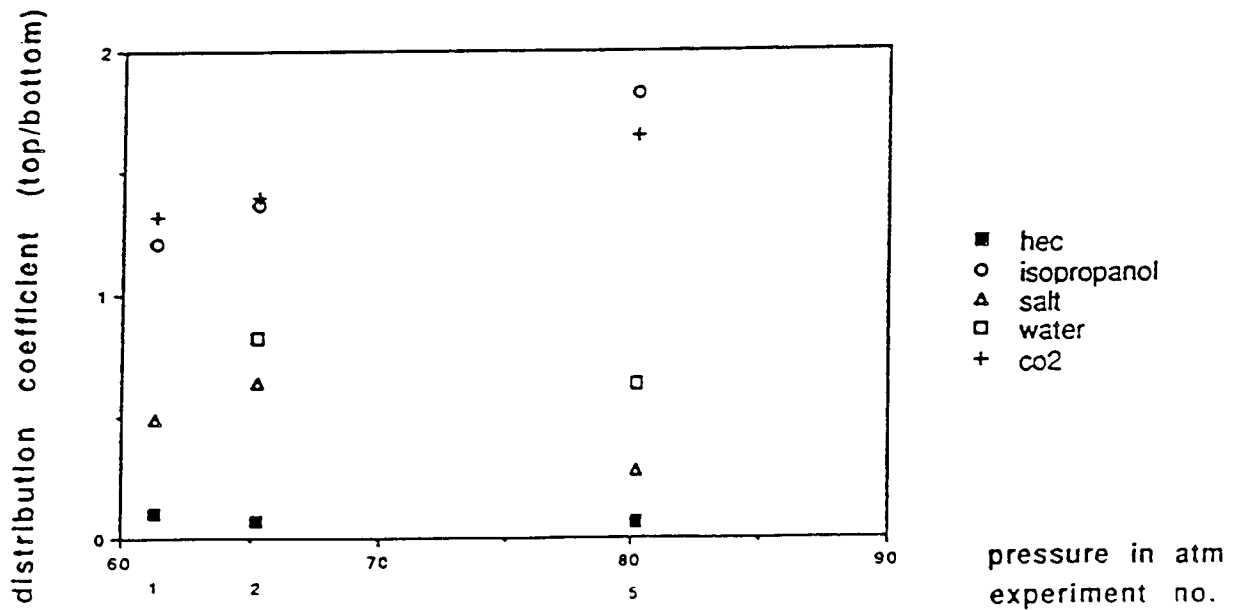
Figure 13: Distribution Coefficients in Exp. #1,2 and 5 at 40°C
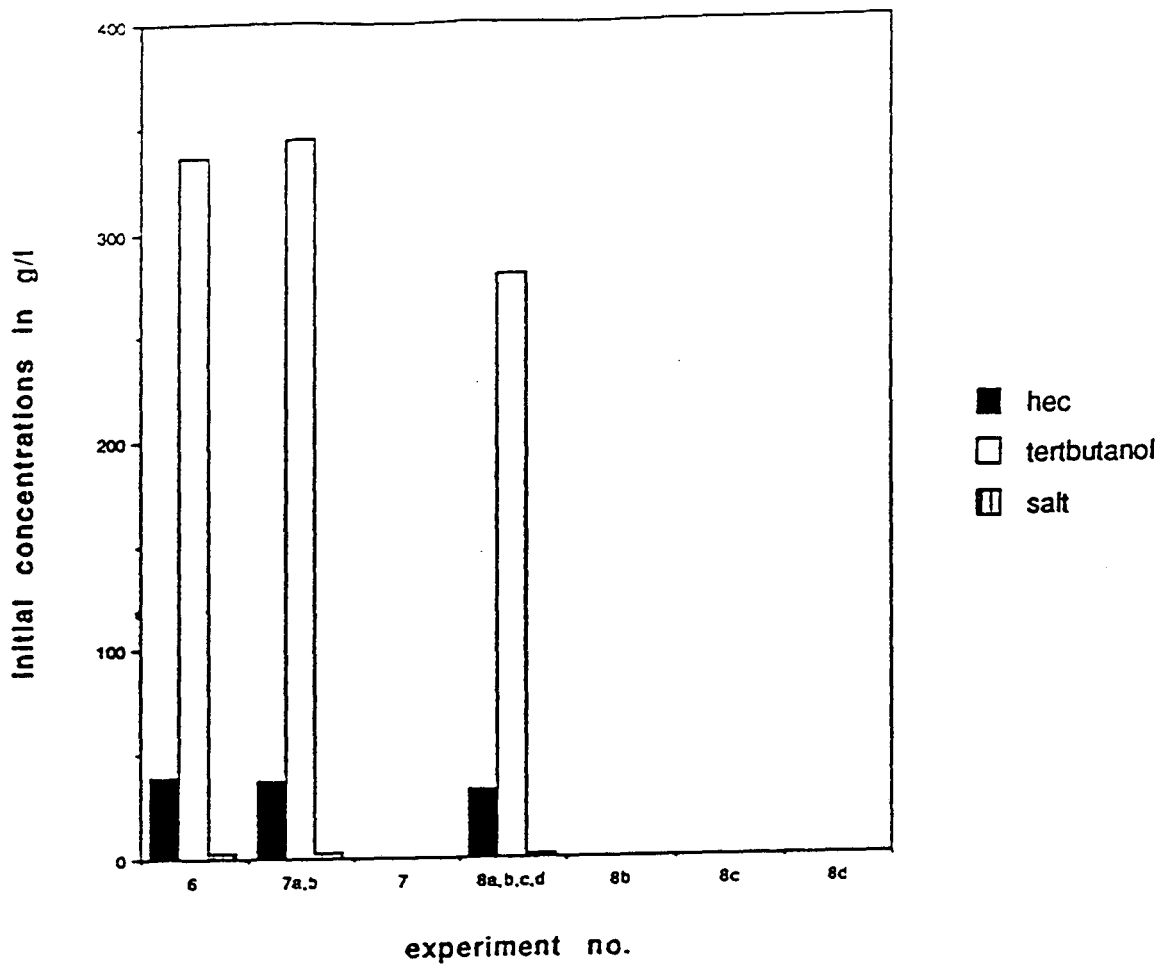
Figure 14: Initial Compositions of Polymer Solutions #6,7 and 8
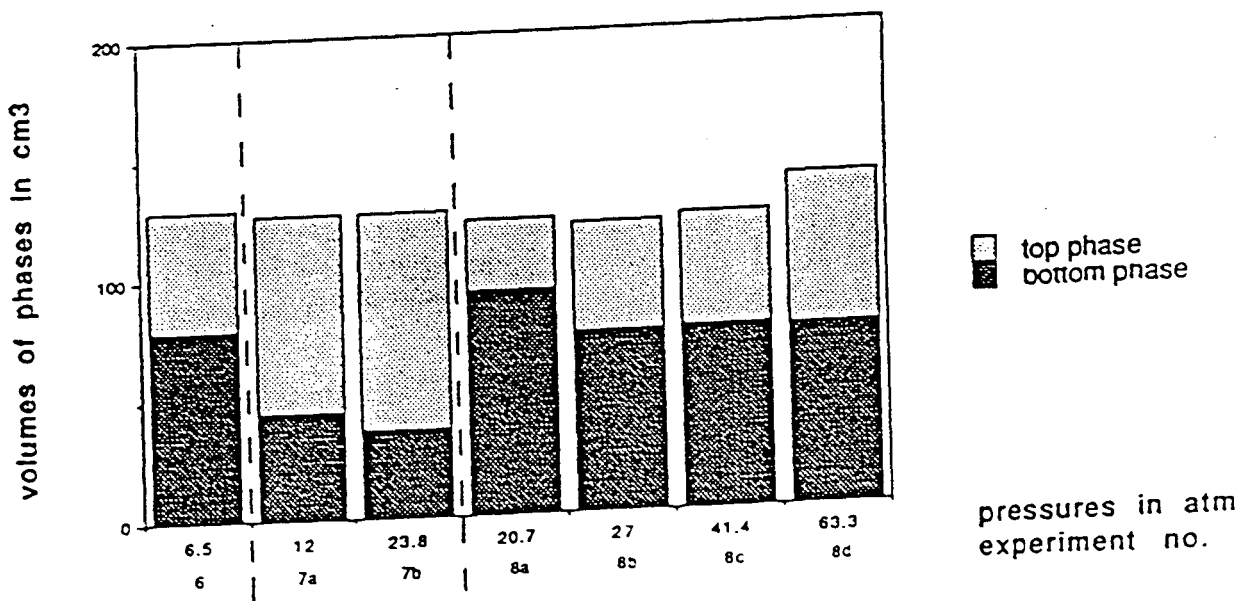
Figure 15: Volumes of the Two Liquid Phases at 40°C in Exp. #6,7 and 8
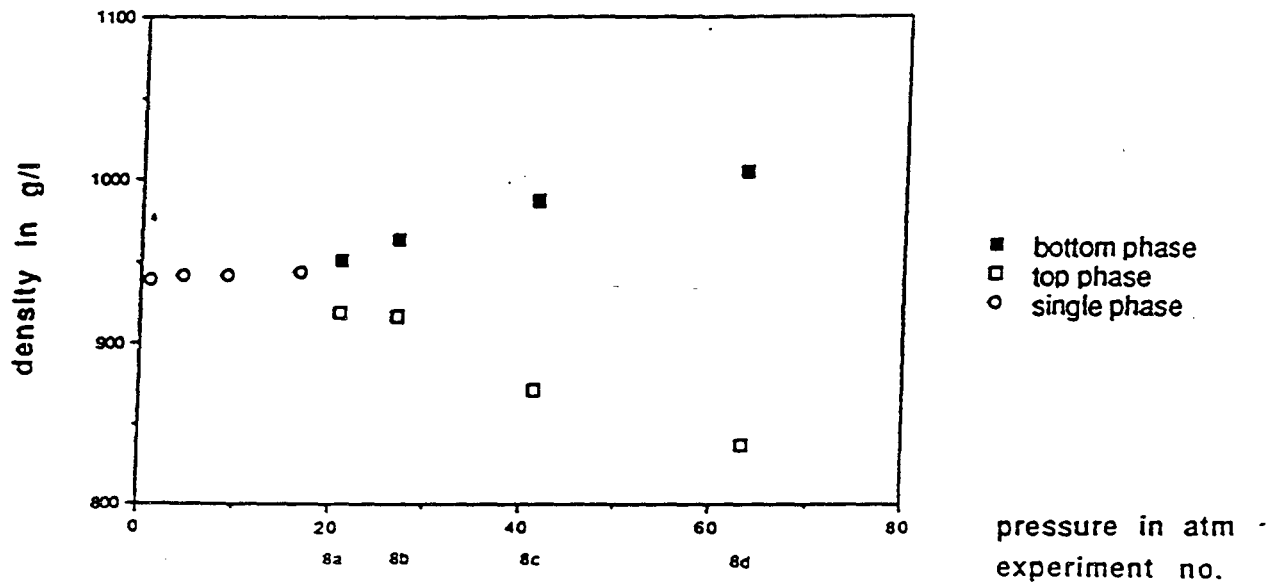
Figure 16: Density in Experiment #8 (40°C)
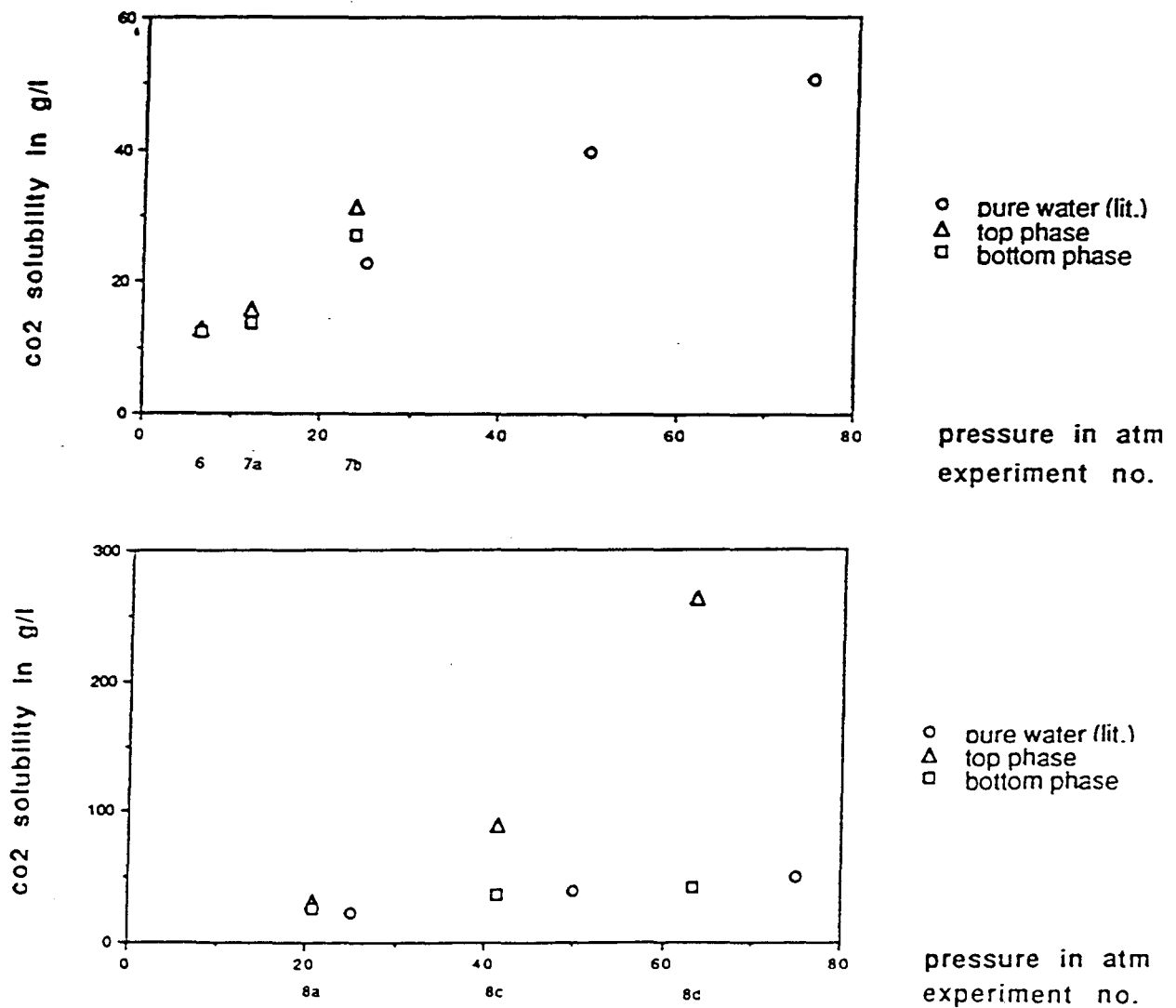
Figure 17: CO₂-Solubility in Both Liquid Phases of Exp. #6,7 and 8
and in Pure Water at 40°C (data for water from (15))
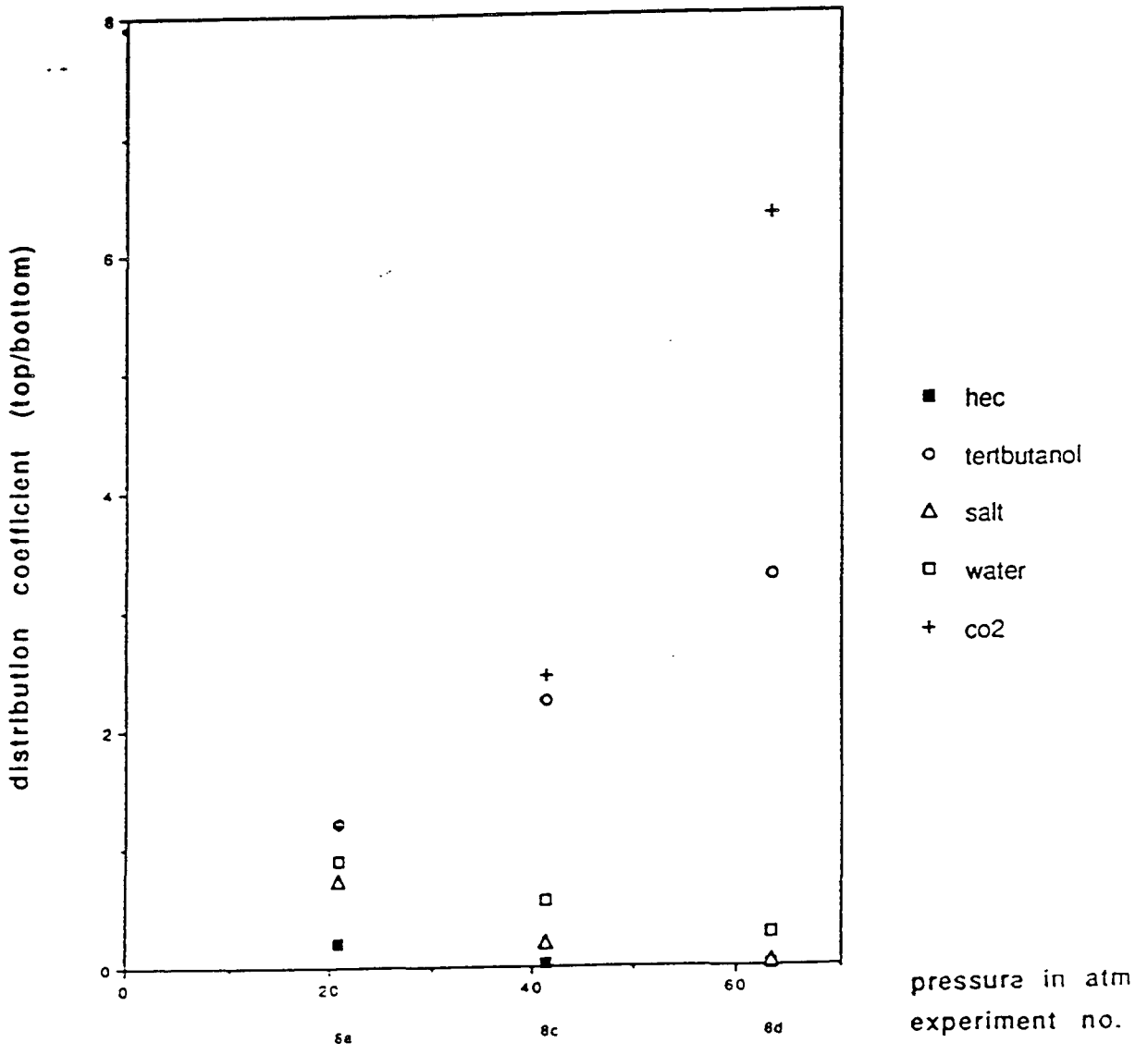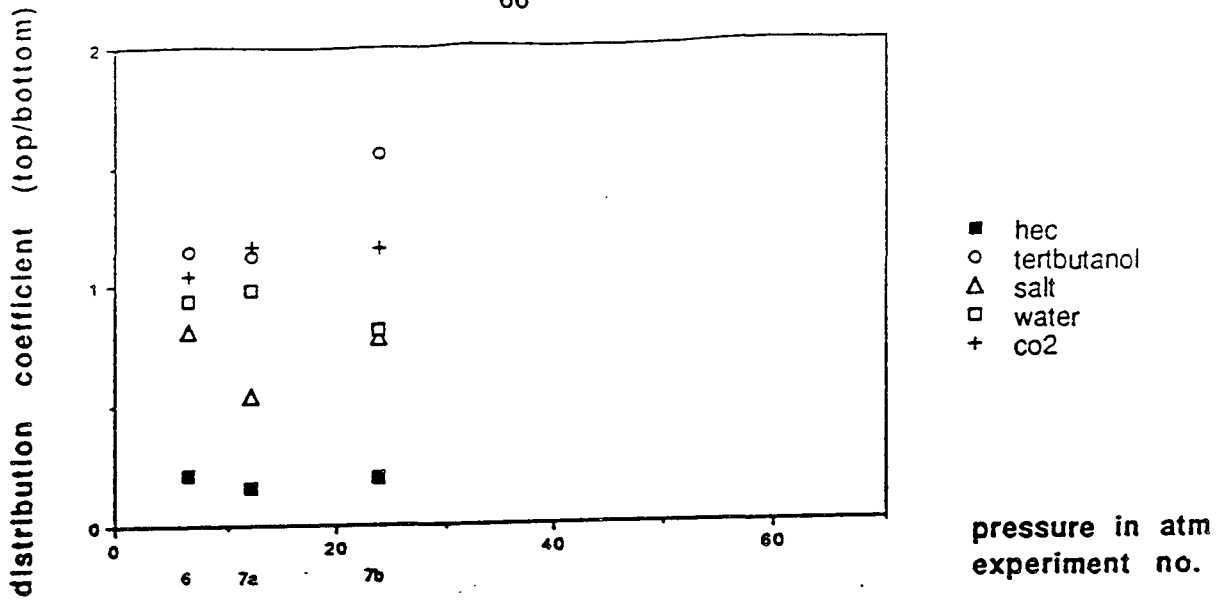
Figure 18: Distribution Coefficients for Experiment #6-8 (40°C)
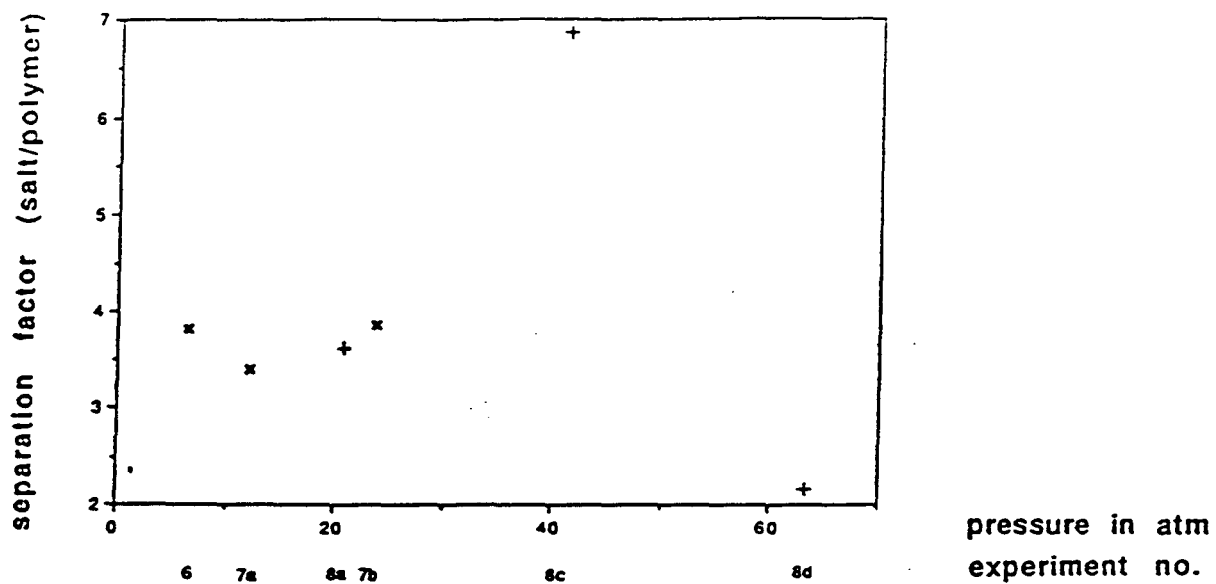
Figure 19: Separation Factor in Exp. #6,7 and 8

isopropanol   tertiary butanol   secondary butanol
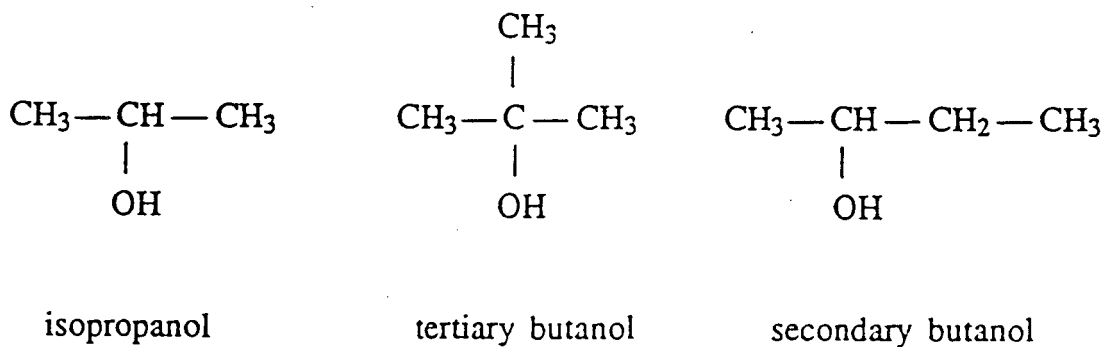
Figure 20: Chemical Structure of the Alcohols Used as Co-Solvents
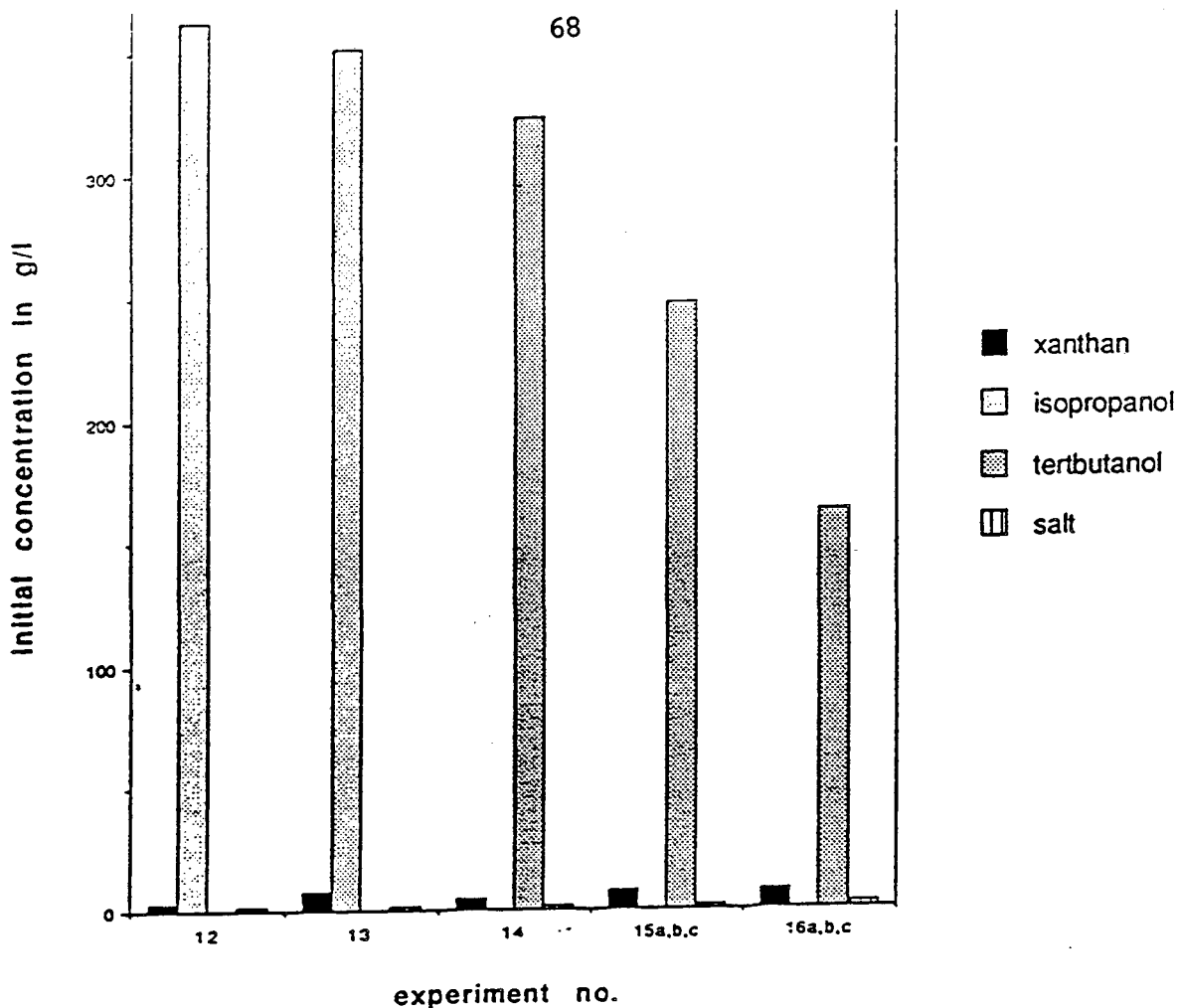
Figure 21: Initial Compositions of Polymer Solutions #12-16
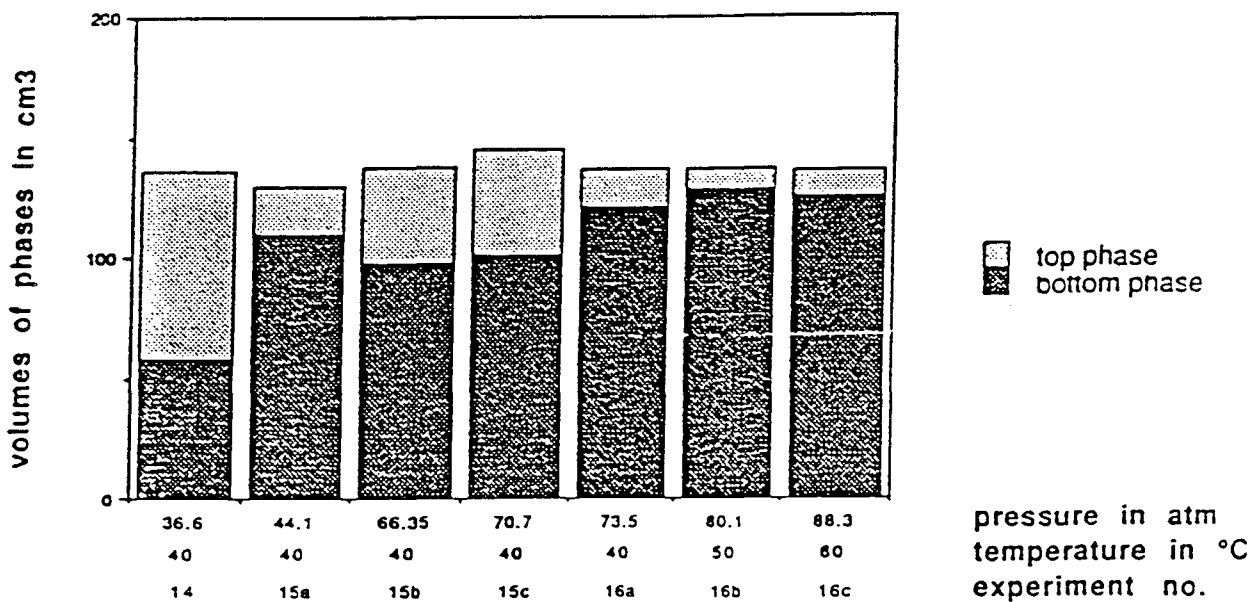
Figure 22: Volumes of the Two Liquid Phases in Exp. #14-16
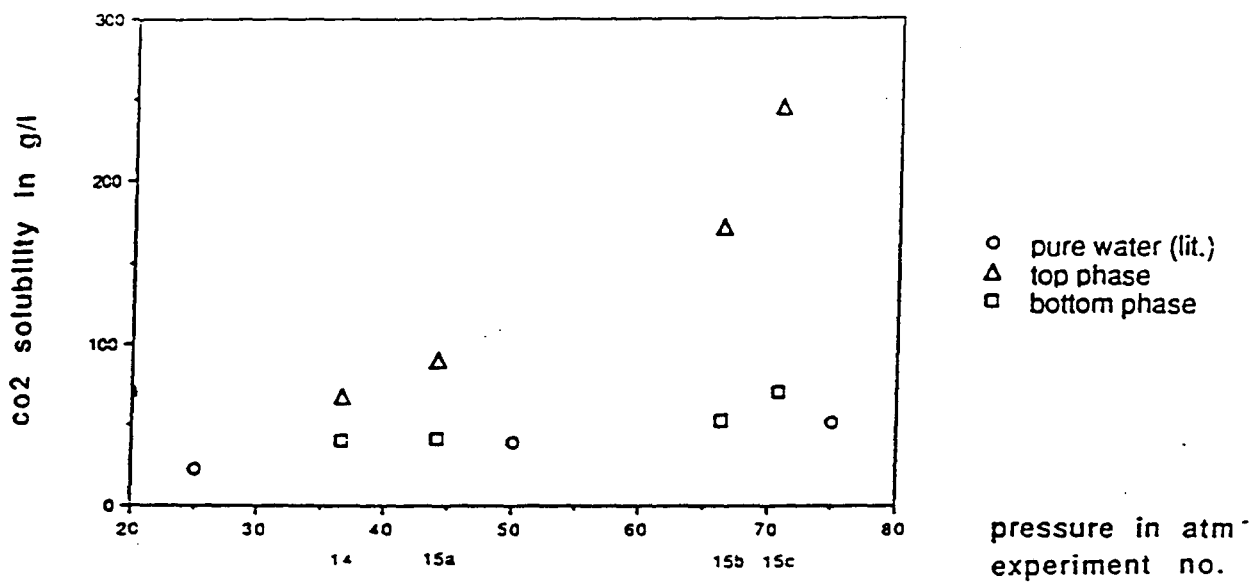
Figure 23: CO_2-Solubility in Both Liquid Phases of Exp. #14 and #15, and in Pure Water at 40°C (data for water from (15))
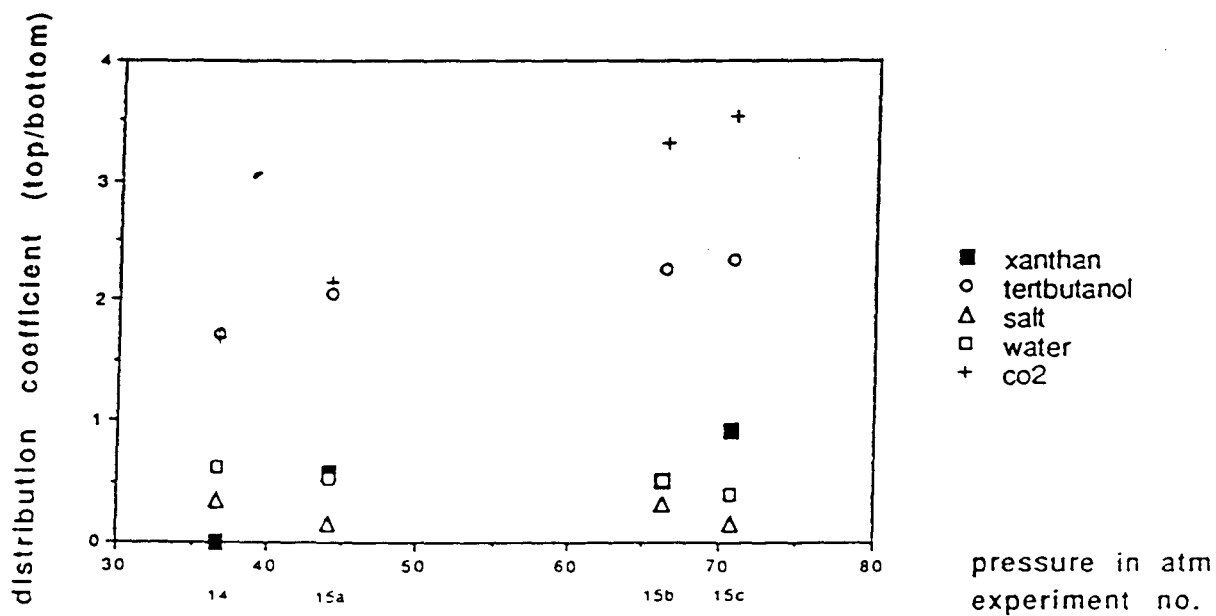
Figure 24: Distribution Coefficients in Exp. #14 and #15

Figure 25
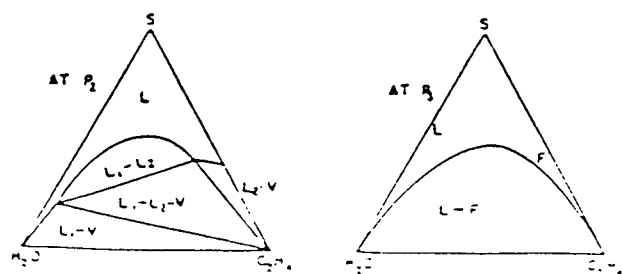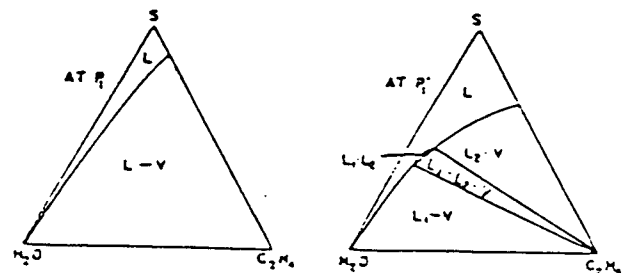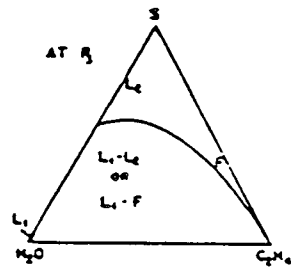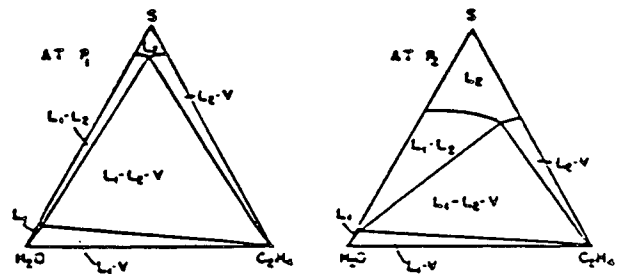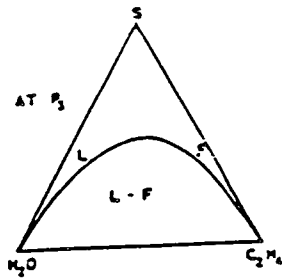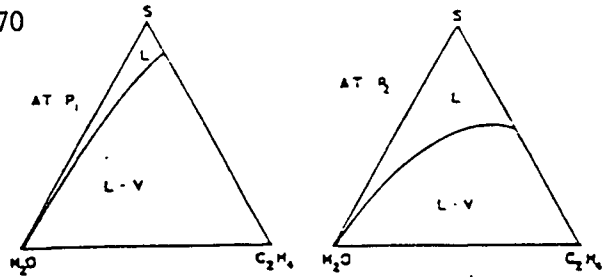
Type 1
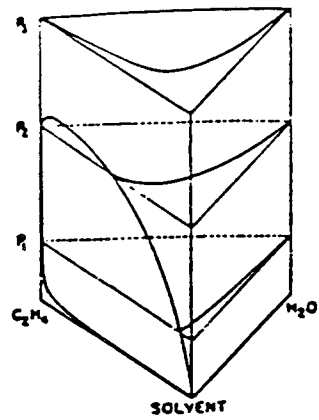
type 2
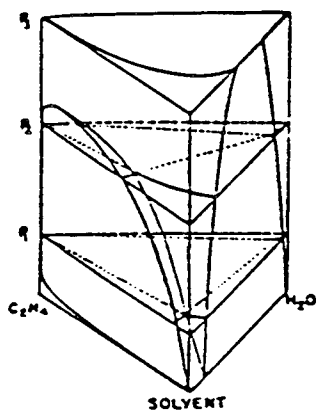
vpe 3
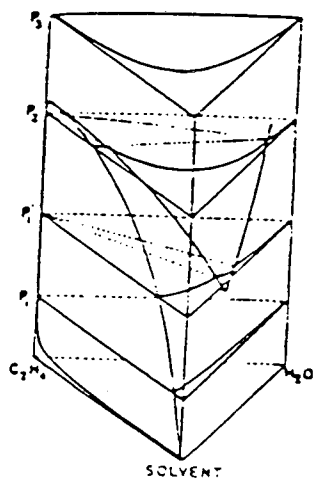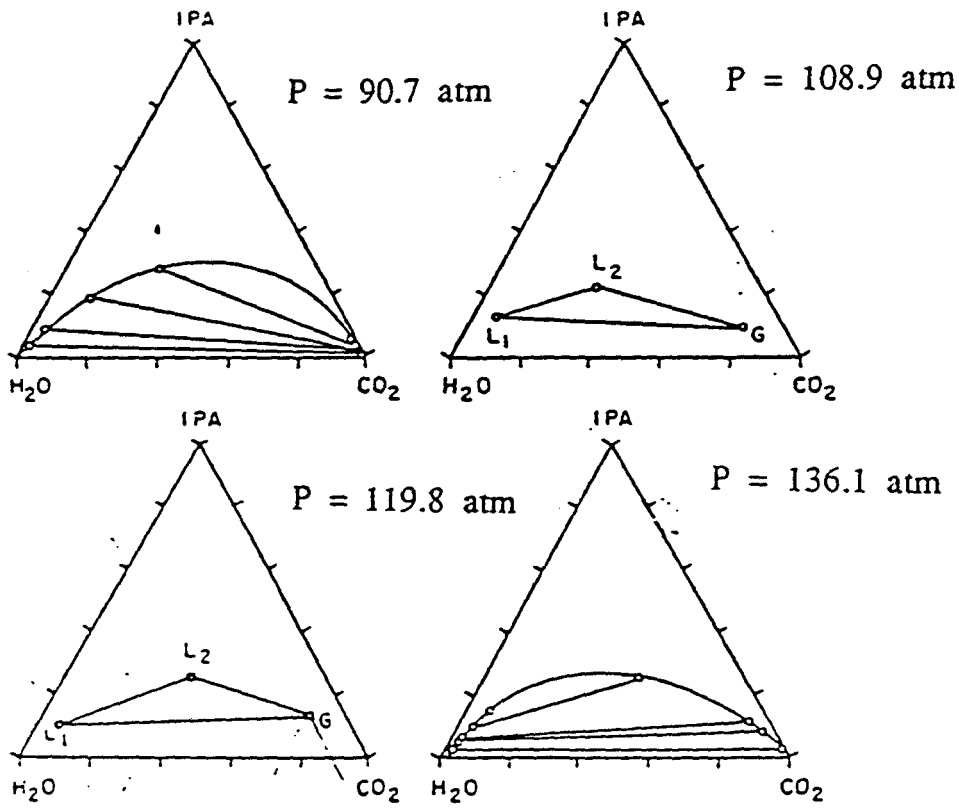
Figure 26

Behavior of the water - isopropanol (IPA) - CO2 system at 60 °C and different pressures.

Figure 27 : The Water/Isopropanol/CO2/Polymer/Salt

System at Equilibrium

T = 40°C

v	pure CO2
α	water isopropanol CO2 salt
β	water isopropanol CO2 polymer salt

Figure 28 : Influence of Polymer Concentration on Excess
Scattered Light Intensity for Two Sodium-Acetate Concentrations

HEC (5% NaAc)

HEC concentration g/l

□ 1
■ 2
○ 3
● 5

HEC (10%NaAc)

◆ 0.25
□ 1
□ 1.25
● 5
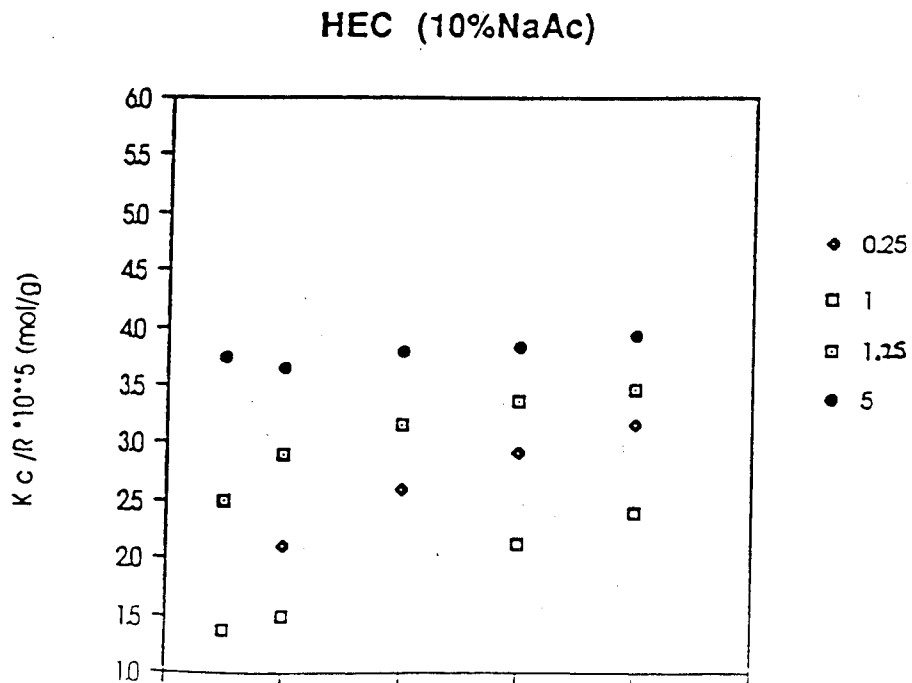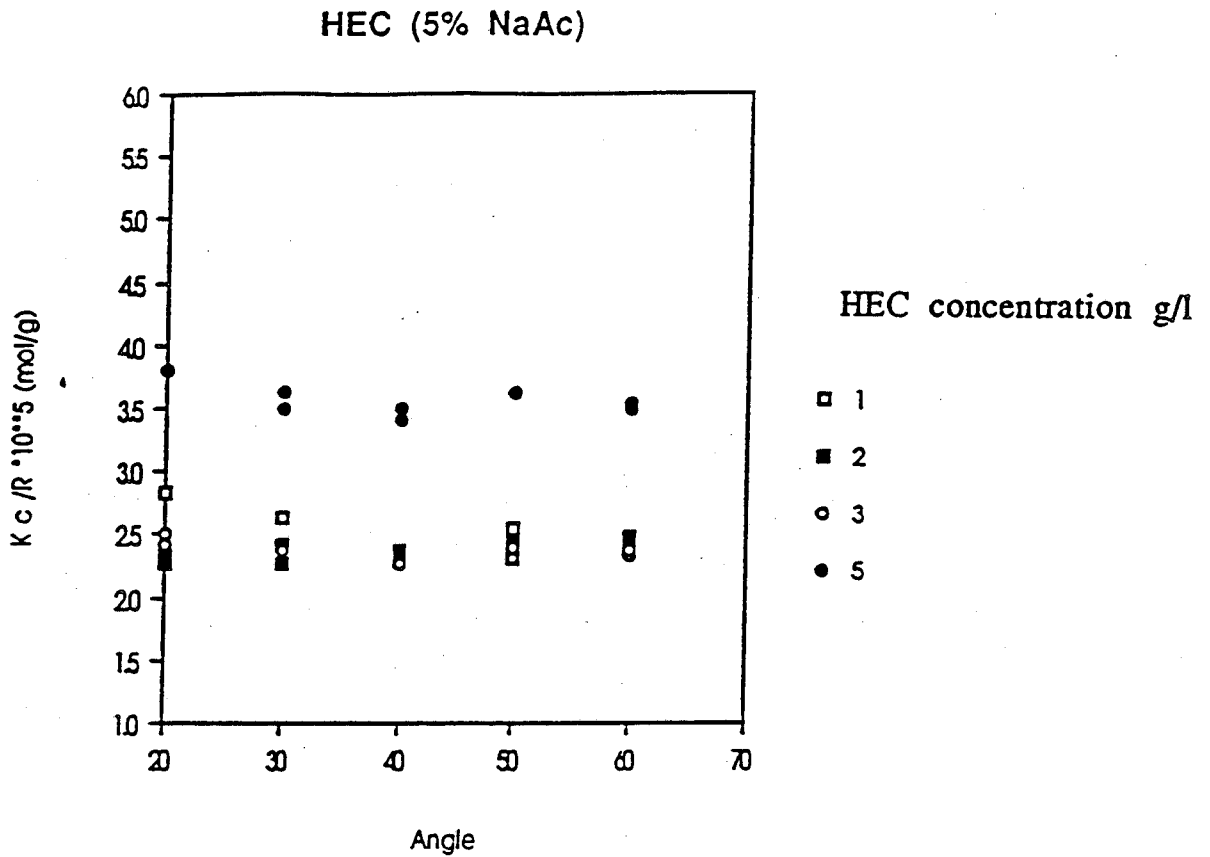
Figure 29 : Influence of Polymer Concentration on Excess
Scattered Light Intensity for Three Potassium-Sulfate
Concentrations

HEC(2%NaAc) 0.1 g/l K2SO4

HEC(2%NaAc) K2SO4 0.5 g/l

Potassium Sulfate
concentration , g/l

- ● 5.
- ◆ 10
- ▣ 15
- ◇ 20
- ■ 25

HEC(2%NaAc) 1g/l K2SO4
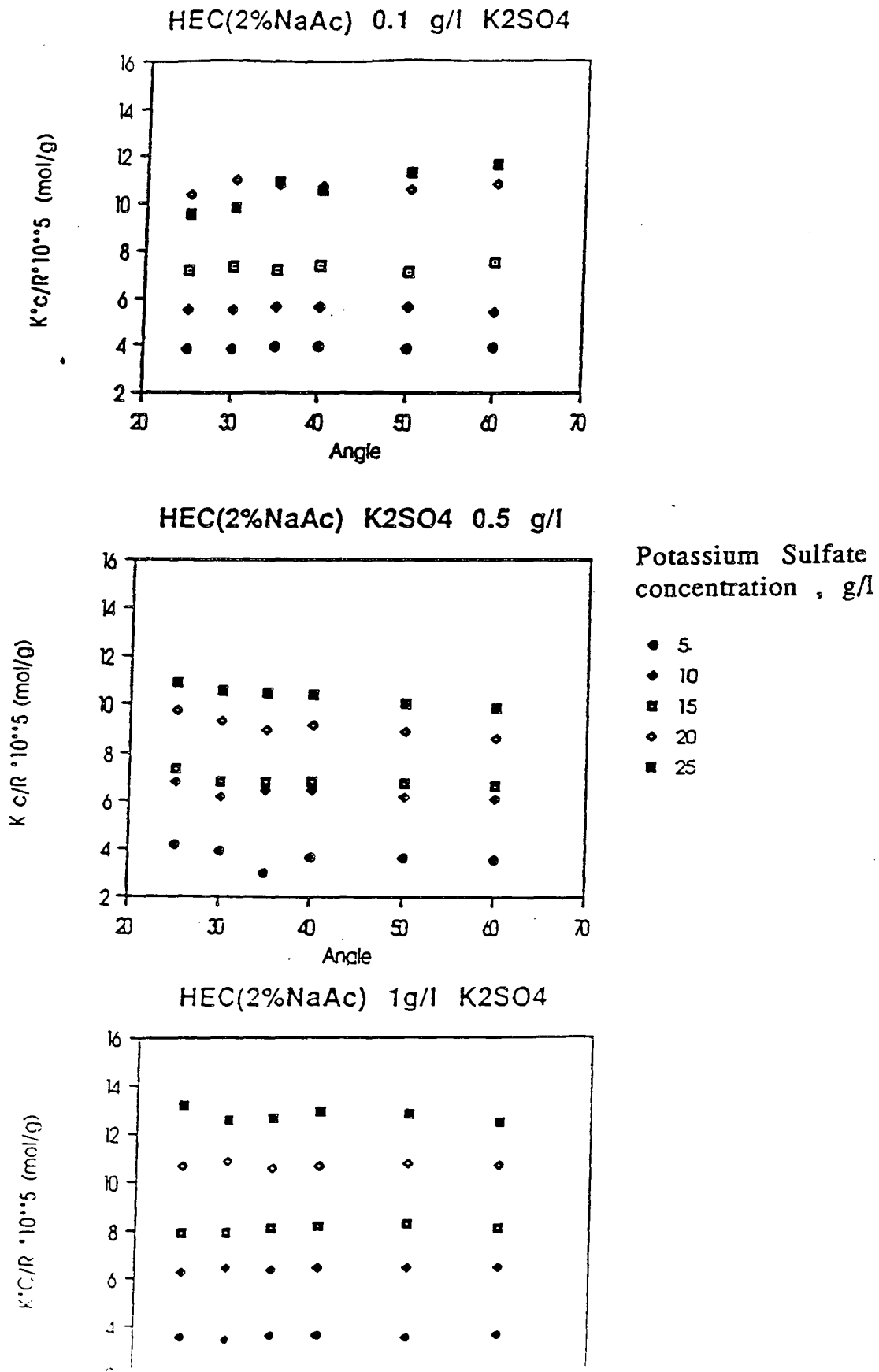
Figure 30 : Influence of Polymer Concentration on Excess
Scattered Light Intensity for Three isopropanol
Concentrations

HEC(2%NaAc)

HEC(5%NaAc) isop(10%)

HEC concentration g/l

- ● 5.
- ◆ 10
- ○ 15
- ■ 20
- □ 25

HEC(2%NaAc) isop(20%)
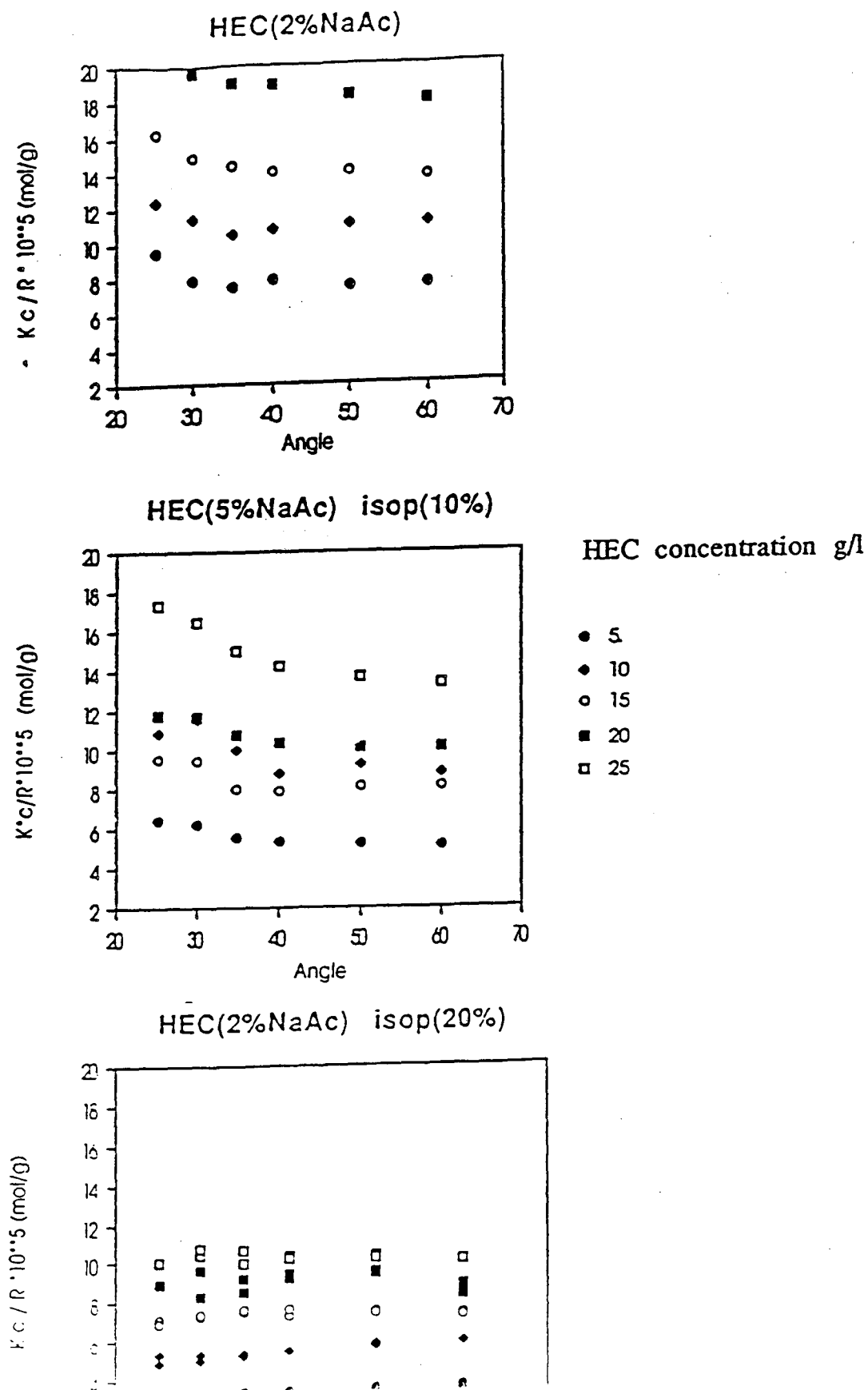
Figure 31 : Influence of Salt Concentrations on Excess Scattered Light Intensity
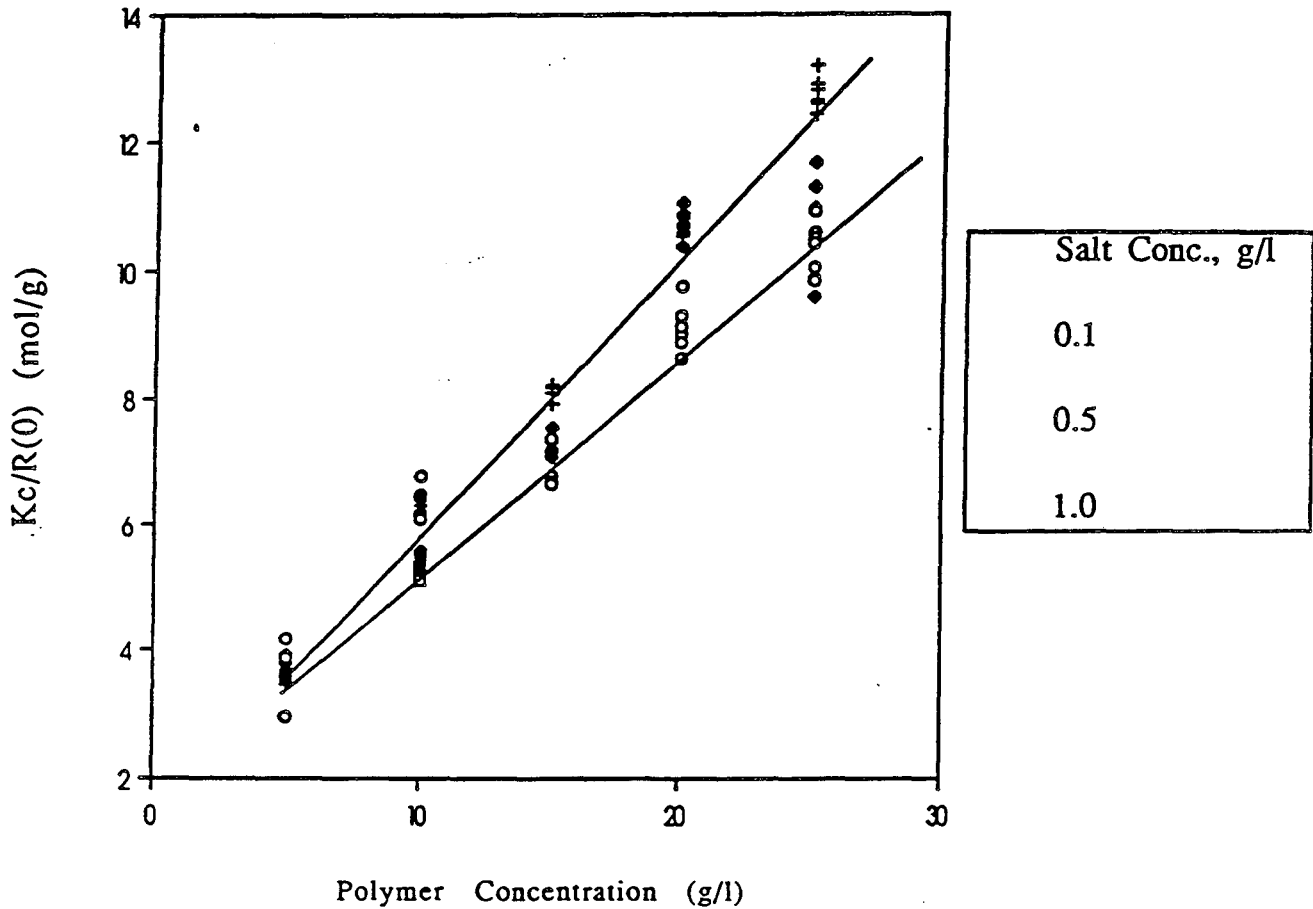
Salt Conc., g/l
0.1
0.5
1.0

K : Optical Constant

c : Polymer Concentration (g/l)

R(0) : Excess Scattered Light Intensity for c=0

Figure 32 : Influence of Isopropanol Concentrations on Excess Scattered Light Intensity
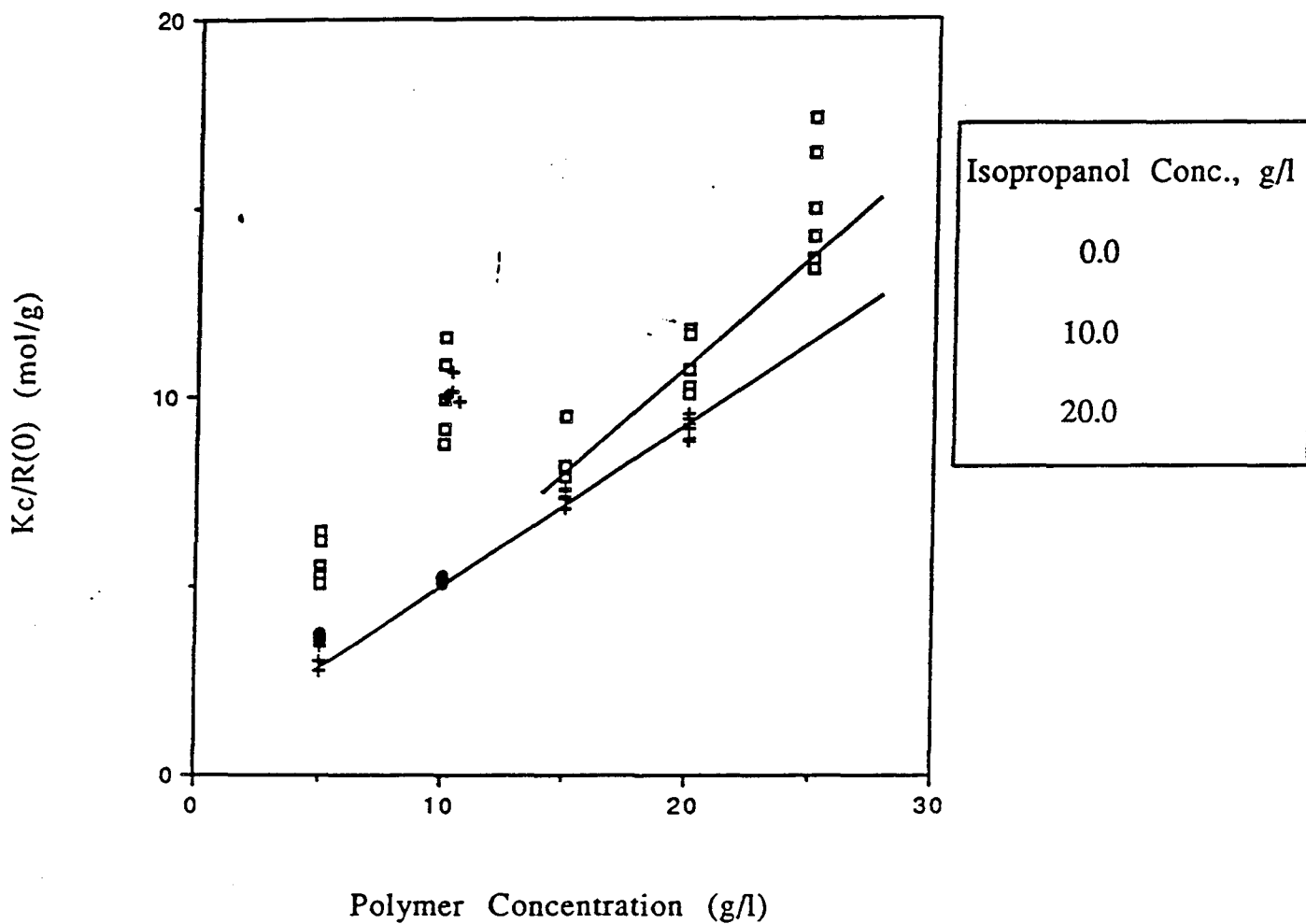
K : Optical Constant

c : Polymer Concentration (g/l)

R(0) : Excess Scattered Light Intensity for c=0

Figure 33 : Experimental Liquid-Vapor Coexistence Curve for the Water-Isopropanol-CO_2 system at 40°C and 103.1 atm.
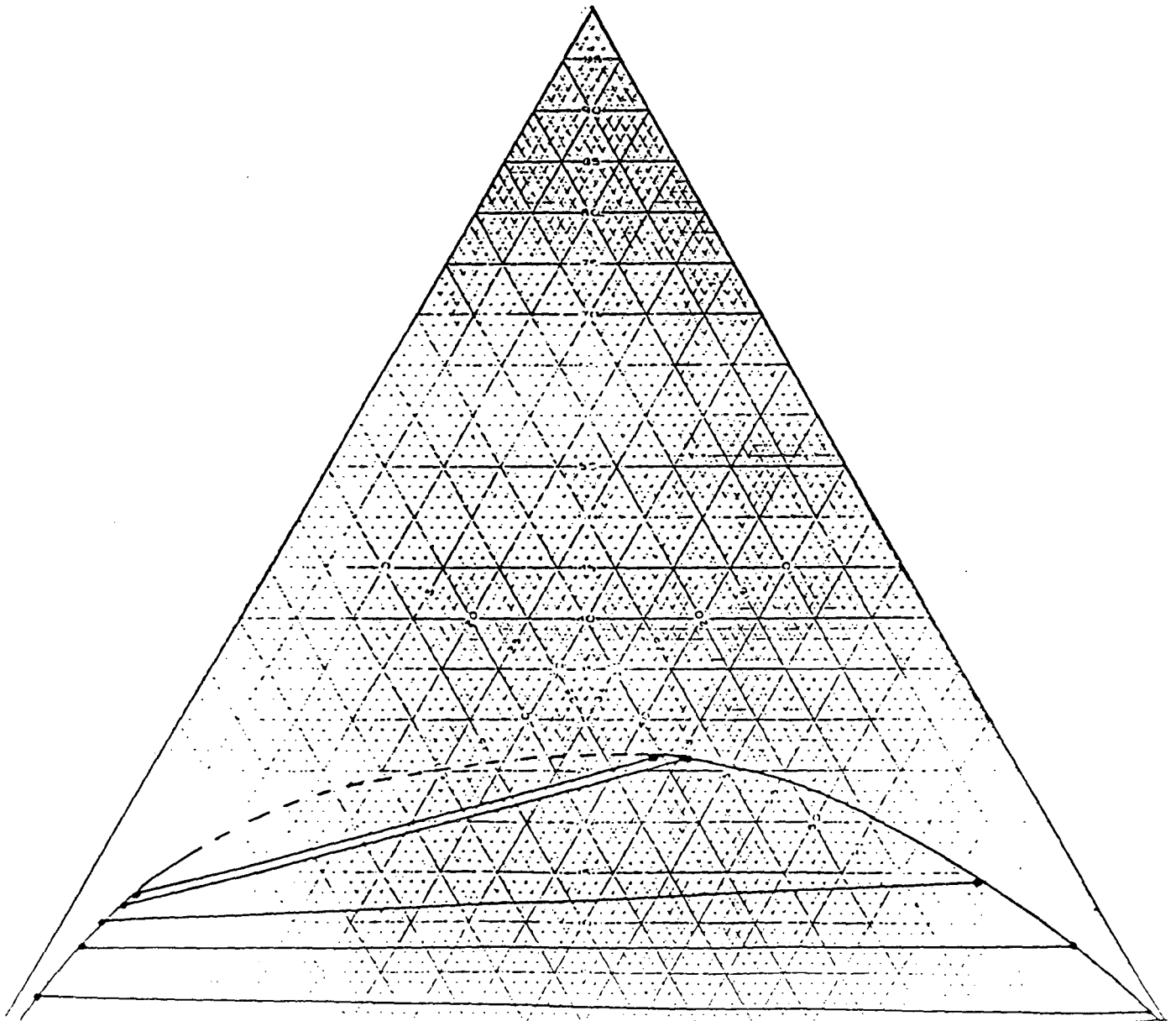
ISOPROPANOL

Figure 34 : Comparison Between Calculated (————) and Experimental
(— — —) Coexistence Curves at 40°C and 103.1 atm.
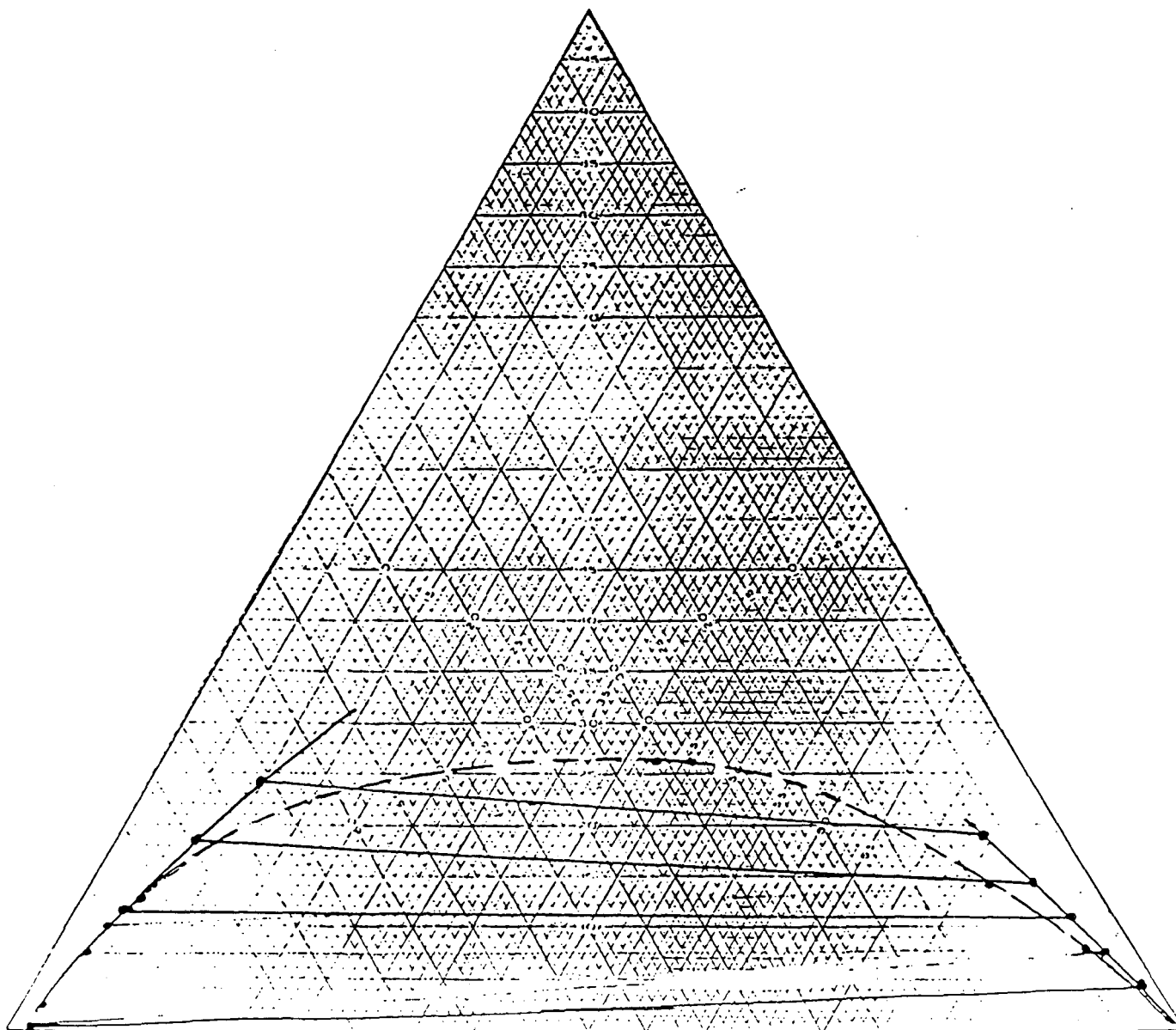
ISOPROPANOL

Figure 35 : Water/Isopropanol/CO_2 Flash Calculations at 60°C. Appearance of the Second Liquid Phase
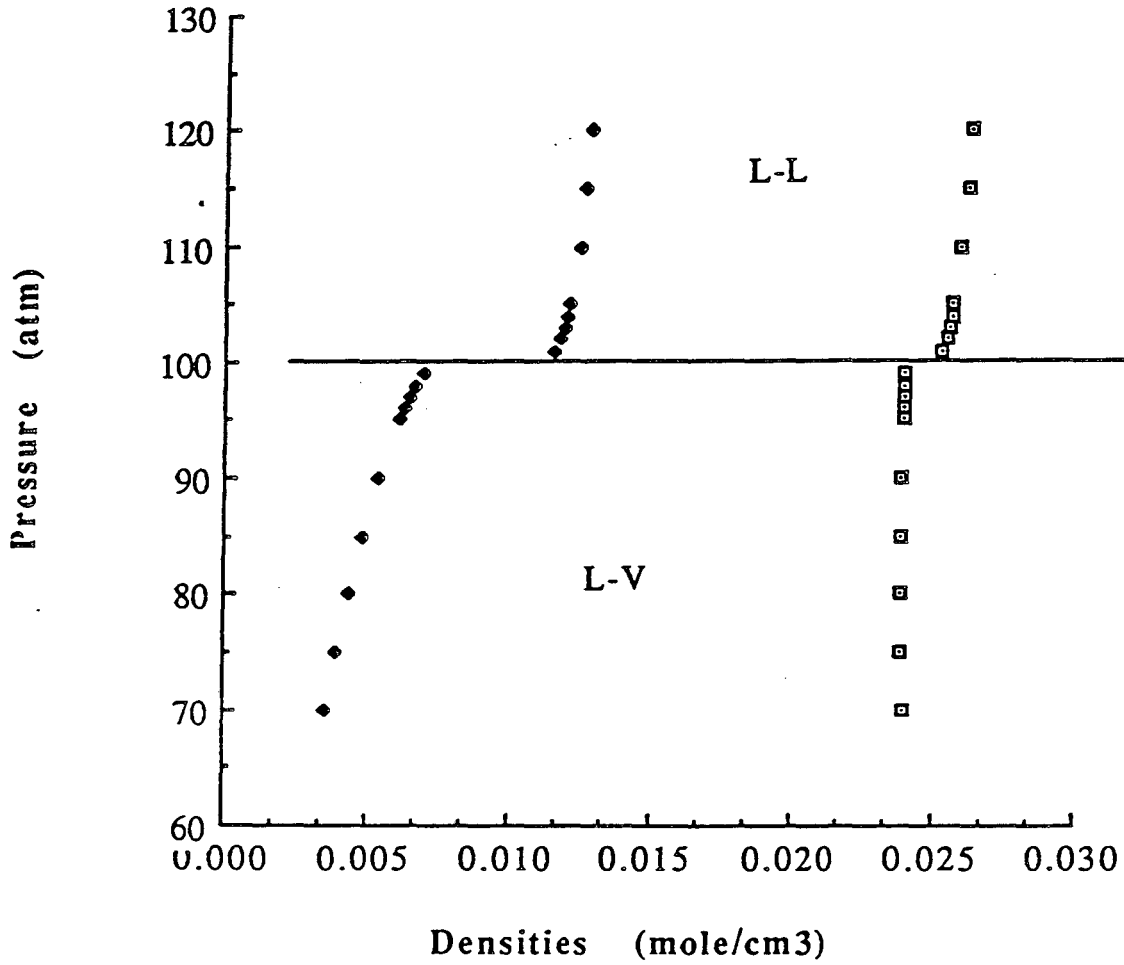
Figure 36 : Computation of the Water/Isopropanol/CO2 Phase-
Diagram at 333 K for a CO_2 Feed Mole Fraction of 0.35
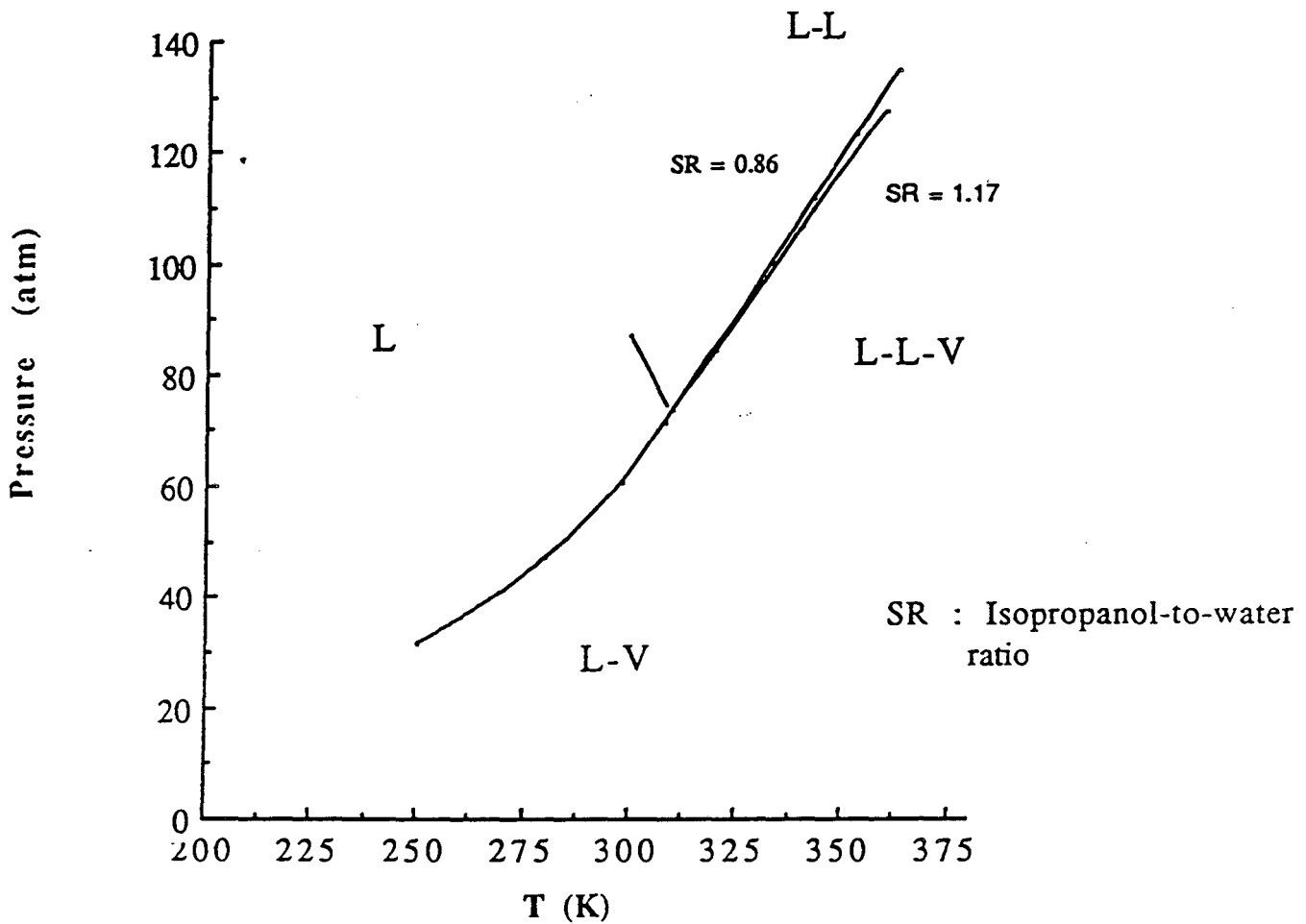
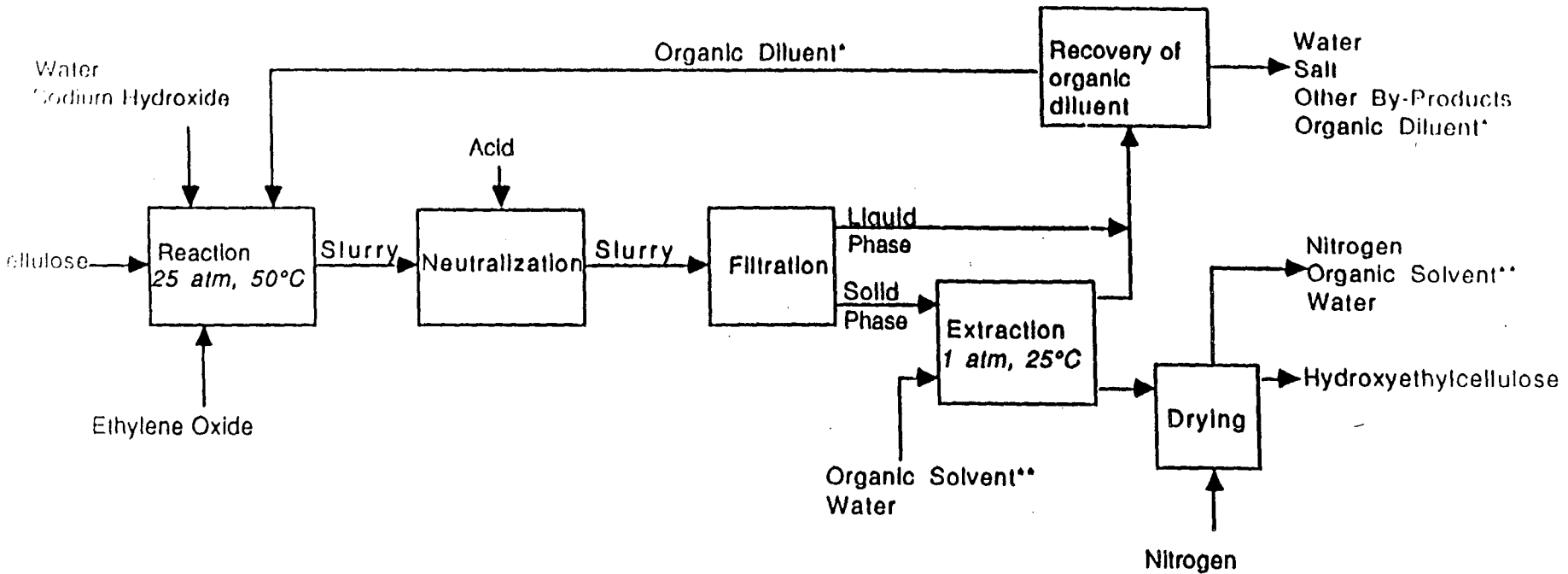# Figure 37 : Experimental and Computed Tie-Lines for the Water/Isopropanol/CO2/HEC/Salt System at 40°C and 80.2 atm

experimental _____   _____ calculated

_ _.Type 1 Diagram _.

x(top) water ======== x(bot) water

x(bot) isop [____] x(top)*isop

10*x(bot) CO2 _____ 10*x(top) CO2

0   Mole Fractions   1

_ _. Type 2 Diagram _

x(top) water _____ x(bot) water

x(bot) isop ____ x(top)*isop

10*x(bot) CO2 _____ 10*x(top) CO2

0   Mole Fractions   1
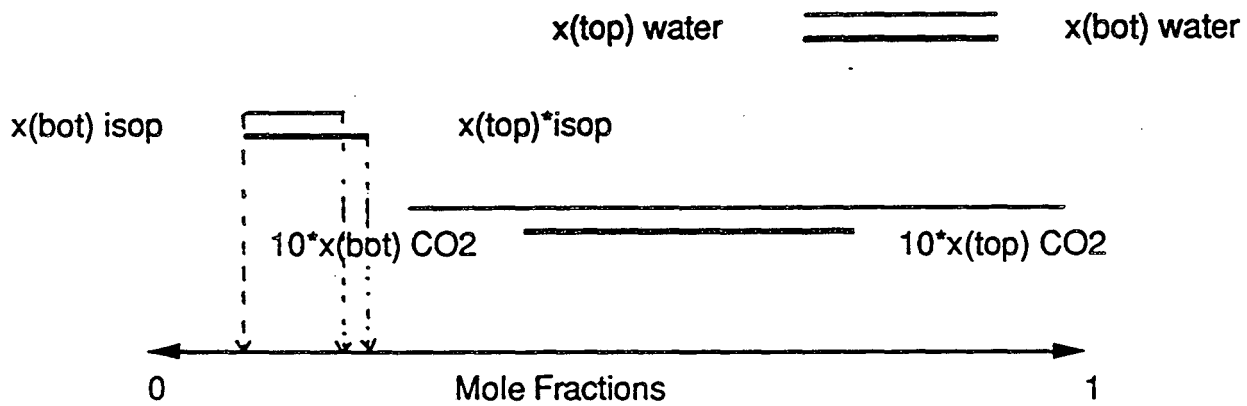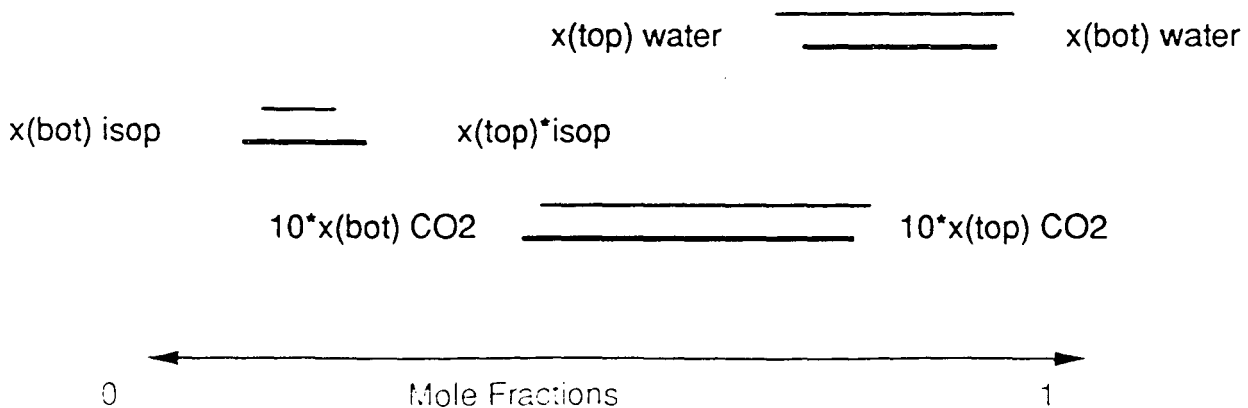
* = Typically Isopropanol, Tertiary Butanol, Acetone or Toluene
** = " Acetone, Methanol or Isopropanol

Figure 38: Current Production Process for Hydroxyethylcellulose
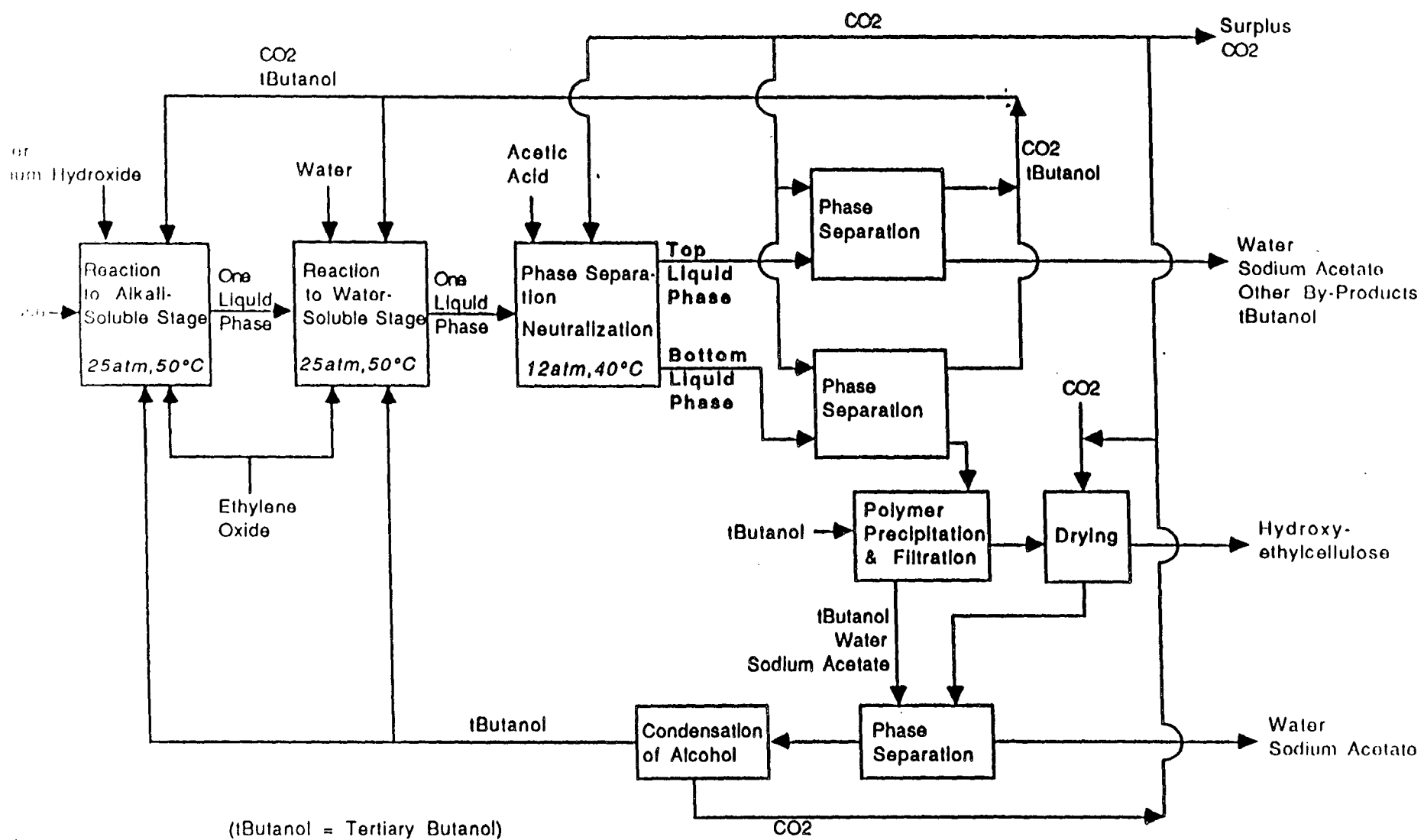
Figure 39: Proposed Production Process for Hydroxyethylcellulose
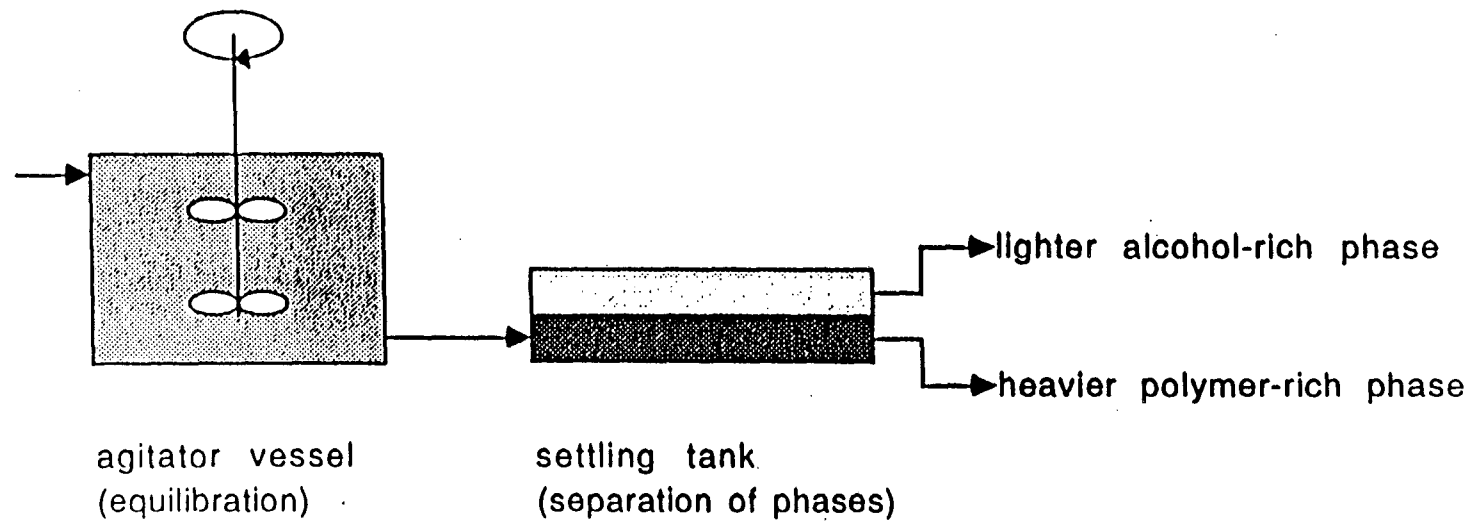
84

ymer, salt,
er, alcohol,
)

agitator vessel
(equilibration)

settling tank
(separation of phases)

lighter alcohol-rich phase

heavier polymer-rich phase

Figure 40: Continuous Purification Step in the New Production
Process of HEC

APPENDIX

A. EXPERIMENTAL DATA

(All concentrations are given in g/l. Results for the bottom liquid phase are referred to as "bot", those of the top to as "top". The initial concentrations are referred to as "init". The dash "-" means that the top phase was not sampled. V = volume of phases, ρ = density of phases.)

HEC (low-viscosity fraction)/Isopropanol

Exp. No.		HEC	Sodium Acetate	Isopropa-nol	Water	Carbon Dioxide
	Init	38.0	1.48	308	577	-
1	Bot	66.3	2.57	258	560	73.0
	Top	6.72	1.27	311	-	96.5
40°C 61.3atm		V(top) = 80ml V(bot) = 50ml		ρ(top) = ρ(bot) =	960.1	g/cm^3
	Init	38.0	1.96	310	573	-
2	Bot	71.8	2.22	236	581	73.8
	Top	4.84	1.42	324	478	103
40°C 65.2atm		V(top) = 87ml V(bot) = 43ml		ρ(top) = ρ(bot) =	911.2 964.7	g/cm^3 g/cm^3
	Init	84.9	1.57	278	598	-
3	Bot	93.8	1.69	268	554	57.1
	Top	-	-	-	-	-
40°C 77.9atm		V(top) = 5ml V(bot) = 132ml		ρ(top) = ρ(bot) =	974.1	g/cm^3
	Init	89.4	1.47	270	606	-
4	Bot	90.3	1.46	214	626	58.0
	Top	-	-	-	-	-
40°C 79.2atm		V(top) = 15ml V(bot) = 115ml		ρ(top) = ρ(bot) =	989.3	g/cm^3
	Init	105.8	2.88	340	500	-
5	Bot	106.5	4.06	233	586	58.7
	Top	6.3	1.14	425	371	97.0
40°C 80.2atm		V(top) = 40ml V(bot) = 100ml		ρ(top) = ρ(bot) =	900.0 987.6	g/cm^3 g/cm^3

Experimental Data for HEC (low viscosity fraction)/Tertiary Butanol

Exp. No.		HEC	Sodium Acetate	Tertiary Butanol	Water	Carbon Dioxide
6	Init	39.4	2.37	336	551	-
	Bot	53.5	2.30	313	556	12.5
	Top	11.4	1.86	360	524	13.0
40°C 6.5atm		V(top) = 50ml V(bot) = 79ml		ρ(top) = ρ(bot) =	910.7 g/cm^3 937.5 g/cm^3	
	Init	37.0	2.40	344	540	-
7a	Bot	81.1	3.49	289	566	13.7
	Top	12.7	1.90	325	555	15.9
40°C 12.0 atm		V(top) = 82ml V(bot) = 45ml		ρ(top) = ρ(bot) =	910.6 g/cm^3 953.4 g/cm^3	
	Init	identical	with exp.	no. 7a		
7b	Bot	77.2	2.94	238	625	27.0
	Top	15.7	2.30	370	499	31.3
40°C 23.8atm		V(top) = 90ml V(bot) = 37ml		ρ(top) = ρ(bot) =	917.9 g/cm^3 970.0 g/cm^3	
	Init	32.5	2.23	280	624	-
8a	Bot	40.5	2.44	251	631	26.0
	Top	8.25	1.80	305	572	31.1
40°C 20.7atm		V(top) = 30ml V(bot) = 93ml		ρ(top) = ρ(bot) =	918.2 g/cm^3 950.7 g/cm^3	
	Init	identical	with exp.	no. 8a		
8b	Bot	53.3	2.58	235	642	31.6
	Top	-	-	-	-	-
40°C 27.0atm		V(top) = 45ml V(bot) = 75ml		ρ(top) = ρ(bot) =	916.7 g/cm^3 964.1 g/cm^3	
	Init	identical	with exp.	no. 8a		
8c	Bot	48.1	3.26	162	737	36.6
	Top	1.44	0.67	361	418	89.5
40°C 41.4atm		V(top) = 47ml V(bot) = 76ml		ρ(top) = ρ(bot) =	871.0 g/cm^3 986.8 g/cm^3	
	Init	identical	with exp.	no. 8a		
8d	Bot	44.0	3.45	105	810	41.7
	Top	0.77	0.15	345	228	263
40°C 63.3 atm		V(top) = 62ml V(bot) = 75ml		ρ(top) = ρ(bot) =	836.9 g/cm^3 1004.6 g/cm^3	

Experimental Data for HEC (low-viscosity fraction)/Secondary Butanol

Exp. No.		HEC	Sodium Acetate	Secondary Butanol	Water	Carbon Dioxide
9	Init	25.2	1.74	127	825	-
	Bot	26.2	1.80	96.0	835	39.1
	Top	10.5	0.91	399	372	112
40°C 49.7atm		V(top) = 5ml V(bot) = 117ml		ρ(top) = ρ(bot) =	894.4 g/cm^3 997.7 g/cm^3	

Experimental Data for HEC (high-viscosity fraction)/Isopropanol

(HEC precipitated out of solution. The remaining liquid phase was sampled through the bottom recirculation line and is referred to as "Liq.")

Exp. No.		HEC	Sodium Acetate	Isopropanol	Water	Carbon Dioxide
10	Init	16.8	2.60	358	565	-
	Liq.	3.95	1.15	356	370	170
40°C 77.0atm				ρ(Liq.) =	901.2 g/cm^3	
10*	Init	13.6	2.15	268	668	-
	Liq.	7.32	2.15	225	660	71.1
40°C 78.0atm				ρ(Liq.) =	997.7 g/cm^3	

Experimental Data HEC (high-viscosity fraction)/Tertiary Butanol

(HEC precipitated out of solution. The remaining liquid phase was sampled through the bottom recirculation line and is referred to as "Liq.")

Exp. No.		HEC	Sodium Acetate	Tertiary Butanol	Water	Carbon Dioxide
	Init	7.74	2.31	354	551	-
11	Liq.	0	2.24	348	558	2
40°C 6.6atm				ρ(Liq.) =	997.7	g/cm^3

Experimental Data for Xanthan Gum/Isopropanol

(No liquid-liquid phase split or precipitation was observed in exp. #12. In exp. #13, the polymer precipitated and no liquid-liquid phase split was observed. The remaining liquid was analyzed. The analytical re-
sults for xanthan gum have to be viewed with caution, see section "Concentration Measurements")

Exp. No.		HEC	Dipotass. Phosphate	Isopropa-nol	Water	Carbon Dioxide
	Init	3.3	1.83	362	545	-
12	Liq.	2.6	1.65	330	498	93.3
40°C 77.3atm				ρ(Liq.) =	925.3	g/cm^3
	Init	7.8	1.92	352	556	-
13	Liq.	1.9	1.77	316	508	95.2
40°C 76.4atm				ρ(Liq.) =	922.8	g/cm^3

B. List of Tables

C. List of Figures

LAWRENCE BERKELEY LABORATORY
UNIVERSITY OF CALIFORNIA
INFORMATION RESOURCES DEPARTMENT
BERKELEY, CALIFORNIA 94720